UC Berkeley
UC Berkeley Electronic Theses and Dissertations

Title
Regulation of cyanobacterial physiology by the stringent response

Permalink
https://escholarship.org/uc/item/9hn2n87p

Author
Hood, Rachel

Publication Date
2017

Peer reviewed|Thesis/dissertation

eScholarship.org Powered by the California Digital Library
University of California

Regulation of cyanobacterial physiology by the stringent response

by

Rachel D. Hood

A dissertation submitted in partial satisfaction of the

requirements for the degree of

Doctor of Philosophy

in

Molecular and Cell Biology

in the

Graduate Division

of the

University of California, Berkeley

Committee in charge:

Professor David Savage, Chair
Professor Daniel Portnoy
Professor Arash Komeili
Professor Krishna Niyogi

Spring 2017

Abstract

Regulation of cyanobacterial physiology by the stringent response

by

Rachel D. Hood

Doctor of Philosophy in Molecular and Cell Biology

University of California, Berkeley

Professor David Savage, Chair

Signals that communicate a cell's metabolic state allow organisms to adapt to the suboptimal conditions they often encounter in the environment. If a particular nutrient is lacking, the organism reduces the energy it expends on growth and reproduction, instead redirecting its resources to maintain basic cellular functions.

Cyanobacteria were the driving force behind the oxygenation of Earth's atmosphere, the ancestor of the chloroplast, and remain an important group of primary producers today. These 'blue-green' bacteria carry out photosynthesis, capturing solar light energy and converting it into the chemical energy that sustains life. They also perform carbon fixation, reducing carbon dioxide into organic carbon compounds. These processes are both required to sustain cyanobacterial growth, so when the inputs of these pathways – like light – are unavailable, many metabolic changes occur that necessitate physiological adaptations.

Here, I demonstrate a major mechanism by which the cyanobacterium *Synechococcus elongatus* senses and responds to stresses. I find that the stringent response, a conserved bacterial stress response, is induced in response to darkness, photosynthetic inhibition, and nutrient starvation. The second messengers of this response, the phosphorylated nucleotides ppGpp and pppGpp, reprogram gene expression and induce physiological responses that can be either general or nutrient-specific. I have also begun investigating the roles of polyphosphate, a compound that accumulates in response to stress and may help cells adapt to challenging conditions, in *Synechococcus*.

Cyanobacteria like *Synechococcus* are an interesting subject for study of the stringent response due to their unique metabolism and physiology. While the logic of the stringent response – indeed, many stress responses – is similar across many bacteria, the specific mechanisms behind them often differ. Learning more about how the same stress response mechanism has been adapted by diverse organisms will continue to increase our understanding of how bacteria interact with their environments.

Acknowledgments

During the past six years, I have grown a great deal both scientifically and personally. Working towards a PhD has been at times exciting, at times frustrating, but very rewarding overall. For their encouragement and guidance along the way, I have a number of people to thank.

First of all, I am extremely grateful to my advisor, Prof. Dave Savage, for taking me on as a student in the very first year he established his lab at UC Berkeley. It's been great to see the lab grow and develop over the last several years. Most of all, though, I really appreciate the scientific freedom Dave has allowed me in pursuing projects and pushing them in the directions I found most interesting. This independence has been very important to my development as an independent scientist. I am also constantly amazed by Dave's knowledge of many different scientific fields and ability to communicate concepts so clearly.

I would like to thank my thesis committee members – Profs. Dan Portnoy, Arash Komeili, and Kris Niyogi – for their feedback and support over the last few years. Their suggestions ended up shaping the directions in which I took my research, and strengthened it as a result.

I wouldn't have opted to do a PhD in the first place had it not been for the influence of my two former advisors. When I decided to do research in microbiology with Prof. Mark Martin at the University of Puget Sound as an undergraduate, I had no idea that it would take me in the direction it has. Mark's passion for microbiology has profoundly affected how I think about the field I've studied ever since working in his lab, and has instilled in me a love of the world we cannot see. Working in Prof. Joseph Mougous's lab as a technician taught me so much about how to do science well, and provided me with a really solid foundation upon which I could build when I entered graduate school.

One of the best things about working in the Savage lab for the past few years has been the diverse group of people with whom I've gotten to work. I have learned a great deal from each and every one of them, and the different experiences and perspectives they've brought to the group have made it much stronger and more interesting, both scientifically and personally. Caleb Cassidy-Amstutz and I rotated in the lab together and joined at the same time, and by now I consider him to be my lab brother.

UC Berkeley has been a fantastic place to do a PhD – there are so many talented and inspiring people with whom I've interacted during my time here. A number of graduate students and postdocs – too many to list here – have helped me formulate and develop scientific ideas, or with experimental techniques, and have been very generous with their time.

Almost as important as my scientific training has been my experience working as a writer, editor, and Editor in Chief of the *Berkeley Science Review* during graduate school. My experience with the *BSR* not only helped me realize I was interested in science communication, it also helped me improve my writing and editing skills a great deal. The *BSR* connected me with a community of graduate students with similar interests, and I've really enjoyed working alongside and learning from them.

Ever since the beginning of graduate school, my classmates in the MCB program have been a source of inspiration and support. It's been really fun seeing what they've done in the past six years. I wish them all the best as we move on to other endeavors, and I'll miss our lunches, movie nights, and trips to the beach and Tahoe.

Any discussion of classmates could not be complete without thanking one of them most of all. Brett Robison, I'm so grateful for all the time we've spent together. It's hard to imagine how different graduate school would have been without the perspective we've given each other and the adventures we've had. I'm looking forward to many more in the future.

Finally, to my parents Mary and David Hood, my sister Catherine Hood, and longtime friend Julia Ledbetter, thank you all for always being there. I know I can always turn to any of you under any circumstances. I know I always have your unwavering support, and I couldn't ask for anything more than that.

Table of Contents

List of Figures

List of Tables

Chapter 1

Introduction

Some material from this chapter is adapted from, and will be published as (tentatively):
Rubin BE, Welkie D, Diamond S, Hood RD, Savage DF, and Golden SS
The dark side of the cyanobacterium
Trends in Microbiology

1.1 A brief introduction to cyanobacteria – their evolutionary history and environmental relevance

We owe our existence to cyanobacteria, the inventors of oxygenic photosynthesis. Had they not oxygenated Earth's atmosphere over the course of a couple billion years, we – and other species that depend on an aerobic metabolism – could not exist. Cyanobacteria have many enduring legacies, some of which are historical and many of which remain extremely relevant, that make them fascinating subjects of study.

Before foundational work in the 1960s and 1970s, cyanobacteria were classified as blue-green algae. In these decades, Stanier and van Niel established the distinguishing characteristics of prokaryotes and eukaryotes, and work by Woese and Fox elucidated what has become our current tree of life – encompassing bacteria, archaea, and eukaryotes – based on molecular phylogenies (1, 2). Many species names of cyanobacteria have changed in the subsequent decades, as we have gained a greater understanding of the taxonomic relationships among cyanobacteria. No longer the blue-green algae, the cyanobacterial phylum is now a fully-fledged branch on the bacterial tree (3).

Another breakthrough in understanding the context and importance of cyanobacteria came around the same time with the elaboration of the endosymbiotic theory. Work by Margulis (then Sagan) and others (4, 5) supported the idea that formerly free-living bacteria were engulfed by proto-eukaryotic cells and were, in a sense, domesticated into mitochondria and chloroplasts. What were formerly α-proteobacteria and cyanobacteria became metabolic powerhouses that supported the larger cell in which they were housed, and received protection and other benefits in return. In the past several decades, we have come to appreciate the cyanobacterial origins of plant photosynthesis and the parallels that can be drawn between chloroplast and cyanobacterial physiology.

Today, many free-living cyanobacteria survive – and thrive – in diverse environments around the globe. Not only are they abundant in the oceans (6), they are also found in less-expected environments like the soil crusts of deserts (7). It has been estimated that cyanobacteria perform 10-25% of global photosynthesis today (6, 8), making them important primary producers. Most cyanobacteria fix carbon and thereby sequester carbon dioxide into biomass. Furthermore, some cyanobacteria fix atmospheric

molecular nitrogen. Altogether, the metabolic capacities of cyanobacteria mean that they play important roles in the food web, and in global carbon and nitrogen cycles.

The subsequent sections of this introductory chapter cover a range of topics in cyanobacterial biology, with a particular focus on their metabolism and physiology. Chapters 2, 3, and 4 will present our studies on cyanobacterial stress responses and stress physiology, but understanding these complicated and integrated phenomena requires first gaining an appreciation for many aspects of how these organisms live in and adapt to their environment.

1.2 Cyanobacterial cellular organization

Not only do cyanobacteria exist in many environments on Earth, they also exist in many forms. The morphologies of different classes of cyanobacteria vary widely – some are filamentous; some form specialized nitrogen-fixing cells called heterocysts – but from here on, I will focus on single-celled cyanobacteria. *Synechococcus elongatus* PCC 7942 (hereafter, *Synechococcus*) is a model cyanobacterium that lives in freshwater, and is the subject of the studies described herein. This particular strain was one of the first cyanobacteria for which genetic tools were developed (9).

Recent work in microbiology has shed light on specialized intracellular structures and organization in bacteria, and cyanobacteria like *Synechococcus* are particularly noteworthy in these respects. Cyanobacteria are Gram-negative in the sense that they have both an outer and an inner membrane, with a peptidoglycan layer in the middle. Most cyanobacteria, including *Synechococcus*, have a series of internal membranes – the thylakoid membranes – in which the photosynthetic machinery is localized (Figure 1-1). Though these appear as concentric ring-like structures in 2D electron micrographs, 3D cellular reconstructions have indicated that the membranes are discontinuous, allowing cytoplasmic components like ribosomes to contact the inner membrane (10).

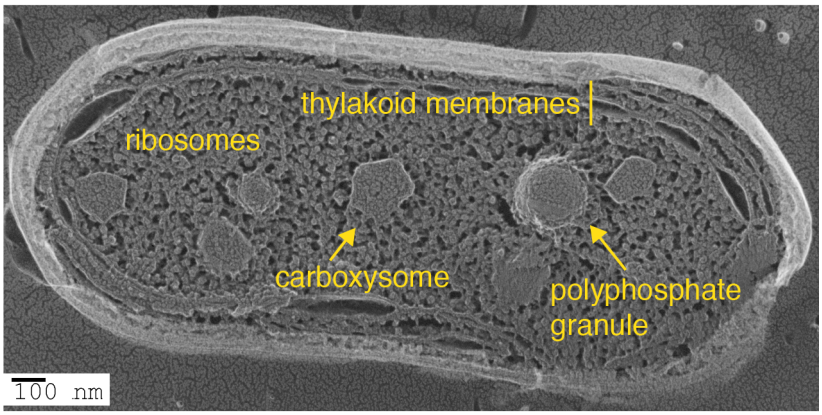

Figure 1-1. Cellular organization of *Synechococcus elongatus* PCC 7942, as revealed by deep-etch electron microscopy. Visible in this image are the thylakoid membranes, carboxysomes (organelles for carbon fixation), polyphosphate granules, and ribosomes. Image acquired by / courtesy of Robyn Roth and Ursula Goodenough, Washington University.

In addition to their unique membrane structures, *Synechococcus* cells contain various "cellular inclusions," including carboxysomes – proteinaceous organelles in which the carbon fixation enzyme Rubisco is contained – and assorted storage granules composed of polyphosphate and glycogen (Figure 1-1) (11). The roles of these compounds will be discussed in greater detail in subsequent sections or chapters.

1.3 Cyanobacterial metabolism

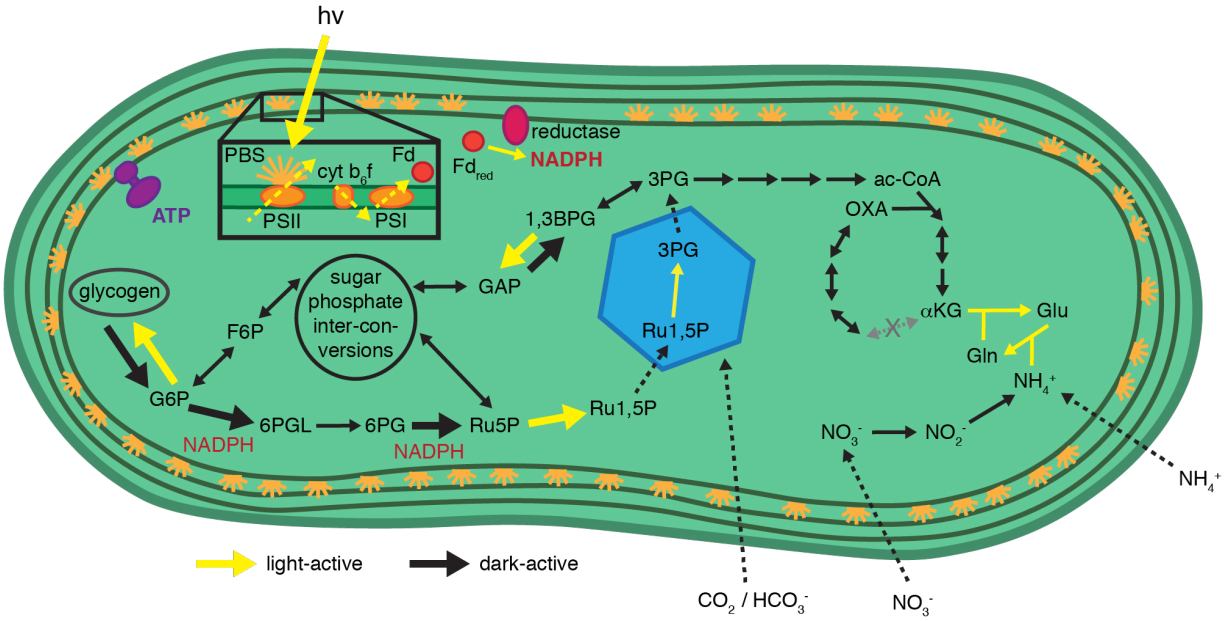

Figure 1-2. Central metabolic pathways and their localization and regulation in *Synechococcus*. Shown are reactions of photosynthesis, the pentose phosphate pathway (both reductive and oxidative branches), the tricarboxylic acid cycle, and nitrogen assimilation. Yellow arrows indicate light-specific reactions, and large black arrows indicate dark-specific reactions. Dashed lines indicate transport reactions. Labels indicating ATP or NADPH depict reactions from which these compounds are produced. Abbreviations: hv, (sun)light; PBS, phycobilisome; PSII, photosystem II; cyt b_6f, cytochrome b_6f; PSI, photosystem I; Fd(red), ferredoxin (reduced); Ru1,5P, ribulose-1,5-bisphosphate; 3PG, 3-phosphoglycerate; 1,3-BPG, 1,3-bisphosphoglycerate; GAP, glyceraldehyde-3-phosphate; F6P, fructose-6-phosphate; G6P, glucose-6-phosphate; 6PGL, 6-phosphogluconolactone; 6PG, 6-phosphogluconate; Ru5P, ribulose-5-phosphate; ac-CoA, acetyl-CoA; αKG, α-ketoglutarate; OXA, oxaloacetate; Glu, glutamate; Gln, glutamine.

1.3.1 Photosynthesis and central carbon metabolism

Each day, a cyanobacterium wakes up to the unenviable task of turning inorganic carbon into the organic molecules of life via photosynthetic carbon dioxide assimilation (Figure 1-2). Its metabolic challenges are numerous. The cell must simultaneously duplicate its molecules to prepare for division, while also storing energetic reserves for the night. These reactions take place in the background of photosynthesis, which

requires significant cellular resources for efficient function and generates reactive oxygen species (ROS) as a primary byproduct (12). Metabolomic analysis has revealed that there is a general upregulation of anabolic metabolism at the onset of light, including pathways related to amino acid, nucleotide, and quinone biosynthesis (13). Upregulation of amino acid and nucleotide production agrees with historical observations that protein translation and DNA replication largely occur during the day (14, 15).

A principal activity during the day is accumulation of excess reduced carbon, which is sequestered as the glucose polymer glycogen. Under growth in light/dark cycles, accumulation of glycogen during the day serves two primary purposes: it is synthesized as the primary energy and carbon storage compound in preparation for night (13, 16), and it serves as a "regulatory valve" for excess reductant under conditions of particularly high light intensity (12, 17, 18).

Glycogen's ability to act as a photosynthetic electron sink has been particularly highlighted by investigations into the nitrogen deprivation response of cyanobacteria. In mutants that cannot synthesize glycogen, nitrogen deprivation causes growth defects and oxidative damage at high light intensities that do not affect wild-type cells (12, 18). Overall, the buffering of cellular redox state through glycogen synthesis and degradation is likely an important mechanism that allows the proper regulation of cellular responses.

1.3.2 Nitrogen assimilation

Nitrogen assimilation is another vital branch of cyanobacterial metabolism, and *Synechococcus* can take up nitrogen sources such as nitrate or ammonium (unlike diazotrophic cyanobacteria, which can fix atmospheric nitrogen) (19). Ammonium feeds directly into the main reaction of nitrogen assimilation, in which glutamine synthetase uses ammonium and ATP to convert glutamate to glutamine (Figure 1-2). Nitrate, however, must first be converted into ammonium before it can be assimilated. This is done through the action of nitrate reductase and nitrite reductase, both of which require reducing equivalents produced by photosynthesis. Central carbon and nitrogen metabolism are tightly linked and must be co-regulated to ensure a proper balance across different branches of metabolism.

1.4 Circadian rhythm

The rotation of the Earth leads to predictable cycles of light and darkness, which for cyanobacteria means frequent, regular metabolic oscillations. Thus, being able to anticipate the timing of these light/dark cycles is beneficial to *Synechococcus* (20). Cyanobacteria are the only bacteria known to have a circadian rhythm – a system that entrains to environmental light/dark cycles, is temperature-compensated, and continues to oscillate even when environmental conditions remain constant (i.e., in constant light).

The discovery that certain cyanobacteria exhibit circadian patterns of nitrogen fixation in the 1980s (21) set off a flurry of research aimed at understanding the underlying

biochemical machinery of the rhythm and its effects on the cell. In the past few decades, circadian rhythm has become a major focus of research in *Synechococcus*, and it has become clear that it is a major regulator of metabolism and physiology (22). While circadian rhythm helps cells anticipate the onset of darkness or the onset of light, metabolic signals indicating light or dark also feed back into the circadian system, signaling to the main timekeeping proteins and affecting cross-talk between circadian rhythm and other signaling pathways.

1.4.1 The post-translational circadian oscillator and its inputs

Genetic screens in the 1990s identified three main protein components of the core circadian machinery in *Synechococcus*: KaiA, KaiB, and KaiC (23). KaiC is the central timekeeper, and undergoes a ~24-hour phosphorylation cycle. The phosphorylation of KaiC is regulated by KaiA and KaiB, which act to promote KaiC's autokinase and autophosphatase activities, respectively (24). Further studies showed that mixing the three Kai proteins with ATP in vitro is sufficient to produce oscillations in KaiC phosphorylation similar to those seen in vivo, and these rhythms persist for several days in constant light (25).

What are the signals that communicate darkness to the circadian oscillator? Both KaiC itself, and two proteins that regulate circadian period (CikA and LdpA), sense the redox state of the quinone pool (24). These electron carriers are reduced when cells are photosynthetically active and oxidized when they are not (i.e., in the dark). ATP:ADP ratios have also been shown to affect the phosphorylation state of KaiC in vitro (26). Rather than directly sensing light (or the absence thereof), the circadian system instead senses the primary products of photosynthesis, ATP and reducing power, to adjust or reset the clock when necessary.

1.4.2 Output mechanisms of the circadian oscillator

Expression of a majority of genes is circadian-regulated in *Synechococcus* (27, 28). None of the Kai proteins themselves are transcription factors, so the KaiC oscillator must be read out by other cellular components to control gene expression. Significant progress has been made in the past few years in understanding how this takes place, and many of these findings center around the transcription factor RpaA. RpaA is the response regulator component of a two-component system, and SasA is its cognate histidine kinase (29). SasA interacts directly with KaiC, but only in one of its four phosphorylated states, and this triggers phosphorylation of RpaA.

Phosphorylated RpaA binds to many sites within the *Synechococcus* genome, thereby directly regulating expression of ~200 genes, including several transcription factors and sigma factors, and noncoding RNAs (30). When RpaA is deleted, normally-rhythmic gene expression becomes arrhythmic, demonstrating the importance of this regulator. Several proteins other than SasA, including CikA, Crm, and RpaB, regulate activity of RpaA (24). The importance of RpaA and its regulon in controlling circadian, and light/dark, physiology only continue to grow – Diamond et al. showed recently that a

mutant lacking this gene dies during light/dark cycles, possibly due to higher levels of ROS (31).

1.5 Effects of light/dark cycles on *Synechococcus* metabolism and physiology

To cyanobacteria, day and night represent extreme contrasts. For an organism like *Synechococcus* that requires light for growth, darkness necessitates metabolic rewiring and cellular reprogramming.

1.5.1 Metabolic changes in the dark, and their regulation

Cyanobacterial metabolism is carefully orchestrated in both space and time. The temporal organization of cyanobacterial metabolism can broadly be characterized as anabolic during the day and catabolic at night. The former is largely driven by photosynthesis, while the latter corresponds to active respiration and the oxidative pentose phosphate pathway (OPPP). In the dark, CP12, a redox-sensitive protein that is a master regulator of the Calvin-Benson-Bassham Cycle (CBBC), becomes oxidized (32). Oxidized CP12 structurally sequesters glyceraldehyde 3-phosphate dehydrogenase (GAPDH) and phosphoribulokinase (PRK) and inhibits the CBBC (33). At the onset of light, photosynthetic reducing equivalents are generated, CP12 is inhibited, and CBBC activity resumes.

One of the first indicators that cyanobacteria undertake active metabolism at night was the observation that glycogen is rapidly degraded upon entering the dark (34). Its importance under diurnal conditions is highlighted by the fact that mutations targeting the glycogen biosynthetic pathway genes *glgA*, *glgC*, and *glgP* significantly attenuate the ability of cells to grow in light/dark cycles (35, 36).

Activation of the OPPP is critical for survival at night, and failure to turn on the OPPP (via the circadian regulator RpaA or post-translational regulatory mechanisms) results in the inability to regenerate essential reducing power in the form of NADPH. Carbon flux through the OPPP is one of the most critical processes for nighttime survival, as inactivation of the core OPPP genes *zwf*, *gap*, or *gnd* causes severely attenuated growth when cells are grown in light/dark cycles (37-39).

An increasing body of evidence indicates that cellular redox homeostasis is of high importance for growth in light/dark cycles. A wide array of metabolic enzymes in cyanobacteria are redox modified, and light/dark cycles drive changes in the oxidation state of redox modified proteins (40). Activation of the OPPP, and the consequent production of NADPH, is vital for the ability of cyanobacteria to survive the dark.

1.5.2 Dark-induced changes in energy charge and cellular redox state

It has been well-established that different branches of metabolism are activated or repressed upon a shift to darkness. Whether the amount of energy and reducing power produced in the dark changes, however, is less clear, and reports from the last several

decades sometimes indicate conflicting results. Ihlenfeldt and Gibson (41) found that ATP levels fell precipitously within the first 2 minutes after a shift to darkness, but rose to pre-dark levels within 20 minutes. More recently, Takano et al. (42) measured similar results: ATP levels dropped quickly, but had recovered within 10 minutes. On the other hand, Rust et al. (26) observed that ATP levels continue to drop during an 8-hour dark pulse. The timepoints at which ATP was measured in these studies do vary, however. The studies that saw the momentary drop only followed ATP levels for 30-60 minutes after the shift to darkness, whereas the other study measured levels for 8 hours, with much lower sampling resolution.

There is greater consensus about the redox state of the cell in light and dark conditions. Though both photosynthesis and the OPPP produce NADPH, studies generally agree that NADPH levels drop in the dark (32, 41) since more reducing equivalents are produced during photosynthesis. Tamoi et al (32) also found that NAD(H) levels rise in the dark, leading to an overall decrease in the NADP(H) / NAD(H) ratio. These changes in redox state set in motion many regulatory responses, not only via CP12, but also through the action of thioredoxins on disulfide bond formation in a variety of central metabolic enzymes (43).

1.5.3 Transcriptional and translational regulation in the dark

Given that energy capacity is more limited when photosynthesis is not operational, it is perhaps not surprising that darkness triggers widespread changes in transcription and translation in *Synechococcus*. Rates of both processes generally decrease (42, 44, 45), but specific genes are induced upon a transition to darkness. Learning more about the identifies and functions of these genes may provide us with clues about how *Synechococcus* survives periods of darkness.

Several studies have conducted transcriptional profiling of *Synechococcus* upon a shift from light to dark (27, 42, 45, 46). The conditions of the light-to-dark shift in these studies were different, however. In Hosokawa et al. (45) and Takano et al. (42), cultures were synchronized and were shifted to the dark at the time consistent with circadian predictions (L12D). In Hood et al. (see Chapter 2; (46)), cultures were also synchronized, but were shifted into the dark at a time of unexpected darkness according to the circadian cycle (L7D).

Are the same genes upregulated by shifts to darkness at times of expected and unexpected darkness? Hosokawa et al. (45) found that expression of many dark-induced genes depends on a functional circadian oscillator, but some of these genes are also upregulated upon a shift to darkness in the middle of the day (46). Comparing the results of these two transcriptional studies as well as those reported by Takano et al. (42), expression of 56 genes is consistently induced in response to darkness. Many of these genes are of unknown function, and some are annotated simply as *dig* (for dark-induced gene, according to (45)). Better-annotated examples within this list include a protein with a high degree of sequence similarity to CP12, a redox-sensitive regulator

of Calvin cycle enzymes (32); *hpf* (*lrtA*), a regulator of ribosomal status (46); and heat shock protein A (*hspA*), a predicted chaperone.

A recent study by Rubin, Welkie, and Golden (47) has identified genes important for survival in light/dark cycles; comparing these data to the dark-induced genes above, nine genes are shared amongst all four datasets. These include genes encoding several components of a respiration-specific cytochrome c oxidase, a regulator of glutamine synthetase (*gifA*), a chaperone (*clpB*) previously implicated in temperature acclimation (48), and a predicted rRNA methyltransferase (*gidB*). These genes represent especially interesting and important candidates for further study, as we aim to understand the cyanobacterial response to darkness in more mechanistic detail.

Considering the specific transcriptional response to darkness, what happens to protein profiles of cells under these circumstances? The answer to this question is less clear. Proteomic studies have shown that the total quantity of a particular protein does not change significantly between light and dark – in Ansong et al. (40), only 4% of proteins changed in abundance. However, several studies have shown that translation rates decrease in the dark (15, 46), and that dark-synthesized proteins differ from those synthesized in the light (49). However, the identities of these dark-synthesized proteins are not yet known.

1.5.4 Light/dark changes in chromosome compaction (cellular organization)

Temporal regulation occurs in cyanobacteria through the activity of the circadian clock in concert with the metabolic state of the cell. What about spatial regulation? One of the best-described examples of spatial changes in cyanobacteria during light and dark is that of chromosome compaction. Several studies have shown that the extent of chromosome or plasmid compaction in *Synechococcus* changes depending on the time of day (28, 50-52). This phenomenon persists in constant light, but not constant darkness, and is thought to be circadian-regulated. Furthermore, when supercoiling is altered using an inhibitor of DNA gyrase, gene expression patterns change (28).

These studies provide insight into how gene expression might be controlled during circadian or diel cycles, but they are mostly correlative, relating DNA compaction or supercoiling with transcriptional outputs. The mechanistic details of how chromatin state and nucleoid organization are controlled – by the circadian oscillator, by histone-like DNA-binding proteins, and/or by changes in DNA topology – remain largely unknown.

1.5.5 An overview of a cyanobacterium in darkness

Though a cyanobacterium in darkness is typically viewed as being in a dormant state, the cell is not inactive – many processes still operate dynamically. Studies on transcription, translation, and metabolism (as described above) have demonstrated a specific, adaptive response to darkness in *Synechococcus*. While overall rates of these processes may be lower (or close to zero, as in the case of DNA replication (53, 54)),

they are coordinated in such a way that the cell can conserve energy, ensuring its survival until the light shines again.

1.6 Stress responses of *Synechococcus*

It is clear that a shift to darkness causes many changes to cyanobacterial metabolism and physiology. Other conditions – stressors such as nutrient starvation, temperature shifts, high light levels, and osmotic or oxidative stress – can cause analogous responses. Under these conditions, photosynthetic capacity – especially reductant production – can become imbalanced with other metabolic capacities within the cell, leading to accumulation of toxic ROS.

One of the best-studied nutrient starvation responses in *Synechococcus* is its adaptation to nitrogen deprivation. Preferential usage of more-reduced nitrogen sources, like ammonium, to less-reduced nitrogen sources, like nitrate, is largely controlled by a transcription factor called NtcA (55). This protein regulates genes of nitrogen metabolism and acclimation in a hierarchical manner, thereby tuning the severity of the response (56). Another protein involved in the nitrogen starvation response is P_{II}, a sensor of α-ketoglutarate levels (an intermediate in the TCA cycle that accumulates when nitrogen metabolism slows). This protein largely works at the level of controlling protein-protein interactions, and overlaps with NtcA in some aspects of nitrogen starvation adaptation (55). Glutamine synthetase, the key enzyme of nitrogen assimilation, is also heavily regulated in response to many environmental and metabolic factors (19).

On the cellular level, dramatic changes occur in response to nitrogen starvation. The typical intracellular organization of *Synechococcus* (described above in Section 1.2) changes dramatically within ~1 week after nitrogen deprivation – thylakoid membranes are no longer obvious, and many glycogen granules are visible (55). Mutants of *Synechococcus* that cannot synthesize glycogen during nitrogen starvation do not survive as well as wild-type, suggesting that this storage compound serves as an important sink of carbon and reducing power when nitrogen is unavailable (12, 18).

Responses of *Synechococcus* to phosphate, sulfur, and iron deprivation vary somewhat, but starvation for each nutrient provokes a response in which the cell tries to acquire more of the nutrient it lacks. This might include upregulating transporters or scavenging proteins for a particular element, and/or downregulating proteins or processes that require that nutrient. During many types of nutrient starvation, *Synechococcus* modifies its photosynthetic machinery to compensate for decreased activity in other aspects of cellular metabolism (in addition to storing excess energy as glycogen, when it can). This photosynthetic regulation will be discussed in greater detail in Chapter 3.

1.7 The stringent response is a conserved bacterial stress response pathway

As single-celled organisms, bacteria are susceptible to extreme fluctuations in nutrient availability. How do these organisms cope with such situations? Research into stress responses of bacteria goes back at least several decades, and a sizable body of literature exists on a widespread phenomenon called the stringent response.

Cashel and Gallant discovered in the late 1960s that when *Escherichia coli* encounters nutrient downshift (amino acid starvation), it makes two compounds, which they called "magic spot I" and "magic spot II" and identified as guanosine derivatives (57). It is now known that "magic spot I" is guanosine 3'-diphosphate 5'-diphosphate, or ppGpp, and "magic spot II" is guanosine 3'-diphosphate 5'-triphosphate, or pppGpp. Because the two nucleotides serve similar functions, we will refer to both as (p)ppGpp when appropriate. These nucleotides are synthesized by transfer of a pyrophosphoryl group from ATP onto the 3' end of either GTP (forming pppGpp) or GDP (forming ppGpp).

Since its initial discovery, microbiologists have grown to realize that the stringent response plays a fundamentally important role in controlling stress responses of diverse bacteria. The enzymes of the stringent response are conserved in nearly all bacteria, with some notable exceptions of obligate intracellular symbionts or pathogens (58). Homologs are also found in algal and plant chloroplasts (58, 59). The typical architecture of Rel proteins, so-named because mutants in these genes displayed a *relaxed* (as opposed to *stringent*) phenotype in response to stress, consists of four domains: (p)ppGpp hydrolase, (p)ppGpp synthetase, and regulatory ACT and TGS domains (60).

Aligning the Rel protein of *Synechococcus elongatus* PCC 7942 and those of several other cyanobacteria – *Synechocystis* sp. PCC 6803, *Synechococcus* sp. PCC 7002, and *Prochlorococcus marinus* MED4 – shows a high degree of similarity across Rels from cyanobacteria. All of these proteins are more similar to the bifunctional (p)ppGpp synthetases/hydrolases, Rel and SpoT, from *Streptococcus equisimilus* (whose structure was partially determined (61)) and *E. coli*, respectively, than with the (p)ppGpp synthetase RelA from *E. coli*.

Though the primary enzymes of (p)ppGpp metabolism may be generally conserved, the mechanisms by which these nucleotides induce cellular responses vary depending on the bacterium. *E. coli* has become the classic model organism for studying the stringent response, probably because it was both the first organism in which the pathway was described and because it has long been a workhorse of molecular biology, a 'typical' Gram-negative bacterium. As studies of the stringent response have expanded to many organisms other than *E. coli*, we have learned that how (p)ppGpp works within the cell at a molecular level varies, but the end result is similar: adjust cellular physiology in a way that helps restore and maintain homeostasis, even in the face of challenging environmental conditions.

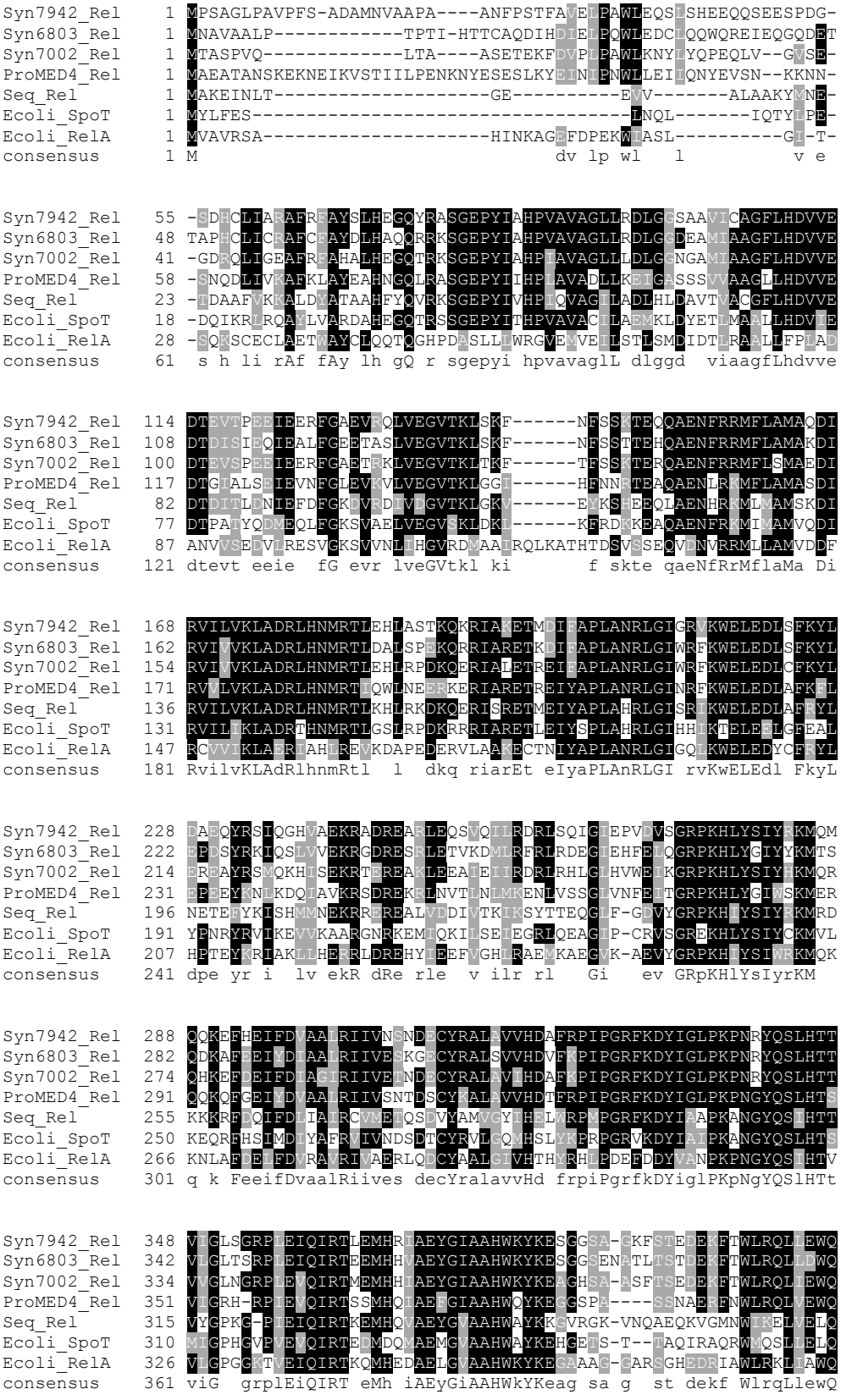
Syn7942_Rel
Syn6803_Rel
Syn7002_Rel
ProMED4_Rel
Seq_Rel
Ecoli_SpoT
Ecoli_RelA
consensus

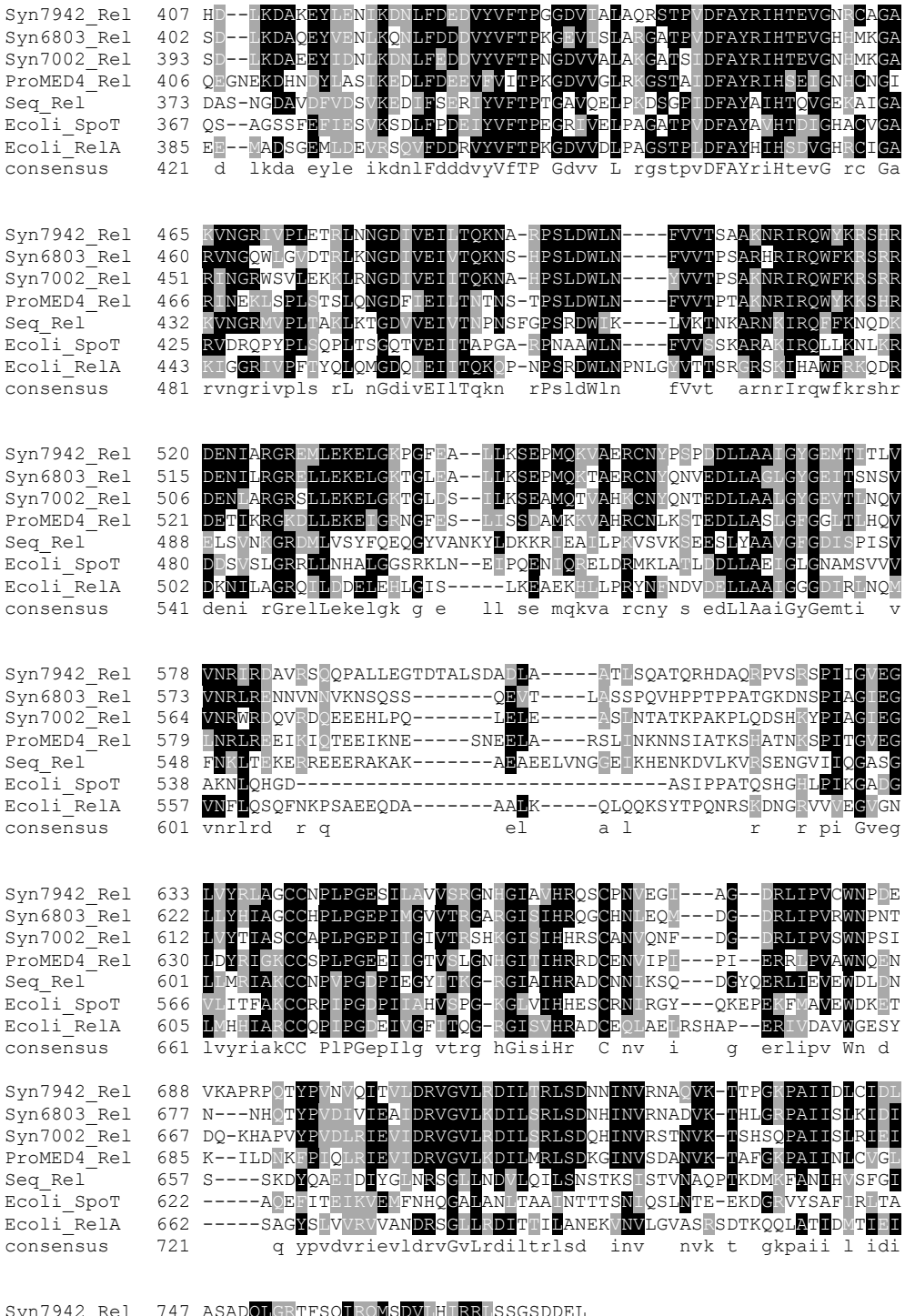
Syn7942_Rel 407 HD--LKDAKEYLENIKDNLFDEDVYVFTPGGDVIALAQRSTPVDFAYRIHTEVGNRCAGA
Syn6803_Rel 402 SD--LKDAQEYVENLKQNLFDDDVYVFTPKGHVLSLARGATPVDFAYRIHTEVGHRMKGA
Syn7002_Rel 393 SD--LKDAEEYIDNLKDNLFDDVYVFTPNGDVVALAKGATSLDFAYRIHTEVGNRMKGA
ProMED4_Rel 406 QEGNEKDHNDYLASIKEDLFDEEVEVLTPKGDVVGLRKGSTALDFAYRIHSEIGNRCNGI
Seq_Rel 373 DAS-NGDAVDFVDSVKEDTFSERIYVFTPTGAVQELPKDSGPIDFAYAIHTQVGEKAIGA
Ecoli_SpoT 367 QS--AGSSFEEFIESVKSDLFPDEIYVFTPEGRIVELPAGATPVDFAYAVHTDIGHACVGA
Ecoli_RelA 385 EE--MADSGEMLDEVRSQVFDDRVYVFTPKGDVVDLPAGSTPLDFAYHIHSDVGHRCIGA
consensus 421 d lkda eyle ikdnlFdddvyVfTP Gdvv L rgstpvDFAYriHtevG rc Ga
Syn7942_Rel 465 KVNGRIVPLETRLNNGDTVEIITQKNA-RPSLDWLN----FVVTSAAKNRIRQWVKRSHR
Syn6803_Rel 460 RVNGQWLGVDTRLKNGDTVEIVTQKNS-HPSLDWLN----FVVTPSARHRIRQWFKRSRR
Syn7002_Rel 451 RINGRWSVLEKKLRNGDTVEIITQKNA-HPSLDWLN----YVVTPSAKNRIRQWFKRSRR
ProMED4_Rel 466 RINEKLSPLSTSLQNGDFIEIITNTNS-TPSLDWLN----FVVTPTAKNRIRQWVKRSHR
Seq_Rel 432 KVNGRMVPLDARLKTGDVVEIVTNPNSFGPSRDWLK----LVKTNKARNKIRQFFKNQDK
Ecoli_SpoT 425 RVDRQPYPLSQPLTSGQTVEIITAPGA-RPNAAWLN----FVVSSKARAKIRQLLKNLKR
Ecoli_RelA 443 KIGGRIVPFIYQLQMGDQTEIITQKQP-NPSRDWLNPNLGYVTTSRGRSKIHAWFKRQDR
consensus 481 rvngrivpls rL nGdivEIlTqkn rPsldWln fVvt arnrIrqwfkrshr
Syn7942_Rel 520 DENIARGREMLEKELGKPGFEA--LLKSEPMQKVAERCNYPSPDDLLAAIGYGEMTITLV
Syn6803_Rel 515 DENILRGRELLEKELGKTGLEA--LLKSEPMQKTAERCNYQNVEDLLAGLGYGEITSNSV
Syn7002_Rel 506 DENLARGRSLLEKELGKTGLES--ILKSEAMQTVAHKCNYQNTEDLLAALGYGEVTTNQV
ProMED4_Rel 521 DETIKRGKDLLEKEIGRNGFES--LISSDAMKKVAHRCNLKSTEDLLASLGFGGITTHQV
Seq_Rel 488 ELSVNKGRDMLVSYFQEQGYVANKYLDKKRIEALLPKVSVKSEESLYAAVGIGDISPISV
Ecoli_SpoT 480 DDSVSLGRRLLNHALGGSRKLN--EIPQENIQFELDRMKLATLDDLLAEIGLGNAMSVVV
Ecoli_RelA 502 DKNILAGRQILDDELEHLGIS-----LKEAEKHILPRYNFNDVDELLAAIGGGDIRLNQM
consensus 541 deni rGrelLekelgk g e ll se mqkva rcny s edLlAaiGyGemti v
Syn7942_Rel 578 VNRIRDAVESQQPALLEGTDTALSDADLA-----ATLSQATQRHDAQRPVSRSPIIGVEG
Syn6803_Rel 573 VNRLRENNVNNVKNSQSS-------QEVT----LASSPQVHPPTPPATGKDNSPIAGIEG
Syn7002_Rel 564 VNRWRDQVEDQEEEHLPQ-------LELE-----ASLNTATKPAKPLQDSHKYPIAGIEG
ProMED4_Rel 579 LNRLREEIKIQTEEIKNE-----SNEELA----RSLINKNNSIATKSHATNKSPITGVEG
Seq_Rel 548 FNKLTEKERREEERAKAK-------AEAEELVNGGEIKHENKDVLKVRSENGVIIQCASG
Ecoli_SpoT 538 AKNLQHGD----------------------------ASIPPATQSHGHLPIKGADG
Ecoli_RelA 557 VNFLQSQFNKPSAEEQDA-------AALK-----QLQQKSYTPQNRSKDNGRVVVEGVGN
consensus 601 vnrlrd r q el a l r r pi Gveg
Syn7942_Rel 633 LVYRLAGCCNPLPGESILAVVSRGNHGIAVHRQSCPNVEGI---AG--DRLIPVCWNPDE
Syn6803_Rel 622 LLYHIAGCCHPLPGEPIMGVVTRGAGISIHRQGCHNLEQM---DG--DRLIPVRWNPNT
Syn7002_Rel 612 LVYTIASCCAPLPGEPIIGIVTRSHKGISIHHRSCANVQNF---DG--DRLIPVSWNPSI
ProMED4_Rel 630 LDYRIGKCCSPLPGEEIIGTVSLGNHGITIHRRDCENVIPI---PI--ERRLPVAWNQDN
Seq_Rel 601 LLMRIAKCCNPVPGDPIEGYITKG-RGIAIHRADCNNIKSQ---DGYQERLIEVEWDLDN
Ecoli_SpoT 566 VLITFAKCCRPIPGDPIIAHVSPG-KGLVIHHESCRNIRGY---QKEPEKFMAVEWDKET
Ecoli_RelA 605 LMHHIARCCQPIPGDEIVGFITQG-RGISVHRADCEQLAELRSHAP--ERIVDAVWGESY
consensus 661 lvyriakCC PlPGepIlg vtrg hGisiHr C nv i g erlipv Wn d
Syn7942_Rel 688 VKAPRPQTYPVNVQITVLDRVGVLRDILTRLSDNNINVRNAQVK-TTPGKPAIIDICIDL
Syn6803_Rel 677 N---NHQTYPVDIVIEAIDRVGVLKDILSRLSDNHINVRNADVK-THLGRPAIISLKIDI
Syn7002_Rel 667 DQ-KHAPVYPVDLRIEVIDRVGVLRDILSRLSDQHINVRSTNVK-TSHSQPAIISLRIDI
ProMED4_Rel 685 K--ILDNKTPHQLRIEVIDRVGVLKDILMRLSDKGINVSDANVK-TAFGKPAIINLCVGL
Seq_Rel 657 S----SKDYQAEIDIYGLNRSGLLNDVLQILSNSTKSISTVNAQPTKDMKFANIHVSFGI
Ecoli_SpoT 622 -----AQEGITEIKVEMFNHQGALANLTAALNTTTSNIQSLNTE-EKDGRVYSAFIRLTA
Ecoli_RelA 662 -----SAGYSLVVRVVANDRSGLLRDITTIISANEKVNVLGVASKSDTKQQLATIDVTIEI
consensus 721 q ypvdvrievldrvGvLrdiltrlsd inv nvk t gkpaii l idi
Syn7942_Rel 747 ASADQLGRTFSQIRQMSDVLHIRRLSSGSDDEL
Syn6803_Rel 733 HDYQQLLGIMAKIKNMSDVLDIRRVIS---G--
Syn7002_Rel 725 RNAQQLAHSLNQIKNMSDTLNVRRVTQIEQE--
ProMED4_Rel 742 ESYSQLHKTLDQIKSMADVLDIARVGIS-----
Seq_Rel 713 PNLTHLTTVVEKIKAVPDVYSVKRTNG------
Ecoli_SpoT 676 RDRVHLANIMRKIRVMPDVIKVTRNRN------
Ecoli_RelA 717 YNLQVLGRVLGKLNQVPDVIDARRLHGS-----
consensus 781 qLgrim kikqm Dvl irRl

Figure 1-3. Alignment of cyanobacterial Rel protein sequences with those of characterized stringent response enzymes from Firmicutes or Proteobacteria. Protein sequences were aligned using T-COFFEE, and amino acid conservation was determined and symbolized by shading using BoxShade. Abbreviations correspond to the following genes (with the corresponding species and locus tags indicated):
Syn7942_Rel: *Synechococcus elongatus* PCC 7942, Synpcc7942_1377
Syn6803_Rel: *Synechocystis* sp. PCC 6803, slr1325
Syn7002_Rel: *Synechococcus* sp. PCC 7002, SYNPCC7002_A2816
ProMED4_Rel: *Prochlorococcus marinus* sp. MED4, PMM0191
Seq_Rel: *Streptococcus equisimilus*, SDEG_0231
Ecoli_SpoT/RelA: *Escherichia coli* K-12 MG1655, SpoT: b3650 / RelA: b2784

Studies of the stringent response in *E. coli* and *Bacillus subtilis* have established paradigms for how the pathway operates in Proteobacteria and Firmicutes, respectively (though there are, of course, a number of differences within these phyla). In *E. coli*, (p)ppGpp binds to RNA polymerase and works alongside a transcription factor called DksA and alternative sigma factors to enact widespread changes in gene expression (60). In *B. subtilis*, (p)ppGpp affects transcription through an entirely different, more indirect mechanism. Intracellular levels of GTP drop in this organism for two reasons: (1) the (p)ppGpp synthesis reaction uses GTP as a substrate, and (2) (p)ppGpp inhibits GTP biosynthetic enzymes (62). In *B. subtilis,* low GTP levels activate the transcription factor CodY and lower expression of genes, including those encoding rRNA, for which GTP serves as the initiating nucleotide (63, 64). In both *E. coli* and *B. subtilis*, nutrient scavenging and/or specific biosynthetic processes (like amino acid biosynthesis) are upregulated, but this is brought about via distinct molecular mechanisms.

Studies of the stringent response have extended far beyond *E. coli* and *B. subtilis*, and the pathway has been explored in many pathogens, such as *Mycobacterium tuberculosis*, and in non-pathogens like *Myxococcus xanthus* and *Caulobacter crescentus* (65). Additionally, studies in *E. coli* have found that lower concentrations of (p)ppGpp can control growth rate and maintain cellular homeostasis, even when an organism is not experiencing acute stress (64, 66).

Because the stresses various bacteria encounter differ depending on the environment in which they live, the specifics of each organism's stringent response also differ. Learning more about the breadth of this stress response pathway – and how it has been adapted to a variety of bacterial lifestyles – can teach us a great deal about bacterial physiology and how they sense and respond to their environment.

1.8 Nucleotide signaling in cyanobacteria

Recent work in *Synechococcus* has mainly focused on photosynthesis, regulation of nitrogen metabolism, and circadian rhythm. A number of studies did investigate stress response pathways and other aspects of cyanobacterial physiology in the 1970s and 1980s, however. Many of these investigations described and characterized metabolic

phenomena and how these pathways were controlled, but did not – in many cases, were not able to – address the mechanisms behind their observations.

The labs of Carr, Smith, Farkas, Borbely, and others tested conditions under which (p)ppGpp levels increase in *Synechococcus* (which was then called *Anacystis*) in the 1970s and 1980s. Several groups reported increases in (p)ppGpp upon a shift from light to dark, and one group found that ppGpp also increased when cultures were treated with an inhibitor of photosynthesis (67-69). Other stresses found to induce (p)ppGpp synthesis were nitrogen starvation (either by nitrogen deprivation or treatment with an inhibitor of glutamine synthetase), treatment with a proton uncoupler (affecting ATP production via both photosynthesis and respiration), and temperature shifts (49, 69, 70). Though collectively these studies provide good evidence for a stringent response mechanism that can sense a variety of stresses, these studies never went further than this. They leave many open questions about whether (p)ppGpp affects downstream processes, and if so, how it changes *Synechococcus* physiology in response to these starvation signals.

Cyanobacteria are also known to produce a number of other signaling nucleotides, including cyclic AMP (cAMP), cyclic GMP (cGMP), cyclic-di-AMP (c-di-AMP), and cyclic-di-GMP (c-di-GMP). Accumulation of cAMP and c-di-GMP has been found to be light dependent in various cyanobacterial species (71). Rubin and colleagues have shown recently that *Synechococcus* makes c-di-AMP in response to darkness, and a mutant that cannot synthesize this nucleotide faces increased oxidative stress, which may be a cause of its decreased survival during dark periods (72).

1.9 Objective

Many of the initial studies that investigated the stringent response in cyanobacteria were conducted several decades ago, before genetic tools or genome sequences became available. I set out to characterize this pathway in *Synechococcus* and learn more about how it changes cellular physiology in response to diverse environmental stressors.

The following chapters will describe this research, which has shown that the stringent response does indeed help *Synechococcus* sense and respond to a variety of changes in its environment, including darkness, photosynthetic inhibition, and nitrogen starvation. Mutants that lack the ability to make (p)ppGpp in response to these stresses are impaired in their ability to survive, because they cannot activate responses that alter metabolism and physiology accordingly. This work helps expand our understanding of cyanobacterial physiology, and the strategies these remarkable organisms use to adapt to the challenges they face.

1.10 References

1. Stanier RY, van Niel CB (1962) The concept of a bacterium. *Archiv fur Mikrobiologie* 42:17–35.

2. Woese CR, Fox GE (1977) Phylogenetic structure of the prokaryotic domain: the primary kingdoms. *Proc Natl Acad Sci USA* 74(11):5088–5090.

3. Stanier RY (1977) The position of cyanobacteria in the world of phototrophs. *Carlsberg Res Commun* 42:77–98.

4. Sagan L (1967) On the origin of mitosing cells. *J Theoret Biol* 14:225–274.

5. Schwartz RM, Dayhoff MO (1978) Origins of prokaryotes, eukaryotes, mitochondria, and chloroplasts. *Science* 199(4327):395–403.

6. Flombaum P, et al. (2013) Present and future global distributions of the marine Cyanobacteria Prochlorococcus and Synechococcus. *Proc Natl Acad Sci USA* 110(24):9824–9829.

7. Rajeev L, et al. (2013) Dynamic cyanobacterial response to hydration and dehydration in a desert biological soil crust. *The ISME Journal* 7(11):2178–2191.

8. Field CB, Behrenfeld MJ, Randerson JT, Falkowski P (1998) Primary Production of the Biosphere: Integrating Terrestrial and Oceanic Components. *Science* 281:237–240.

9. Golden SS, Vann C, Sherman LA (1984) Cloning of photosynthesis genes from the cyanobacterium Anacystis nidulans R2. *Advances in Photosynthesis Research*:1–4.

10. Nevo R, et al. (2007) Thylakoid membrane perforations and connectivity enable intracellular traffic in cyanobacteria. *EMBO J* 26:1467–1473.

11. Allen MM (1984) Cyanobacterial cell inclusions. *Annu Rev Microbiol* 38:1–25.

12. Latifi A, Ruiz M, Zhang C-C (2009) Oxidative stress in cyanobacteria. *FEMS Microbiol Rev* 33(2):258–278.

13. Diamond S, Jun D, Rubin BE, Golden SS (2015) The circadian oscillator in Synechococcus elongatus controls metabolite partitioning during diurnal growth. *Proc Natl Acad Sci USA* 112:E1916–E1925.

14. Mori T, Binder B, Johnson CH (1996) Circadian gating of cell division in cyanobacteria growing with average doubling times of less than 24 hours. *Proc Natl Acad Sci USA* 93:10183–10188.

15. Singer RA, Doolittle WF (1975) Control of gene expression in blue-green algae. *Nature* 253:650–651.

16. Hanai M, et al. (2014) The Effects of Dark Incubation on Cellular Metabolism of the Wild Type Cyanobacterium Synechocystis sp. PCC 6803 and a Mutant Lacking the Transcriptional Regulator cyAbrB2. *Life* 4(4):770–787.

17. Hickman JW, et al. (2013) Glycogen synthesis is a required component of the nitrogen stress response in Synechococcus elongatus PCC 7942. *Algal Research* 2(2):98–106.

18. Work VH, et al. (2015) Lauric Acid Production in a Glycogen-Less Strain of Synechococcus sp. PCC 7002. *Front Bioeng Biotechnol* 3:48.

19. Luque I, Forchhammer K (2008) Nitrogen assimilation and C/N balance sensing. *The Cyanobacteria: Molecular Biology, Genomics and Evolution*, eds Herrero A, Flores E (Caister Academic Press, Norfolk, UK), pp 335–382.

20. Woelfle MA, Ouyang Y, Phanvijhitsiri K, Johnson CH (2004) The Adaptive Value of Circadian Clocks: An Experimental Assessment in Cyanobacteria. *Current Biology* 14(16):1481–1486.

21. Grobbelaar N, Huang TC, Lin HY, Chow TJ (1986) Dinitrogen-fixing endogenous rhythm in Synechococcus RF-1. *FEMS Microbiol Lett* 37:173–177.

22. Shultzaberger RK, Boyd JS, Diamond S, Greenspan RJ, Golden SS (2015) Giving Time Purpose: The Synechococcus elongatus Clock in a Broader Network Context. *Annu Rev Genet* 49:485–505.

23. Kondo T, et al. (1994) Circadian clock mutants of cyanobacteria. *Science*:1–4.

24. Cohen SE, Golden SS (2015) Circadian Rhythms in Cyanobacteria. *Microbiol Mol Biol Rev* 79(4):373–385.

25. Nakajima M, et al. (2005) Reconstitution of circadian oscillation of cyanobacterial KaiC phosphorylation in vitro. *Science* 308(5720):414–415.

26. Rust MJ, Golden SS, O'Shea EK (2011) Light-Driven Changes in Energy Metabolism Directly Entrain the Cyanobacterial Circadian Oscillator. *Science* 331(6014):220–223.

27. Ito H, et al. (2009) Cyanobacterial daily life with Kai-based circadian and diurnal genome-wide transcriptional control in Synechococcus elongatus. *Proc Natl Acad Sci USA* 106:14168–14173.

28. Vijayan V, Zuzow R, O'Shea EK (2009) Oscillations in supercoiling drive circadian gene expression in cyanobacteria. *Proc Natl Acad Sci USA* 106:22564–22568.

29. Takai N, et al. (2006) A KaiC-associating SasA-RpaA two-component regulatory system as a major circadian timing mediator in cyanobacteria. *Proc Natl Acad Sci USA* 103(32):12109–12114.

30. Markson JS, Piechura JR, Puszynska AM, O'Shea EK (2013) Circadian Control of Global Gene Expression by the Cyanobacterial Master Regulator RpaA. *Cell* 155(6):1396–1408.

31. Diamond S, et al. (2017) Redox crisis underlies conditional light-dark lethality in cyanobacterial mutants that lack the circadian regulator, RpaA. *Proc Natl Acad Sci USA* 114:E580–E589.

32. Tamoi M, Miyazaki T, Fukamizo T, Shigeoka S (2005) The Calvin cycle in cyanobacteria is regulated by CP12 via the NAD(H)/NADP(H) ratio under light/dark conditions. *Plant J* 42(4):504–513.

33. Matsumura H, et al. (2011) Structure Basis for the Regulation of Glyceraldehyde-3-Phosphate Dehydrogenase Activity via the Intrinsically Disordered Protein CP12. *Structure* 19(12):1846–1854.

34. Lehmann M, Wober G (1976) Accumulation, mobilization and turn-over of glycogen in the blue-green bacterium Anacystis nidulans. *Arch Microbiol*:93–97.

35. Osanai T, Azuma M, Tanaka K (2007) Sugar catabolism regulated by light- and nitrogen-status in the cyanobacterium Synechocystis sp. PCC 6803. *Photochem Photobiol Sci* 6(5):508–514.

36. Gründel M, Scheunemann R, Lockau W, Zilliges Y (2012) Impaired glycogen synthesis causes metabolic overflow reactions and affects stress responses in the cyanobacterium Synechocystis sp. PCC 6803. *Microbiology* 158:3032–3043.

37. Scanlan DJ, Sundaram S, Newman J, Mann NH, Carr NG (1995) Characterization of a zwf mutant of Synechococcus sp. strain PCC 7942. *J Bacteriol* 177(9):2550–2553.

38. Broedel SE, Wolf RE (1990) Genetic tagging, cloning, and DNA sequence of the Synechococcus sp. strain PCC 7942 gene (gnd) encoding 6-phosphogluconate dehydrogenase. *J Bacteriol* 172(7):4023–4031.

39. Doolittle WF, Singer RA (1974) Mutational analysis of dark endogenous metabolism in the blue-green bacterium Anacystis nidulans. *J Bacteriol* 119(3):677–683.

40. Ansong C, et al. (2014) Characterization of protein redox dynamics induced during light-to-dark transitions and nutrient limitation in cyanobacteria. *Front Microbiol* 5:325.

41. Ihlenfeldt MJA, Gibson J (1975) CO2 fixation and its regulation in Anacystis nidulans (Synechococcus). *Arch Microbiol* 102:13–21.

42. Takano S, Tomita J, Sonoike K, Iwasaki H (2015) The initiation of nocturnal dormancy in Synechococcus as an active process. *BMC Biol* 13(1):36.

43. Lindahl M, Florencio FJ (2003) Thioredoxin-linked processes in cyanobacteria are as numerous as in chloroplasts, but targets are different. *Proc Natl Acad Sci USA* 100(26):16107–16112.

44. Doolittle WF (1979) The cyanobacterial genome, its expression, and the control of that expression. *Adv Microb Physiol* 20:1–102.

45. Hosokawa N, et al. (2011) Circadian transcriptional regulation by the posttranslational oscillator without de novo clock gene expression in Synechococcus. *Proc Natl Acad Sci USA* 108:15396–15401.

46. Hood RD, Higgins SA, Flamholz A, Nichols RJ, Savage DF (2016) The stringent response regulates adaptation to darkness in the cyanobacterium Synechococcus elongatus. *Proc Natl Acad Sci USA* 113(33):E4867–E4876.

47. Rubin BE, Welkie DG, Golden SS, personal communication.

48. Eriksson MJ, Clarke AK (1996) The heat shock protein ClpB mediates the development of thermotolerance in the cyanobacterium Synechococcus sp. strain PCC 7942. *J Bacteriol* 178(16):4839–4846.

49. Suranyi G, Korcz A, Palfi Z, Borbely G (1987) Effects of light deprivation on RNA synthesis, accumulation of guanosine 3'(2‘)-diphosphate 5’-diphosphate, and protein synthesis in heat-shocked Synechococcus sp. strain PCC 6301, a cyanobacterium. *J Bacteriol* 169:632–639.

50. Smith RM, Williams SB (2006) Circadian rhythms in gene transcription imparted by chromosome compaction in the cyanobacterium Synechococcus elongatus. *Proc Natl Acad Sci USA* 103(22):8564–8569.

51. Woelfle MA, Xu Y, Qin X, Johnson CH (2007) Circadian rhythms of superhelical status of DNA in cyanobacteria. *Proc Natl Acad Sci USA* 104(47):18819–18824.

52. Murata K, Hagiwara S, Kimori Y, Kaneko Y (2016) Ultrastructure of compacted DNA in cyanobacteria by high-voltage cryo-electron tomography. *Sci Rep* 6:34934.

53. Watanabe S, et al. (2012) Light-dependent and asynchronous replication of cyanobacterial multi-copy chromosomes. *Mol Microbiol* 83(4):856–865.

54. Ohbayashi R, et al. (2013) DNA replication depends on photosynthetic electron transport in cyanobacteria. *FEMS Microbiol Lett* 344:138–144.

55. Schwarz R, Forchhammer K (2005) Acclimation of unicellular cyanobacteria to macronutrient deficiency: emergence of a complex network of cellular responses. *Microbiology* 151:2503–2514.

56. Luque I, Flores E, Herrero A (1994) Molecular mechanism for the operation of nitrogen control in cyanobacteria. *EMBO J* 13(12):2862–2869.

57. Cashel M, Gallant J (1969) Two compounds implicated in the function of the RC gene of Escherichia coli. *Nature* 221:838–841.

58. Atkinson GC, Tenson T, Hauryliuk V (2011) The RelA/SpoT Homolog (RSH) Superfamily: Distribution and Functional Evolution of ppGpp Synthetases and Hydrolases across the Tree of Life. *PLoS ONE* 6(8):e23479.

59. Ito D, Ihara Y, Nishihara H, Masuda S (2017) Phylogenetic analysis of proteins involved in the stringent response in plant cells. *J Plant Res*. doi:10.1007/s10265-017-0922-8.

60. Potrykus K, Cashel M (2008) (p)ppGpp: still magical? *Annu Rev Microbiol* 62:35–51.

61. Hogg T, Mechold U, Malke H, Cashel M, Hilgenfeld R (2004) Conformational Antagonism between Opposing Active Sites in a Bifunctional RelA/SpoT Homolog Modulates (p)ppGpp Metabolism during the Stringent Response. *Cell* 117:57–68.

62. Kriel A, et al. (2012) Direct regulation of GTP homeostasis by (p)ppGpp: a critical component of viability and stress resistance. *Mol Cell* 48(2):231–241.

63. Krásný L, Gourse RL (2004) An alternative strategy for bacterial ribosome synthesis: Bacillus subtilis rRNA transcription regulation. *EMBO J* 23(22):4473–4483.

64. Gaca AO, Colomer-Winter C, Lemos JA (2015) Many means to a common end: the intricacies of (p)ppGpp metabolism and its control of bacterial homeostasis. *J Bacteriol* 197(7):1146–1156.

65. Boutte CC, Crosson S (2013) Bacterial lifestyle shapes stringent response activation. *Trends Microbiol* 21(4):174–180.

66. Traxler MF, et al. (2011) Discretely calibrated regulatory loops controlled by ppGpp partition gene induction across the “feast to famine” gradient in Escherichia coli. *Mol Microbiol* 79(4):830–845.

67. Mann N, Carr NG, Midgley J (1975) RNA synthesis and the accumulation of guanine nucleotides during growth down shift in the blue-green alga Anacystis nidulans. *Biochim Biophys Acta* 402:41–50.

68. Smith RJ (1977) The regulation of stable RNA synthesis in the blue-green alga Anacystis nidulans, the effect of DCMU inhibition. *FEMS Microbiol Lett* 1:129–132.

69. Borbely G, Kaki C, Gulyás A, Farkas GL (1980) Bacteriophage infection interferes with guanosine 3“-diphosphate-5-”diphosphate accumulation induced by energy and nitrogen starvation in the cyanobacterium Anacystis nidulans. *J Bacteriol* 144(3):859–864.

70. Friga GM, Borbely G, Farkas GL (1981) Accumulation of guanosine tetraphosphate (ppGpp) under nitrogen starvation in Anacystis nidulans, a cyanobacterium. *Arch Microbiol* 129:341–343.

71. Agostoni M, Montgomery B (2014) Survival Strategies in the Aquatic and Terrestrial World: The Impact of Second Messengers on Cyanobacterial Processes. *Life* 4(4):745–769.

72. Rubin BE, Golden SS, personal communication.

Chapter 2

The stringent response regulates adaptation to darkness in the cyanobacterium *Synechococcus elongatus*

Adapted from *Proceedings of the National Academy of Sciences of the United States of America*, Volume 113, Hood RD, Higgins SA, Flamholz A, Nichols RJ, and DF Savage, The stringent response regulates adaptation to darkness in the cyanobacterium *Synechococcus elongatus*, Pages E4867-76, Copyright 2016, with permission from *PNAS*.

Abstract

The cyanobacterium *Synechococcus elongatus* relies upon photosynthesis to drive metabolism and growth. During darkness, *Synechococcus* stops growing, derives energy from its glycogen stores, and greatly decreases rates of macromolecular synthesis via unknown mechanisms. Here, we show that the stringent response, a stress response pathway whose genes are conserved across bacteria and plant plastids, contributes to this dark adaptation. Levels of the stringent response alarmone ppGpp rise after a shift from light to dark, indicating that darkness in cyanobacteria triggers the same response as starvation in heterotrophic bacteria. High levels of ppGpp are sufficient to stop growth and dramatically alter many aspects of cellular physiology including levels of photosynthetic pigments and polyphosphate, DNA content, and the rate of translation. Cells unable to synthesize ppGpp display pronounced growth defects after exposure to darkness. The stringent response regulates expression of a number of genes in *Synechococcus*, including ribosomal hibernation promoting factor (*hpf*), which causes ribosomes to dimerize in the dark and may contribute to decreased translation. Although the metabolism of *Synechococcus* differentiates it from other model bacterial systems, the logic of the stringent response remains remarkably conserved, while at the same time having adapted to the unique stresses of the photosynthetic lifestyle.

Significance Statement

Cyanobacteria are an important group of photosynthetic bacteria that rely upon light energy for growth but frequently must adapt to darkness. Cells stop growing and decrease overall rates of gene expression and protein synthesis in the dark, but the molecular mechanisms behind these observations remain unknown. We find that a widespread bacterial stress response, the stringent response, helps cells conserve resources during darkness. In the dark, cells produce higher levels of the stringent response signaling molecule ppGpp, which alter gene expression patterns and affect the protein synthesis machinery. These results help explain previous observations in the cyanobacterial literature and extend our knowledge of how the same signaling pathway has been adapted to different bacterial lifestyles and metabolisms.

2.1 Introduction

The conversion of solar light energy to chemical energy through photosynthesis ultimately supports the majority of life on Earth. Light harvesting by photosynthetic antenna complexes and photosystems is directly tied to light availability, which can fluctuate greatly over the course of a single day (1). The growth and reproduction of photosynthetic organisms therefore depends upon their ability to capture light efficiently, and they have evolved several mechanisms that allow them to adapt to changing light conditions (2).

Cyanobacteria comprise a diverse bacterial phylum that oxygenated the atmosphere, gave rise to the plant chloroplast, and perform 10-25% of global photosynthesis today. *Synechococcus elongatus* PCC 7942 (hereafter, *Synechococcus*) is a model cyanobacterium that relies exclusively upon photosynthesis and carbon assimilation to grow. Its obligate photoautotrophic lifestyle makes *Synechococcus* a useful system in which to investigate the coordination and regulation of these inherently essential metabolic processes.

Cyanobacteria frequently encounter transitions between light and dark in their environment, and these transitions fall into two distinct categories. One is due to the rising and setting of the sun, which yields predictable transitions from light to dark and back to light again. *Synechococcus* has a circadian rhythm that anticipates the timing of dawn and dusk and regulates the expression of a majority of its genes in a time-dependent manner (3, 4). The second type of light/dark transition is unpredictable, and can occur due to transient cloud cover or shade cast by other organisms or geological features, for example. These transitions cannot be anticipated, and may require a rapid restructuring of metabolism. Studies of circadian rhythm in *Synechococcus* have provided insight into regulatory strategies that persist in constant light, but few studies have addressed the mechanisms by which cells adapt to darkness, predictable or otherwise.

Nearly all aspects of cyanobacterial physiology are affected by a shift from light to dark; cells stop elongating and dividing, cease DNA replication, and exhibit decreased rates of transcription and translation (5-7). Proteins produced in the dark differ from those produced in the light (8), and recent studies have identified genes that are differentially expressed between light and dark (9, 10). How the cell coordinates these transcriptional and translational changes remains largely unknown.

Not only does *Synechococcus* physiology change a great deal between light and dark, but its metabolism also shifts dramatically. Photosynthetically active cells reduce carbon dioxide into carbohydrates, which they accumulate as glycogen. When light is no longer available, cells catabolize their glycogen stores through respiration. Metabolism must be tightly controlled in the dark, as total energy supply is finite and must be rationed (5). This raises the question of whether dark periods are analogous to starvation for *Synechococcus* and whether bacterial stress response mechanisms mediate adaptation to darkness.

Here, we show that the stringent response – a stress response pathway whose enzymes are conserved in nearly all bacteria as well as plant plastids – is involved in dark adaptation in *Synechococcus*. We find that this pathway is active in *Synechococcus*, and that it exerts dramatic effects on cellular physiology. Furthermore, this response is required for cells to adapt properly to darkness, as cells lacking the stringent response display pronounced growth defects in diurnal light/dark cycles and loss of viability after prolonged exposure to darkness. We investigate which genes are regulated by the stringent response in *Synechococcus*, and find that one of them, ribosomal hibernation promoting factor, causes ribosomes to dimerize in the dark. Altogether, these results suggest that the stringent response mediates a coordinated transcriptional and translational reaction to periods of darkness.

2.2 Materials and Methods

2.2.1 Bacterial strains and culture conditions

Synechococcus elongatus PCC 7942 was grown in BG-11 media (11) at 30°C with shaking (185 rpm) under white fluorescent lights at 60-100 µE. Cultures grown in diurnal (12 hour light/12 hour dark) cycles were incubated in a programmable photosynthetic incubator (Percival Scientific, Perry, IA); otherwise, cultures grown in constant light were incubated in an environmental (30°C) room. All processing of samples under dark conditions was performed in a dark room with a minimal amount of light provided by a green LED. Unless otherwise indicated, *Synechococcus* cultures were induced with 50 µM isopropyl β-D-1-thiogalactopyranoside (IPTG) when appropriate. Single antibiotics (chloramphenicol, kanamycin) were used at 10 µg/ml, and double antibiotics at 2 µg/ml each. *Escherichia coli* was grown in LB media at 37°C with shaking (250 rpm), unless otherwise noted. When appropriate, chloramphenicol was used at 25 µg/ml, and kanamycin at 60 µg/ml for *E. coli*. Measurements of culture optical density (OD_{600} or OD_{750}, subscript indicating wavelength in nm) were performed using a Thermo Scientific Genesys 20 spectrophotometer (Waltham, MA).

2.2.2 Plasmid and strain construction

All plasmids were constructed using a Golden Gate cloning strategy (12) and were propagated in *E. coli* DH5α. Primers were designed to amplify genes such that a BsaI restriction enzyme site would be added onto both ends, and overhangs generated by digestion with BsaI would be complementary to those present in Golden Gate destination plasmids. Golden Gate reactions (incorporating cycles of restriction enzyme digestion and ligation) were incubated for 50 cycles of 45°C for 5 min and 16°C for 2 min, followed by incubations at 50°C for 10 min and 80°C for 10 min to inactivate the enzymes. Standard methods were used for PCR, gel purification of PCR products, *E. coli* transformation, and DNA sequencing to verify cloned constructs. Table 2-1 lists the plasmids and primers used in this study.

Synechococcus was transformed by growing cultures to log phase (OD_{750} 0.2-0.6), harvesting cells by centrifugation (16000 g, 2 min, 25°C), washing cells once in 0.5X volume of 10 mM NaCl, and resuspending cells in 0.1X volume of BG-11 media. Approximately 200 ng of the plasmid to be transformed was added, and cultures were wrapped in foil and incubated overnight at 30°C. The next day, transformations were plated on BG-11 plates containing the appropriate selective antibiotic. All deletion strains were verified by colony PCR, using primers to detect both the native locus and the deletion construct, and were fully penetrant. Table 2-2 lists and describes the strains used in this study.

Table 2-1. Plasmids and primers used in Chapter 2.

plasmid name	**reference**
pNS2 (Kan^R)	Clerico, EM, Ditty, JL, and SS Golden (2007) Methods Mol Biol 362: 115-129
pNS2-BSU11600	this study
pNS2-BSU11600_D72G	this study
pNS2-Synpcc7942_1377	this study
pNS3 (Cm^R)	Clerico, EM, Ditty, JL, and SS Golden (2007) Methods Mol Biol 362: 115-129
pUC-ΔSynpcc7942_1377(rel)-Cm^R	this study
pUC-ΔSynpcc7942_2352(hpf)-Kan^R	this study
primer name	**primer sequence**
for plasmid construction	
BSU11600-F-BsaI-GG	CACACCA GGTCTC A GTCC GATGACAAACAATGGGAGCG
BSU11600-R-stop-BsaI-GG	CACACCA GGTCTC A CGCT CTATTGTTGCTCGCTTCCTT
BSU11600-D72G-F-GG	CACACCA GGTCTC A GGTA TTGCTGGCCTTAGAATCATG
BSU11600-D72G-R-GG	CACACCA GGTCTC A TACC CTGCATGGTTTCAATTTCATGC
Synpcc7942_1377-F-BsaI-GG	CACACCA GGTCTC A GTCC ccgtcagccggtttgccg
Synpcc7942_1377-R-stop-BsaI-GG	CACACCA GGTCTC A CGCT tcacagctcatcatcgctgccg
rel-KO-up-F-BsaI-GG	CACACCA GGTCTC A CGCT ctggtcagcaagacttccagca
rel-KO-up-R-BsaI-GG	CACACCA GGTCTC A TACT cgaacgtgcgatcgctcc
rel-KO-down-F-BsaI-GG	CACACCA GGTCTC A TAGC tcactcagctatccaactgatg
rel-KO-down-R-BsaI-GG	CACACCA GGTCTC A GTCC ctggatctgaatccacacgatc
Cm^R-F-BsaI-GG	CACACCA GGTCTC A AGTA cactggagcacctcaa
Cm^R-R-BsaI-GG	CACACCA GGTCTC A GCTA ctgccaccgctgagc
hpf-KO-up-F-BsaI-GG	CACACCA GGTCTC A CGCT gctaacgaactgctgatactgg
hpf-KO-up-R-BsaI-GG	CACACCA GGTCTC A TACT aaatcgcctcccagacaag
hpf-KO-down1-F-BsaI-GG	CACACCA GGTCTC A TAGC tctcaacttgatcaacccttttctcac
hpf-KO-down1-R-BsaI-GG	CACACCA GGTCTC A acga ccaccattggcctgcg
hpf-KO-down2-F-BsaI-GG	CACACCA GGTCTC A tcgt ctctcggaagaggatggtttcg
hpf-KO-down2-R-BsaI-GG	CACACCA GGTCTC A GTCC cgcagaagcagcagttcatgg
Kan^R-F-BsaI-GG	CACACCA GGTCTC A AGTA agcttagatcgacctgcag
Kan^R-R-BsaI-GG	CACACCA GGTCTC A GCTA gcgctgaggtctgcctcg
for qPCR	
Syn7942_2352-qPCR-F (hpf)	CCTTGGCACAGCTACAACTAG
Syn7942_2352-qPCR-R (hpf)	CCTTCTCTGAGTTGCCTTCG
Syn7942_0900-qPCR-F (gifA)	TCGCGTGAACTGGTGATG
Syn7942_0900-qPCR-R (gifA)	TGAATGGTGCCGTTGTAGTG
Syn7942_1475-qPCR-F (sbtA)	TCATCGGGTCAAAATCTGGC
Syn7942_1475-qPCR-R (sbtA)	CCTTCGTAGACACTTTCTGGAC
Syn7942_2259-qPCR-F (rimM)	ATCTCTACATCGTGCAACTGG
Syn7942_2259-qPCR-R (rimM)	AAGACGTGAAATTCTCCCTCG
Syn7942_1615-qPCR-F (rnpA)	CTTCCCAGCACTGTATCGAG
Syn7942_1615-qPCR-R (rnpA)	CGCTTGTGAACTTTGAGACTG
Syn7942_0289-qPCR-F (secA)	CGAACGCTACTTCATCCTTCAG
Syn7942_0289-qPCR-R (secA)	AGCCCTCACTCTTATACTCCAG
Syn7942_16SrRNA-qPCR-F	TGGAAACGACTGCTAATACCC
Syn7942_16SrRNA-qPCR-R	TCATCCTCTCAGACCAGCTAC
Syn7942_pre-16SrRNA-qPCR-F	TGGGTTCGGGAAAACTTACG
Syn7942_pre-16SrRNA-qPCR-R	CGTTCGACTTGCATGTGTTAAG

Table 2-2. List of strains used in Chapter 2.

Strain name	Strain genotype	Resistance	Reference
Synechococcus elongatus PCC 7942 wild-type (WT)	WT	–	–
control (WT-Kan^R)	pNS2	Kan	this study
control (WT-Cm^R)	pNS3	Cm	this study
control (WT-Cm^R/Kan^R)	pNS2 + pNS3	Cm, Kan	this study
ppGpp$^+$	pNS2-BSU11600	Kan	this study
ppGpp$^+$ D72G	pNS2-BSU11600_D72G	Kan	this study
Δ*rel*	ΔSynpcc7942_1377-Cm^R	Cm	this study
Δ*rel* (Cm^R/Kan^R)	ΔSynpcc7942_1377-Cm^R +pNS2	Cm, Kan	this study
Δ*rel* + *rel*	ΔSynpcc7942_1377-Cm^R + pNS2-Synpcc7942_1377	Cm, Kan	this study
Δ*hpf*	ΔSynpcc7942_2352-Kan^R	Kan	this study
Escherichia coli W3110 wild-type (CF1943)	WT	–	Michael Cashel (NIH)
E. coli W3110 *relA251::Kan* (CF1944)	*relA::Kan*	Kan	Michael Cashel (NIH)

2.2.3 ppGpp measurements by HPLC and estimation of intracellular concentrations

Synechococcus cultures grown under the conditions specified in the text were harvested by filtration. For the light/dark shift experiment shown in Figure 2-1A, a wild-type culture was grown to log phase (OD_{750} ~0.25), split into seven flasks with 57 ml each (corresponding to ~13 OD_{750} units), and each culture was harvested at the appropriate timepoint. For the experiment shown in Figure 2-1B, cultures of the appropriate strains were grown to log phase (OD_{750} ~0.4), and strains in the light (control and ppGpp$^+$) were induced with IPTG for 17 hours before harvesting 20 OD_{750} units per culture.

Cells were isolated by filtration, resuspended and lysed in 400 µl 13 M formic acid, subsequently flash-frozen in liquid nitrogen, and stored at -80°C until further processing. Lysates were thawed at room temperature, subjected to three freeze/thaw cycles alternating between a dry ice/ethanol bath and room temperature, and were clarified by centrifugation (16000 g, 5 min, 4° C). Extracts were filtered using PES syringe filters, and were flash-frozen in liquid nitrogen and stored at -80°C until HPLC analysis.

Levels of ppGpp were measured using anion-exchange chromatography and a Phenomenex Luna NH_2 column, 50 x 4.60 mm (Torrance, CA). Using a protocol modified from (13), an isocratic method was developed to isolate the ppGpp peak on an Agilent Technologies 1200 series HPLC. The buffer consisted of 0.85 M ammonium phosphate, pH 2.1. Samples were thawed on ice before transfer to a pre-chilled HPLC vial; all samples were kept on ice until just prior to injection. 25 µl was injected at time zero and the method was run at 1 ml/min for 8-10 minutes. The column temperature was maintained at 30°C, and absorbance was monitored at 254 nm. A small ppGpp peak was found to elute at approximately 3.5 minutes. Concentrations were estimated

by manually integrating peaks using Agilent Chemstation software and comparing with a ppGpp standard added to the sample. The ppGpp standard was obtained from TriLink Biotechnologies (San Diego, CA). Using this method, the limit of detection for ppGpp was ~1 μM. We did not measure pppGpp by HPLC, as we were unable to resolve any candidate peaks eluting after ppGpp.

To estimate intracellular ppGpp concentrations, we used the following equation:

$$[\text{ppGpp}](\text{M}) = \frac{(\text{mAU} \cdot \text{sec})(\frac{\text{moles}}{\text{mAU} \cdot \text{sec}} \quad \text{conversion})(\text{fraction of total lysate measured})(\text{efficiency of ppGpp extraction})}{(\text{number of cells})(\text{estimated cell volume (L)})}$$

- mAU*sec : value determined for each sample by integrating ppGpp peaks from HPLC traces
- moles/mAU*sec conversion: determined by running a standard curve with known molar amounts of the ppGpp standard vs. measured mAU*sec and taking the slope of a linear regression (R^2 = 0.998) (value = 2.4 x 10^{-12} moles/mAU*sec).
- fraction of total lysate measured: 25 μl was analyzed by HPLC from an original volume of 400 μl (value = 16)
- efficiency of ppGpp extraction: determined by spiking a known amount of ppGpp into the 400 μl of formic acid used to lyse cells and measuring how much was recovered compared to that measured after spiking in ppGpp at the end of the extract preparation (~37% efficiency; value = 2.69)
- number of cells: determined by plating dilutions from cultures harvested for ppGpp extraction and averaging the number of colony forming units across replicates (value = 4.69 x 10^9 cells)
- estimated cell volume: determined by analyzing microscopy images of wild-type *Synechococcus* using MicrobeTracker software (14) and converting pixels^3 into μm^3 into L (value = 3 fL = 3 x 10^{-15} L)

2.2.4 ppGpp measurements by ^{32}P-TLC

Synechococcus strains were grown in low-phosphate BG-11 media (as in (11), except containing 44 μM rather than 175 μM K_2HPO_4) to log phase (OD_{750} ~0.5). *E. coli* strains were grown in low-phosphate minimal media (50 mM KCl, 10 mM NH_4Cl, 0.5 mM $MgSO_4$, 0.2 mM KH_2PO_4, 50 mM HEPES pH 7.5, 100 μM $FeCl_3$, 0.4% glucose, 0.2% casamino acids) at 30°C to mid-log phase (OD_{600} ~0.5). $H_3{}^{32}PO_4$ (Perkin Elmer, Waltham, MA) was added to the appropriate low-phosphate medium at 20 μCi/ml along with 50 μM IPTG for *Synechococcus* cultures where appropriate, and cell pellets (normalized to 0.5 OD units) were resuspended in low-phosphate media containing $H_3{}^{32}PO_4$. Cultures were incubated without shaking in a 30°C incubator for at least 1 generation time (30 minutes for *E. coli*; 27 hours for *Synechococcus*) to allow for ^{32}P uptake and incorporation. *E. coli* cultures were treated with serine hydroxamate (Sigma-Aldrich, Saint Louis, MO) at 1 mg/ml to mimic amino acid starvation for 10 minutes before harvesting.

Cells were harvested and excess $H_3{}^{32}PO_4$ was removed by centrifugation (10000 g, 2 min, 25°C), and pellets were resuspended in the appropriate ^{32}P -free low-phosphate medium. An equal volume of 13 M formic acid was added to cell suspensions, which

were then subjected to three freeze-thaw cycles alternating between a dry ice/ethanol bath and room temperature. Lysates were clarified by centrifugation (10000 g, 2 min, 25°C), and were spotted onto PEI-cellulose TLC plates (EMD Millipore, Darmstadt, Germany) along with a [γ-^{32}P]-GTP standard (Perkin Elmer). TLC plates were run in a chamber containing 1.5 M KH_2PO_4 pH 3.4 for 30 minutes and exposed to a phosphorscreen for ~24 hours. Imaging and quantitation were performed using a GE Healthcare Typhoon phosphorimager (Sunnyvale, CA). Spot intensities corresponding to ppGpp were normalized to GTP spot intensities from the same sample using ImageQuant software.

2.2.5 Microscopy and image analysis

Synechococcus cultures were harvested at the appropriate timepoint (26 hours after IPTG induction for the experiment shown in Figure 2-3) and were stained with 4',6-diamidino-2-phenylindole (DAPI; Sigma-Aldrich) at 1 mg/ml for 15 minutes in the dark at room temperature. Stained cells were washed two times in phosphate-buffered saline (PBS) and resuspended in BG-11 medium. Cells were immobilized by spotting cultures onto agarose pads (2% agarose in BG-11 medium). Imaging was performed on a Zeiss AXIO Observer.Z1 inverted microscope (Oberkochen, Germany) equipped with a 100X phase-contrast oil objective (NA 1.4) and an Excelitas Technologies X-Cite 120Q fluorescent light source (Fremont, CA). Images were acquired using a Hamamatsu Photonics ORCA-Flash4.0 sCMOS camera (Hamamatsu City, Japan) and Zeiss ZEN 2012 software.

Cyanobacteria naturally fluoresce in the red portion of the visible spectrum due to both chlorophyll-containing photosystems and the light-harvesting pigments present in phycobilisomes, both of which are found in the thylakoid membranes (15). Pigment fluorescence was assayed using a standard red fluorescent protein (RFP) filter set (excitation 572 nm; emission 629 nm). Polyphosphate (polyP) was imaged using a standard cyan fluorescent protein (CFP) filter set (excitation 436 nm; emission 480 nm). Upon binding to negatively-charged polyP, the positively-charged DAPI molecule exhibits a spectral Stokes shift that permits DAPI-polyP fluorescence to be distinguished from DAPI-DNA fluorescence using these wavelengths (16). At the same time, a standard DAPI filter set was used to assay DAPI-DNA fluorescence (excitation 365 nm; emission 445 nm). Microscopy images were analyzed using MicrobeTracker and SpotFinder, bacterial image analysis programs written in Matlab (14). Segmentation of cells was manually verified and corrected when necessary.

2.2.6 Flow cytometry

Synechococcus cultures were diluted to OD_{750} ~0.03 and were stained with Vybrant DyeCycle Green (Thermo Fisher) at 26 hours after IPTG induction. The final dilution of the stain was 1:5000. Cultures were stained for 45 minutes in the dark at 30°C. Stained cells were analyzed on an EMD Millipore Guava EasyCyte HT flow cytometer. 10,000 events were analyzed for each condition.

2.2.7 ^{14}C-Leu protein incorporation measurements

Synechococcus cultures were grown in constant light to log phase (OD_{750} ~0.4), and $ppGpp^+$ cultures were induced with 50 µM IPTG for 12 hours. Aliquots (0.5 ml) of cultures were incubated in the dark for 2 hours where appropriate, and all cultures were then labeled with 0.2 µCi ^{14}C-Leu (Perkin Elmer) for 1 hour. Cells were lysed by adding SDS to a final concentration of 1% and heating at 80˚C for 15 minutes, following by cooling on ice. To precipitate proteins, ice-cold trichloroacetic acid (TCA) was added to cell lysates at a final concentration of 5% and lysates were incubated on ice for 30 minutes. Lysates were centrifuged (21000 g, 10 min, 25°C), pellets washed once in ice-cold 5% TCA to remove unincorporated ^{14}C-Leu, and centrifuged again. The entire protein pellet was resuspended in 8M urea and ^{14}C counts were determined using a Beckman LS6500 scintillation counter.

2.2.8 Absorbance scans

Absorbance scans of *Synechococcus* cultures were performed using a Tecan Infinite M1000 Pro plate reader (Männedorf, Switzerland), measuring absorbance between 350-800 nm at 5 nm intervals. An identical absorbance scan was performed using sterile media, and these values were subtracted from culture readings.

2.2.9 RNA-seq: RNA library preparation, sequencing, and data analysis

RNA was isolated from four different conditions: control-L = wild-type cultures (WT-Cm^R) in the light (+50 µM IPTG for 18 hours); $ppGpp^+$-L = $ppGpp^+$ cultures in the light (induced with 50 µM IPTG for 18 hours); control-D = wild-type cultures (WT-Cm^R) at the end of a 2-hour dark pulse; Δ*rel*-D = Δ*rel* cultures at the end of a 2-hour dark pulse. All cultures were synchronized by two 12-hour light/12-hour dark cycles and were harvested at the same time during the subjective day (L7) to minimize effects of circadian rhythm on gene expression. Cultures (100 ml; OD_{750} 0.2-0.4) were harvested by filtration; cell material was scraped off filters and resuspended in 400 µl AE buffer (50 mM sodium acetate pH 5.5, 10 mM EDTA pH 8.0). Cell suspensions were flash-frozen in liquid nitrogen and stored at -80°C until further processing.

RNA was isolated using a method based on (4) in which cells were lysed using hot acid phenol/SDS and phenol/chloroform extraction. Cell suspensions were thawed at room temperature. 0.1X volume (40 µl) of 10% sodium dodecyl sulfate (SDS) was added to each tube, followed by an equal volume (440 µl) of phenol (equilibrated with AE buffer). Tubes were incubated at 65°C for 4 minutes, frozen in a dry ice/ethanol bath for ~1 minute, and centrifuged to separate aqueous and phenol phases (16000 g, 5 min, 25°C). The aqueous phase was transferred to a phase lock gel heavy tube (5 Prime, Hilden, Germany), to which an equal volume (~350 µl) of acid phenol:chloroform:isoamyl alcohol (125:24:1, pH 4.5) was added. These tubes were centrifuged to separate aqueous and phenol phases (16000 g, 5 min, 25°C). 200 µl of the aqueous phase was further purified using a Qiagen RNeasy Mini kit according to the manufacturer's protocol (Hilden, Germany). RNA concentrations were determined using

a Thermo Scientific Nanodrop 2000 spectrophotometer. Total RNA (5 µg) was treated with 2 units of DNase I (Thermo Scientific) to remove genomic DNA contamination according to the manufacturer's recommendations. 20 units of RNase inhibitor (SUPERaseIn, Thermo Fisher) were added to reactions, which were incubated at 37°C for 75 minutes. EDTA was added to reactions at a final concentration of 2.5 mM, and reactions were incubated at 65°C for 10 minutes to stop DNase I activity. DNase-treated RNA was further purified using a Zymo Research RNA Clean & Concentrator-5 kit (Irvine, CA) according to the manufacturer's protocol. RNA integrity was verified at multiple steps using the Agilent Technologies RNA 6000 Nano kit and an Agilent 2100 Bioanalyzer (Santa Clara, CA) according to the manufacturer's protocol.

Total RNA (~1.5 µg) was depleted of ribosomal RNA using an Illumina RiboZero rRNA depletion kit (Bacteria) (San Diego, CA), and RNA-seq libraries were constructed using the BIOO Scientific, NEXTflex Rapid Illumina Directional RNA-Seq Library Prep Kit (cat no. 5138-08) using 15 cycles of PCR. Samples were barcoded, pooled in equimolar ratios, and sequenced in one lane on an Illumina HiSeq2500, generating 50-bp single-end reads. Each condition sequenced had four biological replicates, except for $ppGpp^+$, which had three.

RNA-seq library adapter contamination was removed using Scythe (http://bioinformatics.ucdavis.edu/software/). The resulting data were aligned to the *Synechococcus* genome, normalized, and analyzed using Rockhopper, a bacterial RNA-seq analysis platform (17). Rockhopper performs upper-quartile normalization to generate RNA-seq expression values for each condition. RNA-seq expression values were plotted in DataGraph (Visual Data Tools, Inc.), and a power regression analysis was performed. Genes with expression values at least one standard deviation higher or lower than the values predicted by the regression line were considered differentially expressed.

2.2.10 Quantitative reverse transcriptase PCR (qPCR)

For qPCR experiments to verify RNA-seq results, RNA isolation, DNase treatment, and RNA cleanup were performed as described for RNA-seq experiments. RNA concentrations were determined using a Thermo Scientific Nanodrop 2000 spectrophotometer, and were standardized to the same amount of input RNA (~1 µg) for reverse transcription reactions, which were performed using Clontech RNA to cDNA EcoDry Premix with random hexamers according to the manufacturer's protocol (Mountain View, CA). The resulting cDNA was diluted 1:10 before amplification in qPCR reactions.

For qPCR experiments to measure pre-16S and 16S rRNA levels, cultures were synchronized by one 12-hour light/12-hour dark cycle, and 50 ml at an OD_{750} of 0.2-0.4 (maintained over the course of the experiment by manual backdilution) was harvested at the appropriate timepoint by filtration. Cell material was scraped off filters, resuspended in 1 ml Trizol reagent (Invitrogen; Carlsbad, CA), flash-frozen in liquid nitrogen, and stored at -80°C until further processing. RNA isolation was performed

according to the manufacturer's protocol, with one additional incubation at 90°C for 5 minutes immediately after thawing frozen samples. DNase treatment and RNA cleanup were performed as described for RNA-seq experiments. Reverse transcription reactions were performed with the same amount of input RNA (1 µg), using Invitrogen SuperScript III reverse transcriptase with random primers according to the manufacturer's protocol. The resulting cDNA was diluted 1:100,000 before amplification in qPCR reactions.

All qPCR reactions were performed using the Thermo Fisher DyNAmo HS SYBR Green qPCR kit according to the manufacturer's instructions with 0.5 µM of each primer (see Table 2-1 for primer sequences). Reactions were run on an Applied Biosystems StepOnePlus real-time PCR machine (Foster City, CA), using fluorescence of the ROX reference dye for normalization. Cycling conditions were: 95°C for 15:00; 40 cycles of 95°C for 0:10, 60°C for 0:30, 72°C for 0:30; and melt curve analysis from 60°C to 95°C. Amplicons ranged from 120-140 base pairs, and product specificity was verified by melt curve analysis and agarose gel electrophoresis. No template controls were performed and showed minimal primer-dimer formation. Three candidate reference genes, *secA* (Synpcc7942_0289), *rimM* (Synpcc7942_2259), and *rnpA* (Synpcc7942_1615), were selected for normalization based on a previous analysis performed with *Synechococcus* sp. PCC 7002 (18) and after confirming similar expression levels across conditions from our RNA-seq data. C_T values for *hpf* (Synpcc7942_2352), *gifA* (Synpcc7942_0900), and *sbtA* (Synpcc7942_1475) were normalized to C_T values for the appropriate reference gene, and expression values were determined relative to the control-L condition (using the $\Delta\Delta$ C_T analysis method).

2.2.11 Polysome analysis by sucrose density gradient centrifugation

Synechococcus cultures (500 ml) were synchronized by one 12-hour dark period, and were grown in constant light to log phase (OD_{750} 0.2-0.5), then shifted into the dark for 2 hours where appropriate. *E. coli* cultures (50 ml) were grown to log phase (OD_{600} ~0.5). All cultures were treated with chloramphenicol at a final concentration of 0.5 mg/ml for 2 minutes to arrest translation elongation. Cultures were poured over crushed ice in centrifuge bottles (to allow rapid cooling), and cells were harvested by centrifugation (10000 g, 10 min, 4°C). Pellets were washed in 5 ml ice-cold polysome lysis buffer (10 mM Tris-HCl pH 8.0, 10 mM $MgCl_2$), centrifuged again (4000 g, 10 min, 4°C), and pellets were resuspended in 1 ml ice-cold polysome lysis buffer. This cell material was transferred to a 2 ml screw-cap tube containing ~0.5 ml 0.1-mm glass beads, which was flash-frozen in liquid nitrogen and stored at -80°C until further processing.

Cell lysates were prepared on the same day as sucrose gradients to minimize the number of freeze-thaw cycles. Cell material was thawed at room temperature and lysed in a bead beater for 3 x 30-second cycles, with 1 minute on ice in between each beating. Tubes were centrifuged quickly (16000 g, 30 sec, 4°C) to sediment beads, the supernatant was transferred to a new tube, and the lysate was clarified by centrifugation (16000 g, 10 min, 4°C). This supernatant was transferred to a new tube, and absorbance at 260 nm was measured using a Nanodrop 2000 spectrophotometer.

Samples in a particular experiment were normalized to the same A_{260nm} (~20 A_{260} units) in a total volume of 300 µl (diluted with polysome lysis buffer where necessary), to which 40 units of RNase inhibitor (SUPERaseIn, Thermo Fisher) was added before loading lysates onto sucrose gradients. For RNase A-treated samples (and negative controls), 33 µl of 3 M NaCl was added to the 300 µl of cell lysate, to which 3 mg of RNase A (Thermo Fisher) was added. Lysates were incubated at room temperature for 10 minutes and were then frozen in liquid nitrogen to stop the reaction (these samples were subjected to one additional freeze-thaw cycle.)

Sucrose gradients (10-40%, w/v) were prepared in ultracentrifuge tubes by layering 6 ml of 40% sucrose buffer solution (20 mM Tris-HCl pH 7.8, 10 mM $MgCl_2$, 100 mM NH_4Cl, 2 mM DTT, 40% sucrose) underneath 6 ml of 10% sucrose buffer solution (20 mM Tris-HCl pH 7.8, 10 mM $MgCl_2$, 100 mM NH_4Cl, 2 mM DTT, 10% sucrose). Linear gradients were created using a Gradient Mate and allowed to equilibrate for at least 15 minutes at 4°C before loading. 300 µl of cell lysate was loaded on top of the sucrose gradient, and gradient tubes were centrifuged in a Beckman ultracentrifuge (40000 g, 105 min, 4°C). Sucrose gradients were then analyzed by a UV-Vis detector, monitoring absorbance at 254 nm. Fractions approximately corresponding to distinct peaks were collected manually and stored at -80°C until further processing. Sucrose gradient fraction analysis was performed using an Agilent RNA 6000 Nano kit and Agilent 2100 Bioanalyzer according to the manufacturer's protocol.

2.3 Results

Darkness presents a major metabolic challenge for cyanobacteria, depriving them of their primary energy source – photosynthetically active radiation. In model heterotrophic bacteria like *Escherichia coli*, metabolic stress by starvation leads to precipitous increases in levels of the alarmones ppGpp (guanosine 3'-diphosphate 5'-diphosphate) and pppGpp (guanosine 3'-diphosphate 5'-triphosphate) (19). Hereafter, we use the notation (p)ppGpp to refer to both molecules simultaneously when appropriate. Increased concentrations of (p)ppGpp, the nucleotide second messengers of the stringent response, cause polyphosphate (polyP) – a linear polymer of orthophosphates – to accumulate in *E. coli* (20). We hypothesized that increased levels of (p)ppGpp might also be responsible for increased polyP levels recently observed in *Synechococcus* in the dark (21). Although previous work has shown that (p)ppGpp is synthesized by *Synechococcus* (8, 22), mechanistic explanations for targets of the stringent response and its physiological effects are lacking. This led us to investigate the role of this pathway more broadly in *Synechococcus*.

2.3.1 ppGpp levels increase in the dark in Synechococcus, and can be genetically manipulated

We hypothesized that the metabolic and physiological changes observed in *Synechococcus* cultures between light and dark could be due to altered levels of (p)ppGpp. We therefore shifted cells grown in the light into the dark, harvested cultures at defined timepoints, and analyzed cell extracts by high-performance liquid chromatography (HPLC) to determine ppGpp levels (Figures 2-1 and 2-2A). Cells growing in the light have low intracellular levels of ppGpp, which we estimate at around 5 μM (see Materials and methods for details). When cells are shifted into the dark, ppGpp levels increase rapidly, peak after ~30 minutes, and remain elevated until cells are shifted back into the light. These results are consistent with those reported previously (8). Peak ppGpp levels in *Synechococcus* (30 minutes after onset of darkness) are approximately 150 μM. We find, therefore, that ppGpp levels increase rapidly in *Synechococcus* in response to darkness.

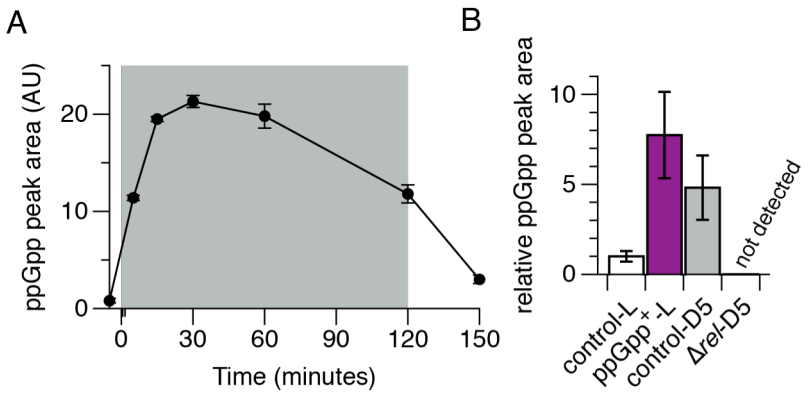

Figure 2-1. ppGpp levels increase in the dark in *Synechococcus*, and can be genetically manipulated. (*A*) *Synechococcus* cultures were shifted from the light (white background) to the dark (gray background) at 0 minutes and were harvested at the timepoints shown. Extracts were analyzed by anion exchange HPLC (AU, arbitrary units). Peaks eluting at the same time as a ppGpp standard were integrated to determine relative ppGpp levels. (*B*) Analysis of ppGpp levels from *Synechococcus* strains in light (white bars) and dark (gray bar). Cultures harvested in the light were induced with IPTG for 17 hours (control = WT-Cm^R). Cultures in the dark were harvested 5 minutes after the light-to-dark shift. ppGpp levels in the Δ*rel* mutant were below the limit of detection (~1 μM). When analyzed using a one-tailed t-test, $ppGpp^+$-L vs. control-L, p = 0.0469; control-D5 vs. control-L, p = 0.0669. Data are presented as mean ± SEM (n = 3).

In order to artificially increase (p)ppGpp levels, we constructed a *Synechococcus* strain that inducibly expresses a small (p)ppGpp synthetase from *Bacillus subtilis*, *yjbM*/SAS1. This gene has been heterologously expressed in *E. coli* and resulted in high levels of (p)ppGpp (23). We refer to this strain as $ppGpp^+$. As expected, the $ppGpp^+$ strain had significantly higher ppGpp levels in the light than a control harboring an empty plasmid, as measured by HPLC and ^{32}P-TLC (Figures 2-1B, 2-2B, 2-2C, and 2-2D). Based on the crystal structure and mutational studies of the homologous Rel (p)ppGpp synthetase from *Streptococcus equisimilus* (24), we generated a point mutant, D72G, to abrogate the activity of the *B. subtilis* synthetase. A recent crystal structure of *yjbM*/SAS1 revealed that Asp72 coordinates a magnesium ion required for catalytic activity (25). The D72G mutation did indeed inactivate (p)ppGpp synthetic activity, restoring ppGpp levels to those of the empty plasmid control (Figures 2-2C and 2-2D). We refer to this strain as $ppGpp^+$ D72G. Using these strains, we can control (p)ppGpp synthesis in *Synechococcus*, allowing us to investigate the cellular effects of manipulating (p)ppGpp levels.

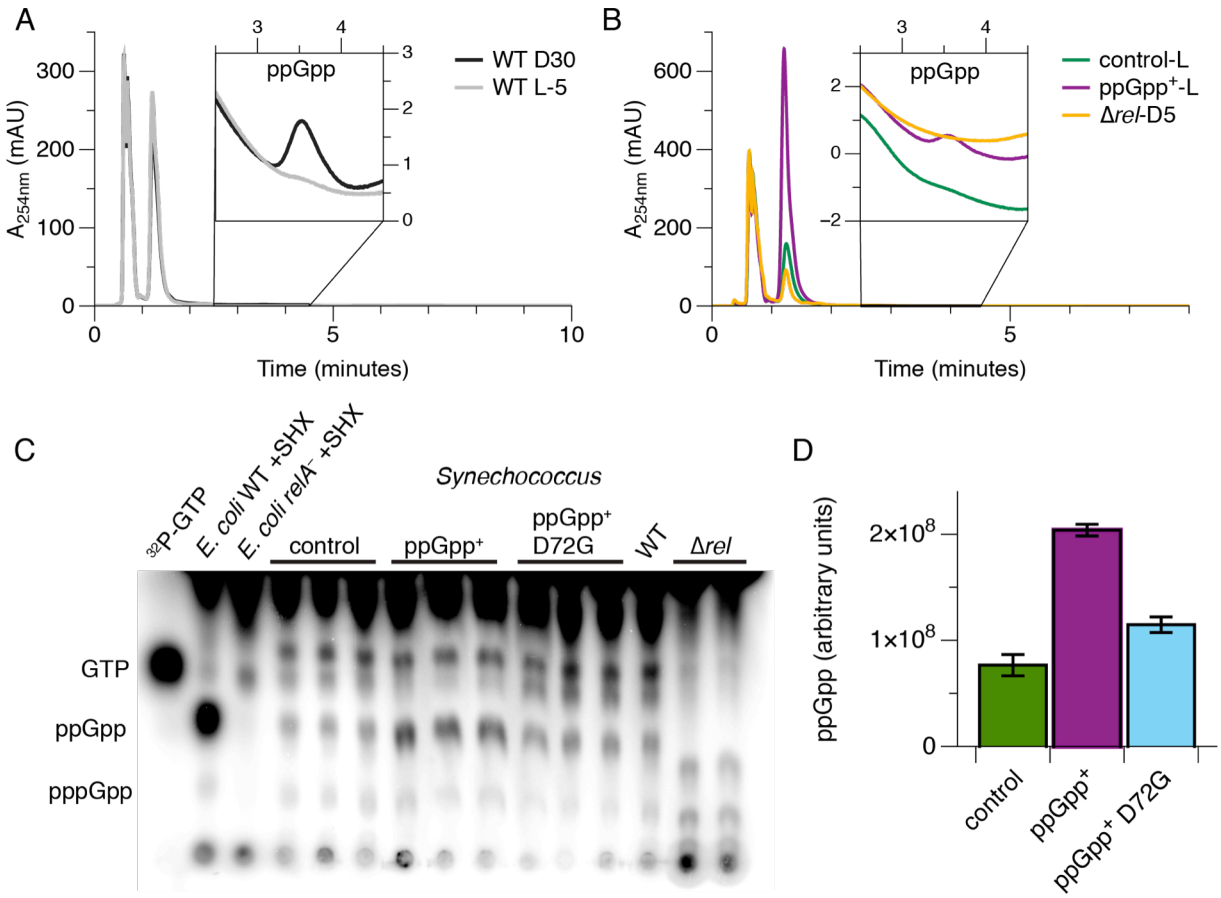

Figure 2-2. Measurement of ppGpp in *Synechococcus* lysates by HPLC and ^{32}P-TLC. (*A, B*) Representative traces from HPLC analysis. *Synechococcus* cell extracts were run on an anion exchange column, monitoring absorbance at 254 nm. Under these conditions, ppGpp elutes at ~3.5 minutes, as shown in the enlarged plots. (*A*) Traces from experiment shown in Figure 1A. Gray line, wild-type (WT) cells in the light at t = -5 minutes (5 minutes before shift to darkness); black line, wild-type cells after 30 minutes in the dark. (*B*) Traces from experiment shown in Figure 2-1B. Green line, control cells (WT-Cm^R) in the light; purple line, ppGpp$^+$ cells in the light after 17 hours of IPTG induction; yellow line, Δ*rel* cells after 5 minutes in the dark. (*C*) *E. coli* and *Synechococcus* (control = WT-Kan^R) were grown in low-phosphate media to mid-log phase. $H_3{}^{32}PO_4$-containing media was added to cultures along with IPTG where appropriate, and they were incubated at 30°C for at least 1 generation time. *E. coli* cultures were treated with serine hydroxamate (SHX) to mimic amino acid starvation for 10 minutes before harvesting. Cells were washed to remove excess $H_3{}^{32}PO_4$ and lysed in 6.5 M formic acid. Cell extracts and [γ-^{32}P]-GTP (a standard) were spotted onto PEI-cellulose TLC plates, run in 1.5 M KH_2PO_4 (pH 3.4) for 30 minutes, and exposed to a phosphorscreen for 24 hours. Imaging and quantitation were performed using a Typhoon phosphorimager. (*D*) Quantitation of ppGpp spot intensities from TLC plate shown in panel C. Data are presented as mean ± SD (n = 3).

2.3.2 High (p)ppGpp levels stop growth and dramatically alter Synechococcus physiology

We next studied the effects of high (p)ppGpp levels on *Synechococcus* growth and physiology. When uninduced, the ppGpp$^+$ strain grows as well as either an empty plasmid control or ppGpp$^+$ D72G (Figure 2-3A). Strikingly, upon addition of the inducer isopropyl β-D-1-thiogalactopyranoside (IPTG), a dramatic decrease in colony forming units is observed in the ppGpp$^+$ strain (Figure 2-3A). When growth in liquid cultures is monitored by absorbance at 750 nm, a similar trend is apparent: ppGpp$^+$ cultures stop growing, while ppGpp$^+$ D72G cultures grow as well as the empty plasmid control (Figure 2-3B). Therefore, high (p)ppGpp levels are sufficient to stop growth of *Synechococcus*. When these cells are imaged by microscopy at 26 hours after induction, a number of physiological changes are visible (Figure 2-3C). For one, ppGpp$^+$ cells are elongated compared to control cells, indicating that cell growth and division are misregulated when (p)ppGpp levels are high (Figure 2-3D).

We noted striking differences in pigmentation between ppGpp$^+$ and control cultures after induction, indicating that cells with high (p)ppGpp levels undergo chlorosis (bleaching) (Figure 2-3E, inset). Microscopy revealed that natural fluorescence from photosynthetic pigments was much lower in ppGpp$^+$ cells than in either control condition (Figures 2-3C, 2-3E, and 2-4; see Materials and methods). Furthermore, absorbance scans indicated that levels of pigments in phycobilisomes, major light-harvesting complexes, were lower in ppGpp$^+$ cells, and chlorophyll absorbance also decreased (Figure 2-5). The lower levels of photosynthetic pigments in ppGpp$^+$ cells could be due to increased pigment degradation, decreased pigment production, or a combination of the two. Based on these results, it is likely that ppGpp$^+$ cells are less photosynthetically active than control cells (26, 27).

We tested whether (p)ppGpp affects levels of polyP by staining cells with DAPI and using an imaging method that distinguishes between DAPI-polyP and DAPI-DNA fluorescence (Figures 2-3C, 2-3F, and 2-6; see Materials and methods). In ppGpp$^+$ cells, the intensity of polyP granules greatly increases (Figure 2-3F) and numbers of polyP granules per cell are slightly higher than controls (Figure 2-6). Overall, these data show that (p)ppGpp regulates polyP granule formation in *Synechococcus*. Considering the finding that polyP granule size and number increase in the dark in *Synechococcus* (21), it is likely that (p)ppGpp stimulates polyP granule formation in the dark.

In ppGpp$^+$ cells, DNA content per cell decreased, as measured by DAPI-DNA fluorescence (Figures 2-3C and 2-3G). We confirmed these results by staining cells with a different DNA-specific dye and analyzing cells by flow cytometry (Figure 2-3G, inset). These results suggest that (p)ppGpp decreases DNA replication in *Synechococcus*, which is consistent with the finding that (p)ppGpp regulates DNA replication in other bacteria. (p)ppGpp directly inhibits DNA primase from *B. subtilis* (28), and causes degradation of the replication initiation protein DnaA in *Caulobacter crescentus* (29).

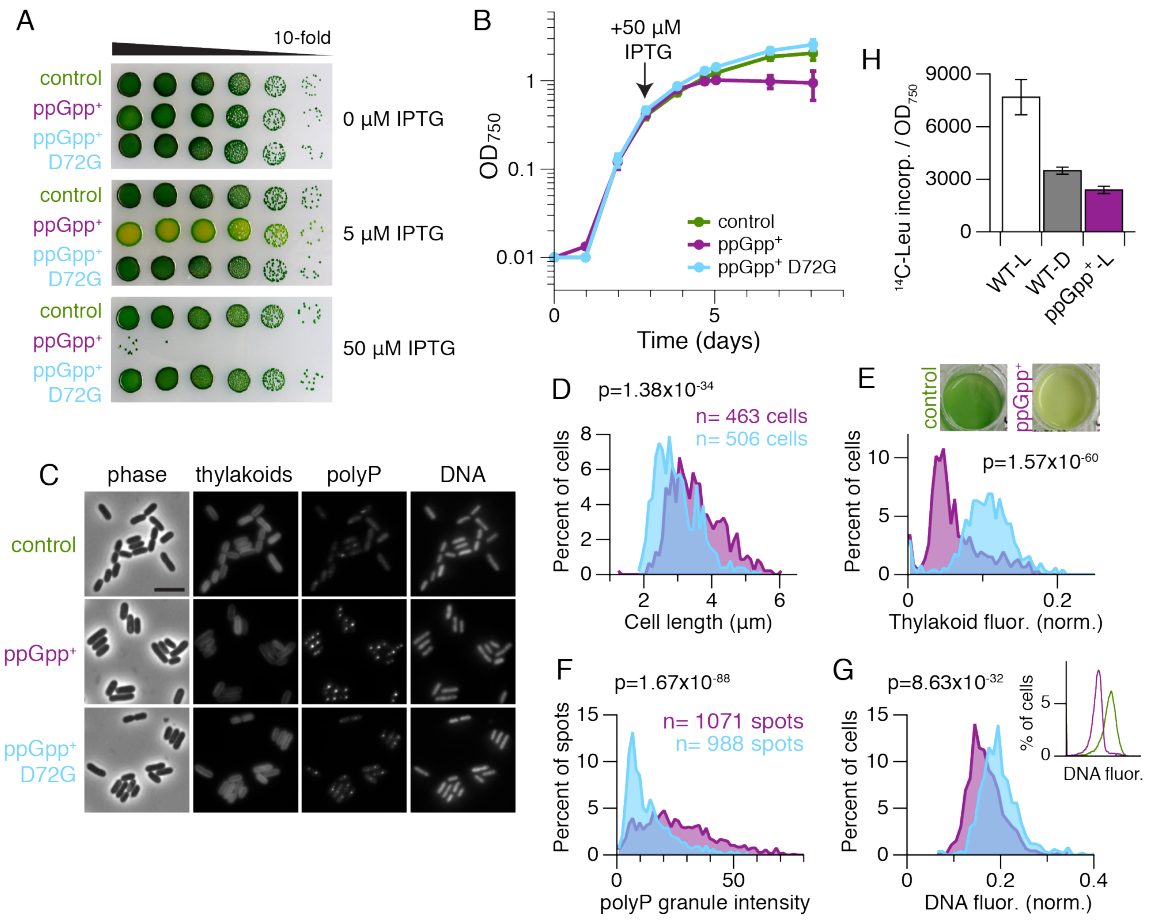

Figure 2-3. High (p)ppGpp levels stop growth and dramatically alter *Synechococcus* physiology. (*A, B*) Inducing high (p)ppGpp levels stops growth of *Synechococcus*. (*A*) When induced with IPTG, viability of the ppGpp$^+$ strain decreases. Images are representative of three independent experiments. (*B*) Cultures of the indicated strains (control = WT-Kan^R) were grown in constant light, induced with IPTG where indicated, and monitored by absorbance at 750nm (OD_{750}). Data are presented as mean ± SD (n = 3). (*C*) At 26 hours after IPTG induction, cultures were stained with DAPI and imaged by fluorescence microscopy. Representative images from three independent experiments are shown. Scale bar = 5 µm. (*D-G*) Microscopy images from two independent cultures at 26 hours after induction were analyzed using MicrobeTracker and SpotFinder. Histogram colors match those in panels A, B, and C: purple, ppGpp$^+$; light blue, ppGpp$^+$ D72G. The same number of cells (ppGpp$^+$: n = 463 cells; ppGpp$^+$ D72G: n = 506 cells) was used for each analysis shown. Data were analyzed with the Mann-Whitney U-test, and p-values are indicated on the histograms. (*D*) ppGpp$^+$ cells are longer than control cells. (*E*) Levels of light-harvesting pigments are lower in ppGpp$^+$ cells than in control cells. Natural fluorescence from thylakoid membranes was normalized to cell area. (*inset*) Pigmentation differences between control and ppGpp$^+$ strains are striking. Cultures were imaged ~48 hours after induction. (*F*) Intensities of polyphosphate (polyP) granules are higher in ppGpp$^+$ cells than in control cells. (*G*) DNA content is lower in ppGpp$^+$ cells than in control cells. Histograms of DAPI-DNA fluorescence (AU; normalized to cell area) in ppGpp$^+$ and ppGpp$^+$ D72G cultures. (*inset*) Analysis of DNA content by flow cytometry confirms that ppGpp$^+$ cells contain less DNA per cell than control cells. Cultures were stained with Vybrant DyeCycle

Green at 26 hours after induction with IPTG. A total of 10,000 events were analyzed by flow cytometry for each condition. Histogram colors match those in panels A, B, and E: green, control; purple, ppGpp$^+$. (*H*) Translation rates decrease in the dark and in ppGpp$^+$ cells. Incorporation of ^{14}C-Leu into trichloroacetic acid-precipitated proteins was measured by scintillation counting, and is plotted as ^{14}C counts per minute / OD_{750}. Labeling was performed for 1 hour with 0.2 µCi ^{14}C-Leu (for WT D, after a 2-hour dark pulse; for ppGpp$^+$, at 12 hours after IPTG induction). Data are presented as mean ± SD (n = 6).

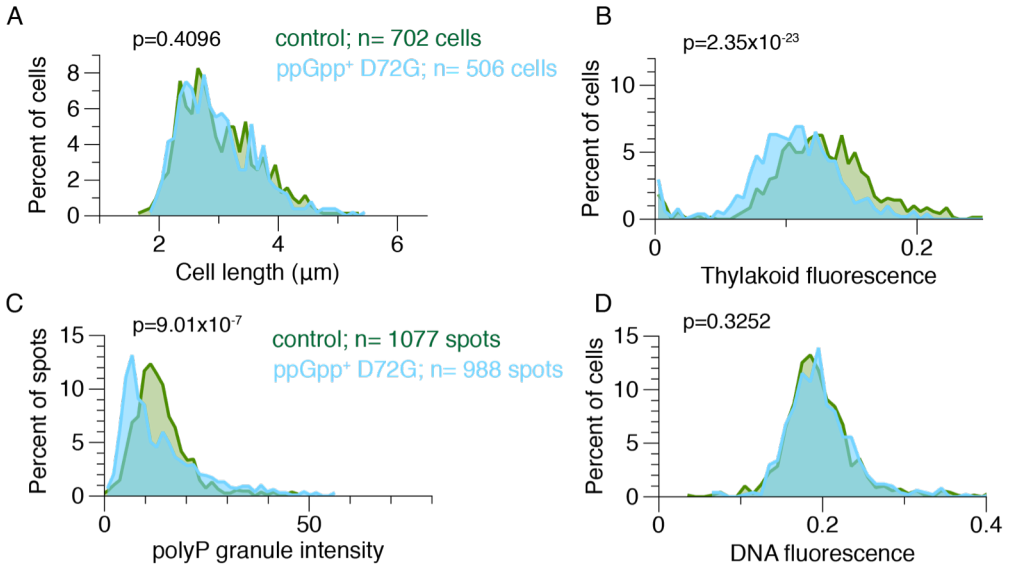

Figure 2-4. The phenotypes of ppGpp$^+$ D72G cells are similar to those of a wild-type control strain. Microscopy images were analyzed using MicrobeTracker and SpotFinder, bacterial image analysis programs written in Matlab. Images were acquired from two independent cultures at 26 hours after induction with 50 µM IPTG, as in Figure 2-3. Histogram colors are the same in all panels: green, control; light blue, ppGpp$^+$ D72G. The same number of cells (control: n = 702 cells; ppGpp$^+$ D72G: n = 506 cells) was used for each analysis shown. Data were analyzed with the Mann-Whitney U-test, and p-values are indicated on the histograms.

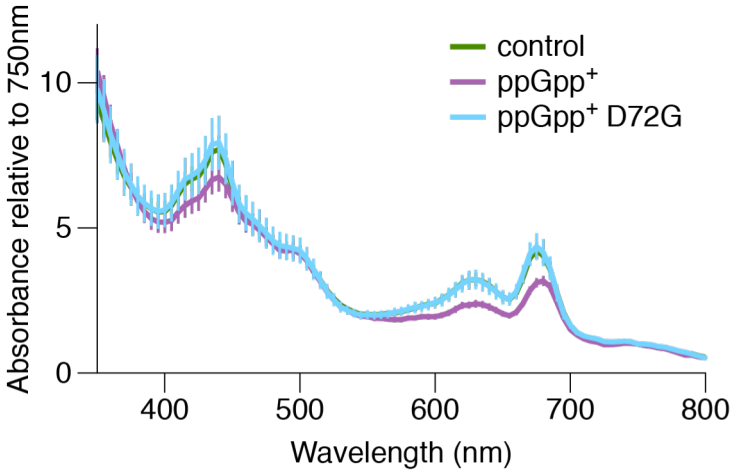

Figure 2-5. (p)ppGpp induces chlorosis (bleaching) in *Synechococcus*. *Synechococcus* cultures of the indicated strains were grown to mid-log phase and induced with 50 μM IPTG for 44 hours. Absorbance scans of cultures were performed using a Tecan M1000 plate reader, reading absorbance between 350-800 nm at 5 nm intervals. An identical absorbance scan was performed using sterile media, and these values were subtracted from culture readings. Spectra from the control and ppGpp$^+$ D72G strains are nearly identical and are therefore hard to resolve. Data are presented as mean ± SD (n = 3).

To investigate whether the stringent response decreases translation rates, we measured incorporation of ^{14}C-leucine into proteins under (p)ppGpp-varying conditions. We first verified that translation rates decrease in the dark in wild-type cells, as has been reported in the literature (30). After a two-hour incubation in the dark, translation rates decrease approximately twofold (Figure 2-3H). Triggering high (p)ppGpp production in the light (ppGpp$^+$) reduced translation rates to a level comparable to that of wild-type cells in the dark (Figure 2-3H). Thus, (p)ppGpp is sufficient to markedly reduce translation rates in *Synechococcus.* Taken together, these results demonstrate a dramatic reshaping of cellular physiology and growth mediated by (p)ppGpp in this cyanobacterium.

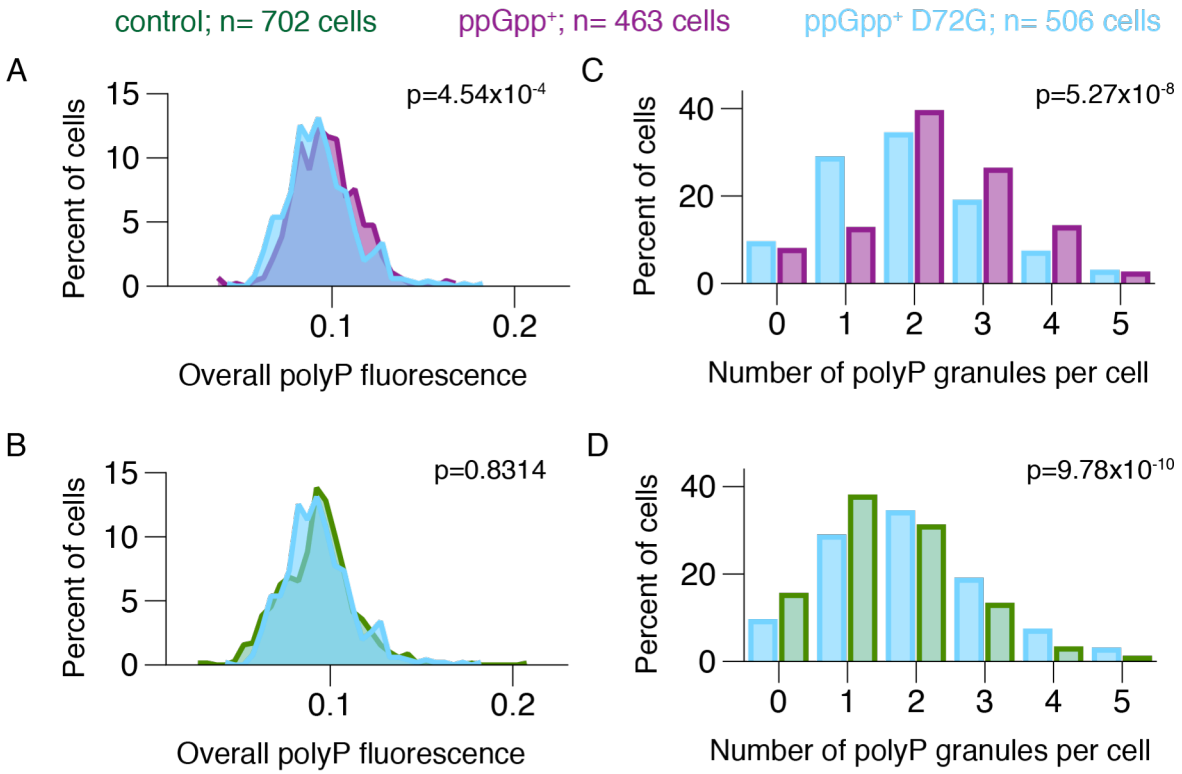

Figure 2-6. (p)ppGpp does not dramatically change overall polyP levels when normalized to cell area, but has a slight effect on polyP granule number. Microscopy images were analyzed using MicrobeTracker and SpotFinder. Images were acquired from two independent cultures at 26 hours after induction with 50 μM IPTG, as in Figure 2-3. Histogram colors are the same in all panels: green, control; purple, ppGpp$^+$; light blue, ppGpp$^+$ D72G. The same number of cells (control: n = 702 cells; ppGpp$^+$: n = 463 cells; ppGpp$^+$ D72G: n = 506 cells) was used for each analysis shown. Data were analyzed with the Mann-Whitney U-test, and p-values are indicated on the histograms. (*A, B*) Histograms of overall polyP fluorescence (AU; normalized to cell area) in control, ppGpp$^+$, and ppGpp$^+$ D72G cultures. A CFP filter set (excitation 436 nm; emission 480 nm) was used to image DAPI-polyP fluorescence; at these wavelengths, DAPI-DNA fluorescence signal is negligible. (*C, D*) Higher (p)ppGpp levels slightly increase the number of polyP granules in *Synechococcus*. Histograms show the number of polyP granules present per cell in each strain.

2.3.3 (p)ppGpp is important for maintaining viability in darkness

The phenotypes exhibited by the ppGpp$^+$ strain led us to investigate the endogenous stringent response pathway in *Synechococcus*. We deleted the *rel* gene, which encodes a bifunctional (p)ppGpp synthetase/hydrolase and is the only protein predicted to synthesize (p)ppGpp in the *Synechococcus* genome. As expected, this strain had very low ppGpp levels that were undetectable using our HPLC method, which has a limit of detection of ~1 μM (Figures 2-1B and 2-2B).

We postulated that (p)ppGpp would be more important for growth under changing environmental conditions than constant conditions. When grown in constant light, the control strain (wild-type harboring the same antibiotic resistance cassette as the mutant) and the Δ*rel* mutant grow similarly until they approach stationary phase, when growth of the Δ*rel* mutant becomes impaired (Figure 2-7A). In 12-hour light/12-hour dark cycling conditions, however, the growth of the Δ*rel* mutant is severely impaired, and this phenotype can be rescued by expressing the *rel* gene from a neutral site in the genome (Figure 2-7B).

These phenotypes become even more pronounced when cells are maintained in darkness for an extended period of time. After a week in constant darkness, the viability of the Δ*rel* strain decreases several orders of magnitude relative to the control strain, while a week in constant light does not affect viability of the Δ*rel* strain (Figure 2-7C). We find, therefore, that the stringent response is of limited import in constant light but helps *Synechococcus* respond to periods of darkness, highlighting the relevance of this pathway in environmental adaptation.

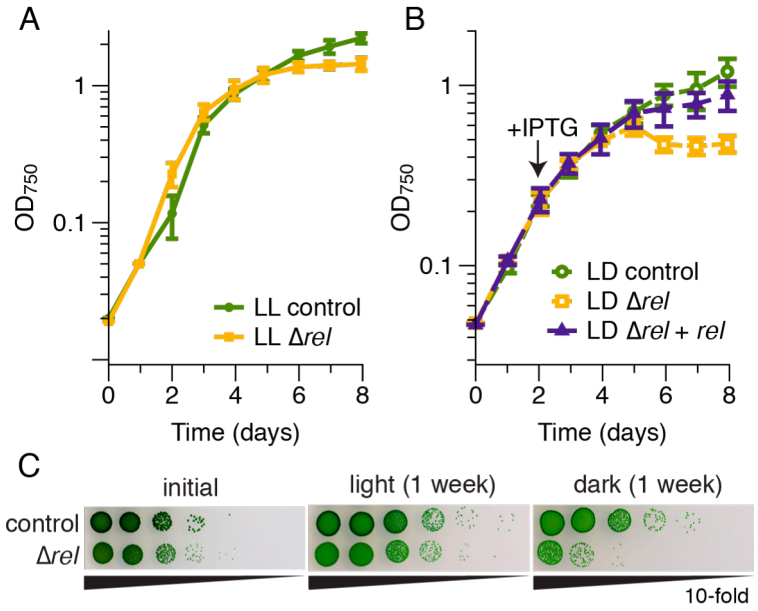

Figure 2-7. (p)ppGpp is important for maintaining viability during darkness. (*A*) Growth of the control (WT-Cm^R) and the Δ*rel* mutant is similar in constant light (LL) until cells reach stationary phase. (*B*) Growth of the Δ*rel* mutant is impaired in 12-hour light/12-hour dark (LD) cycles, but complementation of the Δ*rel* mutant restores nearly wild-type growth (control = WT-Cm^R/Kan^R). An IPTG-inducible copy of the *rel* gene was reintroduced into the Δ*rel* mutant at a neutral site, and IPTG was added to all cultures when indicated by the arrow. Data are presented as mean ± SD (*A*, n = 3; *B*, n = 4). (*C*) Viability of the Δ*rel* strain decreases greatly after incubation in constant darkness. Tenfold serial dilutions of cultures were plated at the beginning of the experiment, after a week in constant light, or after a week in constant darkness. Images are representative of two independent experiments.

2.3.4 (p)ppGpp regulates the expression of many genes in Synechococcus

To determine cellular targets downstream of (p)ppGpp in *Synechococcus*, we compared transcriptional profiles under (p)ppGpp-varying conditions using RNA-sequencing (RNA-seq). The reference conditions for this experiment were control cells (wild-type harboring an antibiotic resistance cassette) in the light or in the dark. We chose a two-hour dark pulse to study the effects of (p)ppGpp on gene regulation because this would give the cells sufficient time to both increase their (p)ppGpp levels and to make resulting changes in gene expression.

We found that expression of many genes changes between light and dark in wild-type cells (Figure 2-8A), as has been seen previously (9, 10), and that some of these gene expression changes are (p)ppGpp-dependent (Figure 2-9). A comparison of gene expression between control-dark and Δ*rel*-dark reveals genes that are (p)ppGpp-regulated in the dark (Figure 2-8B). At the same time, comparing gene expression between ppGpp^{+}-light vs. control-light uncovers genes for which high (p)ppGpp levels are sufficient to alter regulation (Figure 2-8C). In Figure 2-8, each scatter plot is oriented such that the higher (p)ppGpp condition is on the y-axis and the lower (p)ppGpp condition is on the x-axis, to facilitate comparison. Points more than one standard deviation above the regression line are considered upregulated by (p)ppGpp, and points more than one standard deviation below the regression line are considered downregulated by (p)ppGpp. This stringent cutoff results in 7 genes consistently upregulated by (p)ppGpp across the three comparisons presented in Figure 2-8 (listed in Table 2-3). Tables 2-4 and 2-5 list genes upregulated (75 genes) or downregulated (37 genes) by (p)ppGpp, respectively, in at least two comparisons.

Table 2-3. Genes upregulated by (p)ppGpp across all three RNA-seq comparisons.

			RNA-seq expression values			
locus tag	**gene name**	**gene description**	**control-D**	**Δ*rel*-D**	**control-L**	**ppGpp^{+}-L**
Synpcc7942_0182		hypothetical protein	135	43	10	41
Synpcc7942_0900	*gifA*	glutamine synthetase inactivating factor	15228	3075	166	7825
Synpcc7942_1212		hypothetical protein	77	21	8	30
Synpcc7942_1724		hypothetical protein	97	18	27	866
Synpcc7942_2352	*lrtA* / *hpf*	sigma 54 modulation protein / SSU ribosomal protein S30P	27694	4836	1073	8799
Synpcc7942_2411		hypothetical protein	108	31	19	83
Synpcc7942_2412	*phb, hflC*	SPFH domain, Band 7 family protein	337	83	35	126

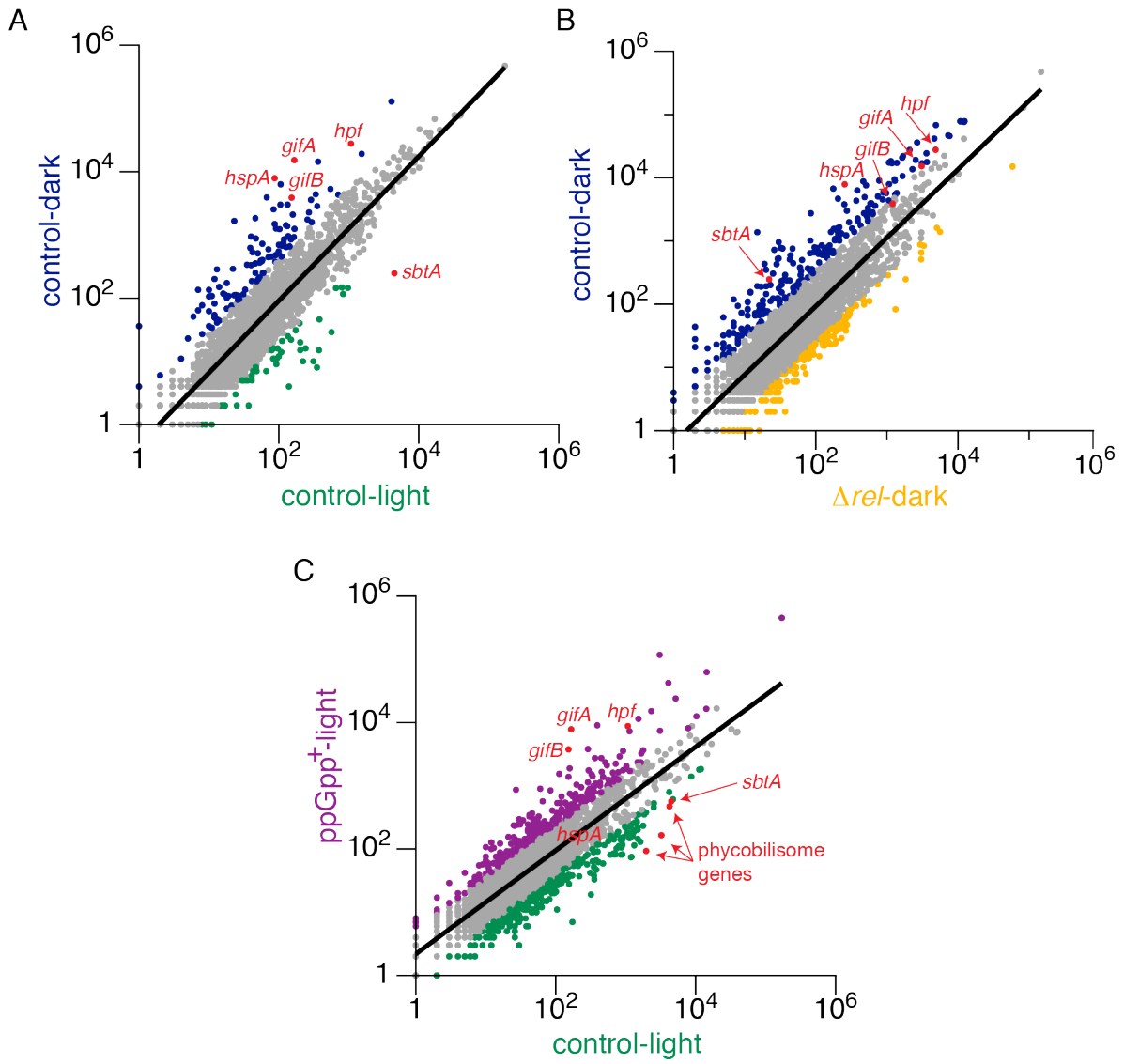

Figure 2-8. (p)ppGpp regulates the expression of many genes in *Synechococcus*. RNA-seq was performed for four different conditions: control (WT-Cm^R)-light; ppGpp$^+$-light = ppGpp$^+$ cultures in the light after 18 hours of IPTG induction; control-dark = WT-Cm^R cultures after a 2-hour dark pulse; Δ*rel*-dark = Δ*rel* cultures after a 2-hour dark pulse. RNA-seq data were analyzed and normalized using Rockhopper. For all conditions except ppGpp$^+$, n = 4 biological replicates; for ppGpp$^+$, n = 3 biological replicates. All panels show scatter plots of expression values based on upper-quartile normalization. The regression line used to identify differentially expressed genes is shown (*A*, R^2=0.81224; *B*, R^2=0.77495; *C*, R^2=0.7258). Genes with expression values at least one standard deviation higher or lower than the values predicted by the regression line are colored according to the condition under which they are more highly expressed. Genes not considered differentially expressed are colored in gray. All plots are shown such that the higher (p)ppGpp condition is on the y-axis and the lower (p)ppGpp condition is on the x-axis: (p)ppGpp-upregulated genes are above the regression line, while (p)ppGpp-downregulated genes are below the regression line. Selected differentially expressed genes discussed in the text are colored in red, with the gene name indicated.

Table 2-4. Genes upregulated by (p)ppGpp across at least two RNA-seq comparisons.

			RNA-seq expression values			
locus tag	**gene name**	**gene description**	**control-D**	**Δ*rel*-D**	**control-L**	**ppGpp$^+$-L**
Synpcc7942_0049	*pilA*	pilin polypeptide PilA-like	36111	2658	14369	62878
Synpcc7942_0108		sulfiredoxin	62	5	10	6
Synpcc7942_0147		hypothetical protein	453	209	78	237
Synpcc7942_0182		hypothetical protein	135	43	10	41
Synpcc7942_0193		hypothetical protein	723	221	58	244
Synpcc7942_0195		hypothetical protein	3918	585	67	121
Synpcc7942_0196		Beta-carotene 15,15'-dioxygenase	622	109	39	44
Synpcc7942_0243	*hliC*	possible high light inducible polypeptide HliC	1012	215	392	9045
Synpcc7942_0251		Exonuclease	941	400	40	244
Synpcc7942_0252	*cp12*	hypothetical protein	14391	5430	363	2738
Synpcc7942_0253		hypothetical protein	6310	383	106	119
Synpcc7942_0267	*gidB*	glucose-inhibited division protein B	3005	933	105	534
Synpcc7942_0291		hypothetical protein	853	121	118	141
Synpcc7942_0316	*digD, orf7.5*	hypothetical protein	4333	370	705	426
Synpcc7942_0398		hypothetical protein	369	77	222	607
Synpcc7942_0465		hypothetical protein	640	83	127	140
Synpcc7942_0497		hypothetical protein	186	110	41	145
Synpcc7942_0623	*trxB*	thioredoxin reductase	696	107	100	82
Synpcc7942_0700		hypothetical protein	5329	1310	546	1007
Synpcc7942_0741		Phage tail protein I	4	8	1	8
Synpcc7942_0781	*ppsA, pps*	phosphoenolpyruvate synthase	1840	659	46	144
Synpcc7942_0801	*sodB, sod1*	Superoxide dismutase	1227	268	916	1761
Synpcc7942_0834		hypothetical protein	106	83	10	76
Synpcc7942_0900	*gifA*	hypothetical protein	15228	3075	166	7825
Synpcc7942_0905		hypothetical protein	128755	83391	4074	42319
Synpcc7942_0906		hypothetical protein	2095	2217	158	1882
Synpcc7942_1002	*psaD*	photosystem I reaction center subunit II	17725	3646	7833	8142
Synpcc7942_1089	*clpB, clpB1, clpBI*	ATPase	444	48	71	66
Synpcc7942_1120		hypothetical protein	20	3	12	127
Synpcc7942_1147		hypothetical protein	44	2	14	8
Synpcc7942_1150		hypothetical protein	290	37	22	36
Synpcc7942_1153	*digE*	hypothetical protein	108	11	11	10
Synpcc7942_1209		hypothetical protein	544	224	99	282
Synpcc7942_1211		probable molybdopterin-guanine dinucleotide biosynthesis protein A	101	63	18	75
Synpcc7942_1212		hypothetical protein	77	21	8	30
Synpcc7942_1302		hypothetical protein	3005	273	133	143
Synpcc7942_1303		hypothetical protein	1424	203	126	136
Synpcc7942_1314	*ftsH*	FtsH-2 peptidase. Metallo peptidase. MEROPS family M41	1586	200	295	138
Synpcc7942_1320		hypothetical protein	201	23	12	23

Synpcc7942_1373		hydrogenase accessory protein	2898	538	565	1245
Synpcc7942_1389	*psbAII, psbA, psbA2*	photosystem q(b) protein	27451	2081	14196	16499
Synpcc7942_1426	*rbcL*	ribulose bisophosphate carboxylase	3935	604	1668	3245
Synpcc7942_1427	*rbcS*	ribulose 1,5-bisphosphate carboxylase small subunit	9456	1280	3089	7402
Synpcc7942_1460		hypothetical protein	476	180	89	406
Synpcc7942_1542	*isiA*	iron-stress chlorophyll-binding protein	203	33	51	79
Synpcc7942_1646		hypothetical protein	1750	744	256	527
Synpcc7942_1648		putative ferric uptake regulator, FUR family	511	43	50	35
Synpcc7942_1649		rubrerythrin	1375	15	132	49
Synpcc7942_1656	*katG, cpx*	catalase/peroxidase HPI	531	278	42	345
Synpcc7942_1689	*rhdA, rhd*	Rhodanese-like	94	8	26	4
Synpcc7942_1722	*sbpA*	Thiosulphate-binding protein	110	11	26	18
Synpcc7942_1724		hypothetical protein	97	18	27	866
Synpcc7942_1845		hypothetical protein	3582	1204	288	3809
Synpcc7942_2043	*speH*	S-adenosylmethionine decarboxylase proenzyme	237	43	238	550
Synpcc7942_2082	*fus*	elongation factor G	591	136	71	56
Synpcc7942_2119		RNA methyltransferase TrmH, group 3	634	124	559	1041
Synpcc7942_2125		hypothetical protein	456	111	109	140
Synpcc7942_2126		hypothetical protein	657	93	142	191
Synpcc7942_2301		hypothetical protein	383	278	57	189
Synpcc7942_2352	*lrtA*	sigma 54 modulation protein / SSU ribosomal protein S30P	27694	4836	1073	8799
Synpcc7942_2401	*hspA, hsp16.6*	heat shock protein Hsp20	7874	255	87	90
Synpcc7942_2411		hypothetical protein	108	31	19	83
Synpcc7942_2412	*phb, hflC*	SPFH domain, Band 7 family protein	337	83	35	126
Synpcc7942_2478	*psb28-2*	photosystem II reaction center W protein	1490	202	87	132
Synpcc7942_2485		hypothetical protein	1233	419	102	383
Synpcc7942_2486		hypothetical protein	1245	511	167	507
Synpcc7942_2529	*gifB*	glutamine synthetase inactivating factor	3874	1199	152	3766
Synpcc7942_2600	*ctaB, cyoE*	protoheme IX farnesyltransferase	354	125	46	218
Synpcc7942_2601	*ctaA*	putative cytochrome aa3 controlling protein	392	201	55	277
Synpcc7942_2602	*ctaC*	cytochrome c oxidase subunit II	670	494	112	1543
Synpcc7942_2603	*ctaD*	Cytochrome-c oxidase	251	258	60	898
Synpcc7942_B2634		hypothetical protein	118	91	16	122
Synpcc7942_B2645		hypothetical protein	19142	2537	1526	2072
Synpcc7942_B2646		two-component sensor histidine kinase	2269	388	269	241
Synpcc7942_B2657		hypothetical protein	27	37	8	55

Table 2-5. Genes downregulated by (p)ppGpp across at least two RNA-seq comparisons.

			RNA-seq expression values			
locus tag	**gene name**	**gene description**	**control-D**	**Δ*rel*-D**	**control-L**	**ppGpp$^+$-L**
Synpcc7942_0293		hypothetical protein	2	37	37	99
Synpcc7942_0358	*dc13, dcl3, trmB*	tRNA (guanine-N(7))-methyltransferase	1	9	11	15
Synpcc7942_0703	*smf*	DNA processing protein DprA, putative	97	362	53	22
Synpcc7942_0718		hypothetical protein	0	1	2	3
Synpcc7942_0719		hypothetical protein	0	3	2	10
Synpcc7942_0724		hypothetical protein	0	1	1	3
Synpcc7942_0915	*aroQ*	3-dehydroquinate dehydratase	21	83	111	323
Synpcc7942_0919		hypothetical protein	25	151	134	191
Synpcc7942_0995	*ycf20*	conserved hypothetical protein YCF20	3	27	24	16
Synpcc7942_1008	*purU*	formyltetrahydrofolate deformylase	2	26	15	14
Synpcc7942_1165		hypothetical protein	0	1	1	3
Synpcc7942_1185		hypothetical protein	8	53	47	38
Synpcc7942_1186	*ribD, ribG*	putative riboflavin-specific deaminase	1	10	9	6
Synpcc7942_1205		phage_integrase-like	0	2	2	4
Synpcc7942_1353		hypothetical protein	5	13	30	3
Synpcc7942_1471		hypothetical protein	16	22	241	67
Synpcc7942_1472		hypothetical protein	29	29	565	133
Synpcc7942_1473	*ndhD5*	putative monovalent cation/H+ antiporter subunit D	10	6	311	42
Synpcc7942_1474		putative monovalent cation/H+ antiporter subunit C	8	8	350	52
Synpcc7942_1475	*sbtA*	sodium-dependent bicarbonate transporter	247	22	4472	569
Synpcc7942_1489	*cmpB, ntrB*	nitrate transport permease	9	3	92	36
Synpcc7942_1538		hypothetical protein	0	2	4	6
Synpcc7942_1547		hypothetical protein	0	7	4	11
Synpcc7942_1560		hypothetical protein	2	12	16	22
Synpcc7942_1564		hypothetical protein	0	5	4	5
Synpcc7942_1744		hypothetical protein	22	22	149	35
Synpcc7942_1970		N-acyl-L-amino acid amidohydrolase	1	7	9	19
Synpcc7942_2085		probable anion transporting ATPase	16	69	59	21
Synpcc7942_2194		hypothetical protein	1	12	8	27
Synpcc7942_2234		NADH dehydrogenase I subunit N	148	146	794	110
Synpcc7942_2235	*trmD*	tRNA (guanine-N(1)-)-methyltransferase	46	70	380	47
Synpcc7942_B2618		transcriptional regulator, BadM/Rrf2 family	0	2	2	11
Synpcc7942_B2620	*srpA*	putative catalase	0	3	2	7
Synpcc7942_B2623	*srpD, cysK*	cysteine synthase A	0	1	2	3
Synpcc7942_B2629	*srpKLM*	sulfonate ABC transporter, periplasmic sulfonate-binding protein, putative	0	1	1	1
Synpcc7942_B2641		hypothetical protein	0	3	2	8
Synpcc7942_B2663	*srpH*	putative serine acetyltransferase	0	2	1	2

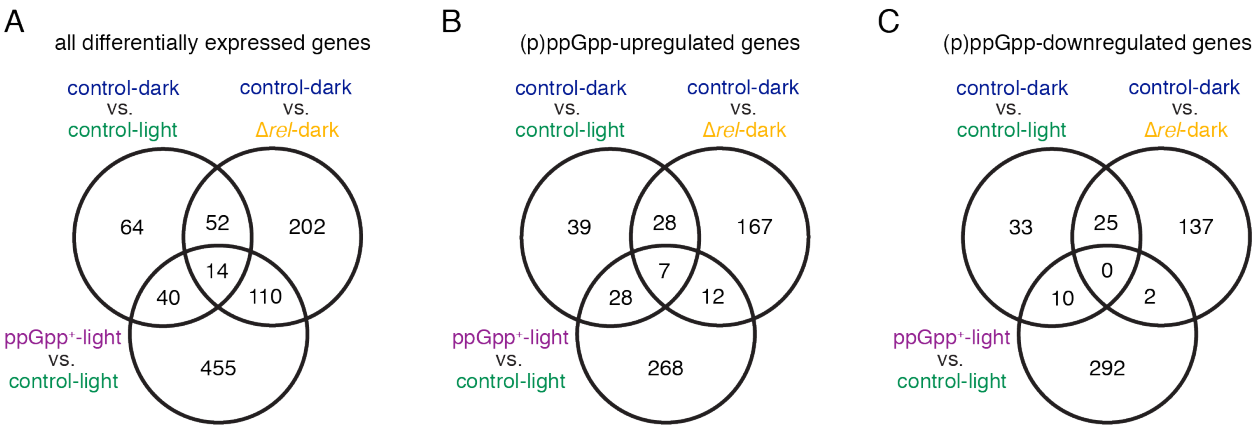

Figure 2-9. Venn diagrams comparing (p)ppGpp-regulated genes across RNA-seq comparisons. (*A*) Overlap among all differentially expressed genes across comparisons. (*B*) Overlap among genes upregulated by (p)ppGpp across comparisons. Genes included here showed expression values at least one standard deviation higher than calculated based on the regression line. See Table S1 for a list of the 14 genes consistently upregulated by (p)ppGpp across all three comparisons. (*C*) Overlap among genes downregulated by (p)ppGpp across comparisons. Genes included here showed expression values at least one standard deviation lower than calculated based on the regression line.

Several (p)ppGpp-upregulated genes were of particular interest (Figure 2-8 and Tables 2-3 and 2-4). Two genes strongly induced by (p)ppGpp are *gifA* and *gifB*, both of which encode glutamine synthetase inactivating factors. As a key link between carbon and nitrogen metabolism, glutamine synthetase is often a target of complex regulation (31). The *gifA* and *gifB* genes encode IF7 and IF17, respectively, both of which are small proteins that bind directly to glutamine synthetase and downregulate its activity (32). When cultures of the cyanobacterium *Synechocystis* sp. PCC 6803 are shifted from one nitrogen source (nitrate) to another (ammonium), *gifA* and *gifB* help tune glutamine synthetase activity and improve cellular growth as a result (33). An analogous balancing could occur in the dark, as metabolic changes necessitate tuning of enzyme activities.

A chaperone-encoding gene known to be highly expressed in the dark, *hspA*, requires (p)ppGpp for its upregulation (Figure 2-8 and (10)). However, high (p)ppGpp levels in ppGpp$^+$-L are not sufficient to induce high levels of the *hspA* transcript. It is likely that additional dark-induced but (p)ppGpp-independent factors are required for induction of *hspA* and other genes with similar expression patterns. (p)ppGpp-downregulated genes were less consistent across comparisons, but one notable example encodes the bicarbonate transporter *sbtA*.

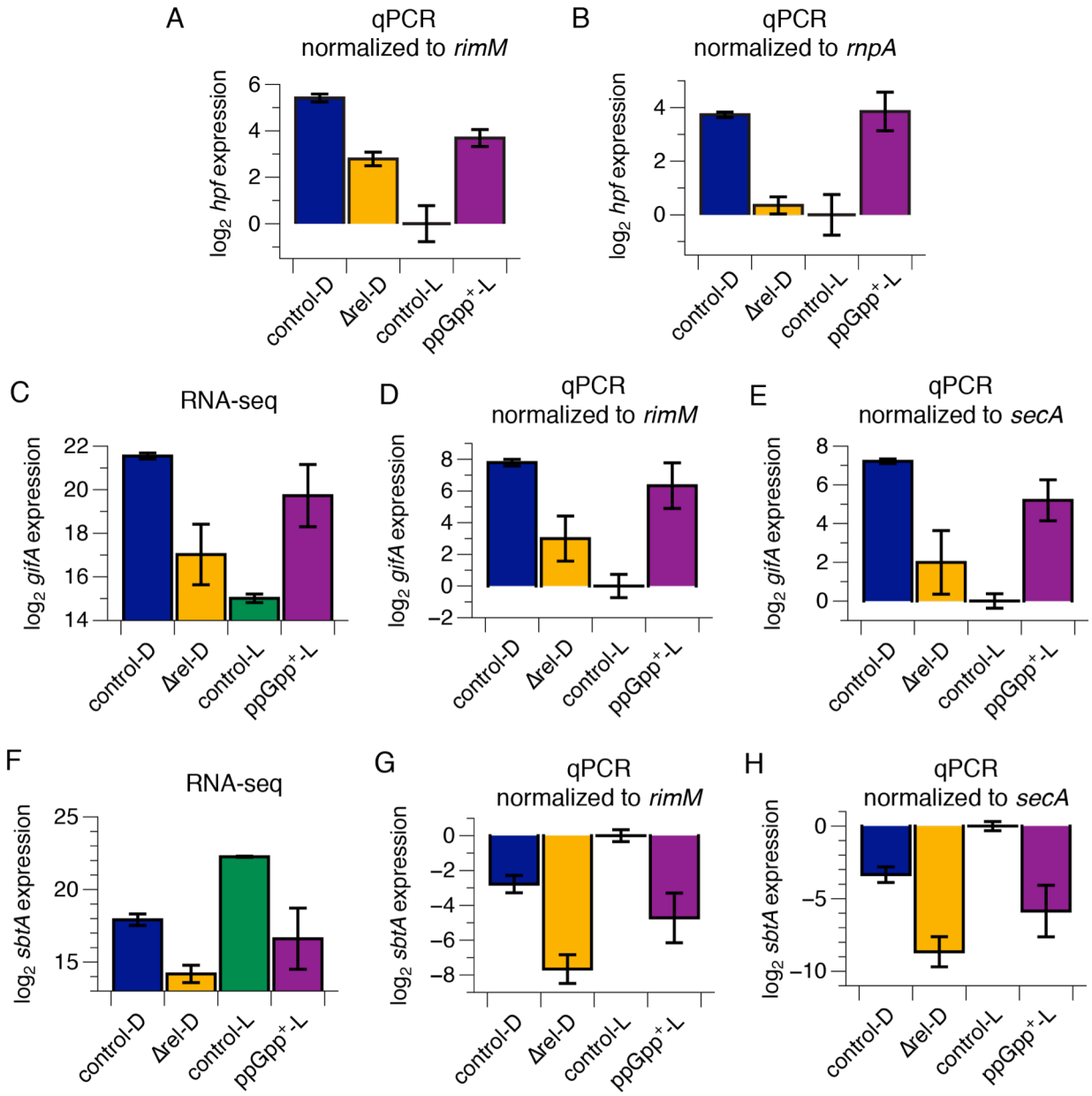

Figure 2-10. Verification of *hpf, gifA,* and *sbtA* gene regulation by qPCR. Three candidate reference genes were selected for qPCR based on a previous analysis (18) and after confirming similar expression levels across conditions from our RNA-seq data. All data are presented as mean ± SEM (n = 4 biological replicates). (*A*) *hpf* expression normalized to *rimM* expression and plotted on a $\log_2$ scale relative to control-L. (*B*) *hpf* expression normalized to *rnpA* expression and plotted on a $\log_2$ scale relative to control-L. (*C*) Rockhopper-normalized *gifA* expression values from RNA-seq, plotted on a $\log_2$ scale. (*D*) *gifA* expression normalized to *rimM* expression and plotted on a $\log_2$ scale relative to control-L. (*E*) *gifA* expression normalized to *secA* expression and plotted on a $\log_2$ scale relative to control-L. (*F*) Rockhopper-normalized *sbtA* expression values from RNA-seq, plotted on a $\log_2$ scale. (*G*) *sbtA* expression normalized to *rimM* expression and plotted on a $\log_2$ scale relative to control-L. (*H*) *sbtA* expression normalized to *secA* expression and plotted on a $\log_2$ scale relative to control-L.

We confirmed (p)ppGpp-dependent gene expression for several genes using quantitative reverse transcriptase PCR (qPCR) and observed trends similar to RNA-seq results (Figures 2-10, 2-11A, and 2-11B). Furthermore, these trends were consistent after using two or three different reference genes for qPCR normalization (Figures 2-10, 2-11A, and 2-11B). Figures 2-11A and 2-11B show expression of a highly (p)ppGpp-upregulated gene, *hpf*, which encodes ribosomal hibernation promoting factor (see the following section). Figure 2-10 contains verification of expression patterns for *gifA* and *sbtA*.

In other bacteria, the stringent response dramatically decreases production of ribosomal RNAs (rRNAs) (34). We performed qPCR experiments to measure total levels of 16S rRNA as well as rRNA precursor transcripts from cultures grown in light and dark and after induction of $ppGpp^+$ strains. During rRNA maturation in bacteria, the 5' leader sequence upstream of the 16S rRNA transcript is processed by RNase III, and this continues even when rRNA transcription slows or stops (35). By measuring amounts of the 16S 5' leader sequence (pre-16S rRNA transcripts), one can infer the rate of change of rRNA levels. Total levels of 16S rRNA did not change under any condition in our experiments (Figures 2-12A and 2-12B). Levels of pre-16S transcripts relative to total 16S transcripts decreased approximately 10-fold after cells had been in the dark for 12 hours (Figure 2-12C), but inducing high (p)ppGpp levels in the light did not affect pre-16S rRNA levels (Figure 2-12D). We conclude that rRNA production rate decreases in the dark but that this requires other factors besides (p)ppGpp.

In sum, (p)ppGpp regulates expression of a number of genes in *Synechococcus*, some of which appear to be controlled solely through (p)ppGpp, and some of which require additional factors for their expression under light/dark conditions. While the functions of some (p)ppGpp-regulated genes are known, the majority of genes lack a predicted function.

2.3.5 (p)ppGpp regulates ribosomal status through hibernation promoting factor

One of the most strikingly (p)ppGpp-upregulated genes encodes ribosomal hibernation promoting factor (*hpf*), a protein that dimerizes ribosomes into a less active state (Figure 2-8; (36, 37)). In *E. coli*, HPF and ribosome modulation factor act together to dimerize ribosomes and block binding of mRNAs, tRNAs, and translation initiation factors to the ribosome (38). HPF is widely conserved across bacterial phyla including cyanobacteria, as well as in plant plastids, and a long form of HPF from several bacterial clades is sufficient to dimerize ribosomes on its own (36, 37).

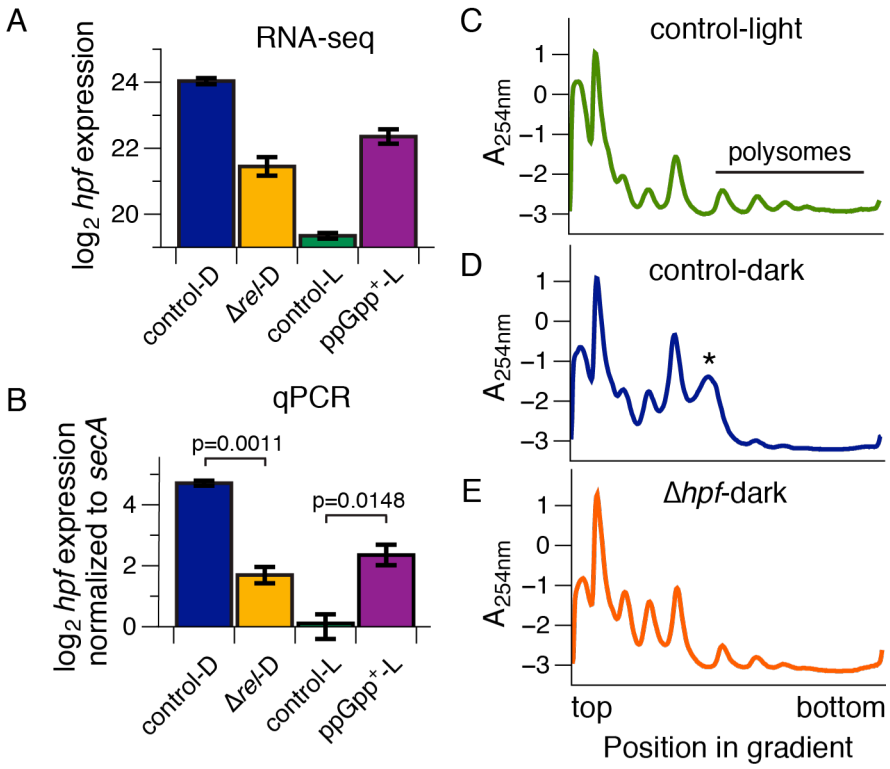

Figure 2-11. (p)ppGpp regulates translation through hibernation promoting factor. (*A*) RNA-seq expression data reveal striking regulation of *hpf* by (p)ppGpp. Rockhopper-normalized expression values plotted on a $\log_2$ scale. Data are presented as mean ± SEM (for all conditions except ppGpp$^+$, n = 4; for ppGpp$^+$, n = 3). (*B*) Verification of *hpf* gene regulation by quantitative reverse transcriptase PCR (qPCR). *hpf* expression was normalized to *secA* expression and plotted on a $\log_2$ scale relative to control-L. A two-tailed t-test between the indicated conditions was performed, and p-values are shown. Data are presented as mean ± SEM (n = 4 biological replicates). (*C, D, E*) Polysome profiles from *Synechococcus* lysates analyzed by sucrose density gradient centrifugation. Cultures were grown to mid-log phase and shifted into the dark for 2 hours where appropriate. Two minutes before harvesting, all cultures were treated with chloramphenicol to arrest translation elongation. Cell lysates were separated on 10-40% sucrose gradients by ultracentrifugation. Abundance of RNA species was monitored by absorbance at 254 nm (A_{254nm}; arbitrary units). All traces are representative of two independent biological replicates. (*C*) Control (wild-type) cells in the light are actively translating, as revealed by their abundant polysomes. (*D*) After a 2-hour dark pulse, control cells exhibit decreased translation and instead contain dimerized ribosomes, as indicated by the asterisk (*). (*E*) *hpf* is required for ribosome dimerization and decreased translation in the dark. After a 2-hour dark pulse, lysate from a Δ*hpf* mutant contains abundant polysomes and completely lacks dimerized ribosomes.

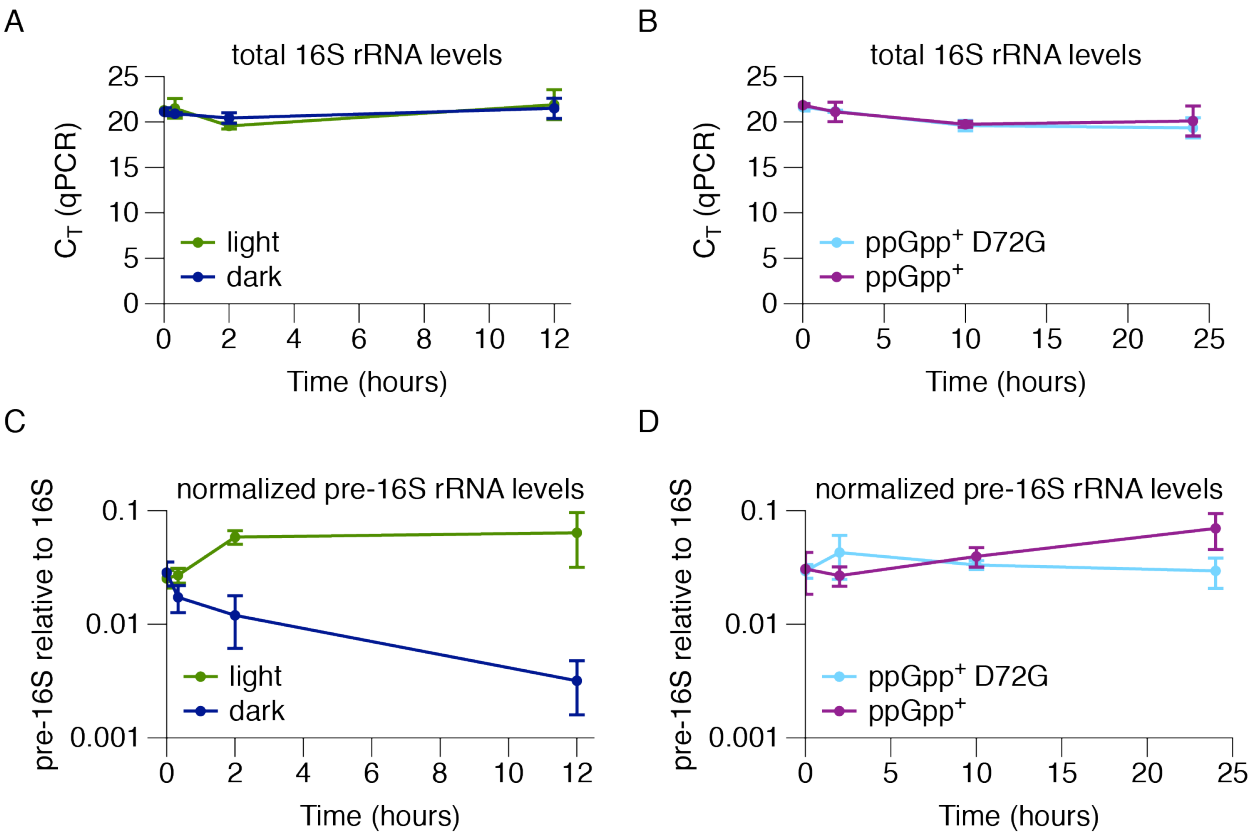

Figure 2-12. Levels of ribosomal RNA precursors decrease in the dark, but do not decrease in the ppGpp$^+$ strain. For the indicated conditions, RNA was isolated, reverse transcribed, and qPCR was performed to amplify sequences from mature 16S rRNAs and pre-16S rRNAs (primers within the 5' leader sequence of the rRNA transcript, which is cleaved during rRNA maturation). All data are presented as mean ± SD (n = 3 biological replicates). (*A, B*) Total 16S rRNA levels are plotted as the threshold cycle (C_T) measured by qPCR, and do not change measurably under any of the indicated conditions. (*C, D*) Pre-16S rRNA levels are plotted relative to total 16S rRNA levels from the same sample (using the calculation 2^(16S C_T – pre-16S C_T)). Levels of pre-16S rRNAs decrease over time when cells are incubated in the dark (*C*; dark begins at time = 0 hours), but are not affected by induction of high (p)ppGpp levels in the ppGpp$^+$ strain (*D*; cultures were induced with 50 μM IPTG at time = 0 hours).

To determine whether HPF acts in a similar manner in *Synechococcus* in the dark, we monitored ribosomal status using sucrose density gradient centrifugation. In actively translating cells, ribosomes exist in multiple forms: small (30S) and large (50S) subunits, assembled 70S monosomes, and polysomes, multiple ribosomes translating the same mRNA. Polysomes can be resolved on sucrose gradients as distinct peaks corresponding to two, three, four, etc. ribosomes bound to one mRNA. The presence of polysome peaks in cell lysates can be used to indicate translational status (39).

We determined polysome profiles from *Synechococcus* and found that *hpf* is necessary for ribosome dimerization in the dark. Since there have been no reports of polysome analyses in *Synechococcus* in the literature, we confirmed peak identities by comparison with *E. coli* lysates (39). *Synechococcus* ribosomes sediment similarly to those of *E. coli*, with characteristic peaks corresponding to small and large ribosomal subunits, monosomes, and polysomes (Figure 2-13A). Treatment of cell lysates with RNase A to cleave mRNA, which should remove polysomes, verified the position of polysome peaks (Figure 2-13B).

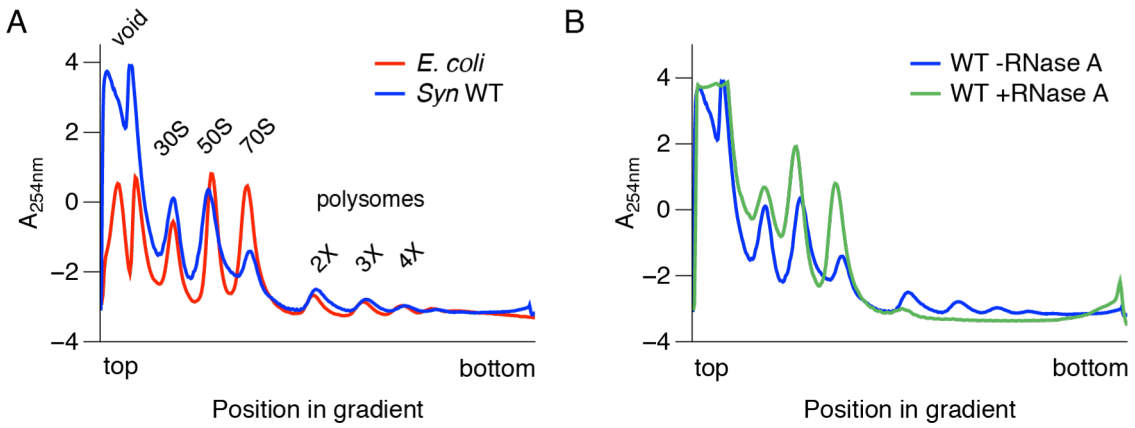

Figure 2-13. Verification of ribosomal peak identities in polysome traces. (*A, B*) Polysome profiles from *E. coli* and *Synechococcus* lysates analyzed by sucrose density gradient centrifugation. Cultures were grown to mid-log phase (in constant light for *Synechococcus*). Two minutes before harvesting, all cultures were treated with chloramphenicol at 0.5 mg/ml to arrest translation elongation and were rapidly cooled on ice before centrifugation. Cells were lysed shortly before preparation of 10-40% sucrose gradients, ultracentrifugation, and analysis. Abundance of RNA species was monitored by absorbance at 254 nm (A_{254nm}). (*A*) Comparison of *E. coli* and wild-type *Synechococcus* (*Syn*) polysome traces. Top labels indicate the identity of each peak. (*B*) Treatment of wild-type *Synechococcus* lysates with RNase A confirms the identity of polysome peaks. *Synechococcus* lysates were treated with RNase A for 10 minutes to cleave mRNAs linking polysomes before continuing with the sucrose density gradient centrifugation protocol.

We tested *Synechococcus* lysates from control (wild-type) cells in the light, and control and Δ*hpf* cells after a two-hour dark pulse. In the light, control cell lysates contained several polysome peaks, indicating active translation (Figure 2-11C). In control cells in the dark, however, a significant fraction of ribosomes exists in a state that sediments between monosomes and the first polysome peak, likely corresponding to dimerized ribosomes (asterisk in Figure 2-11D). Furthermore, few polysomes were observed, consistent with the observation that translation rates are lower after two hours in the dark in *Synechococcus* (Figure 2-3H). In the Δ*hpf* mutant, ribosomes do not dimerize and instead can be found as polysomes (Figure 2-11E). We conclude from these results that ribosomal status is altered in the Δ*hpf* mutant, so that the ribosomal pool of the Δ*hpf* mutant resembles that of wild-type cells in the light. Overall, these data suggest that *hpf* could be one mechanism by which (p)ppGpp controls translation, tuning protein synthesis in response to environmental cues.

2.4 Discussion

Here, we have shown that the stringent response is an important mechanism by which *Synechococcus* adapts to darkness. Levels of (p)ppGpp rise in response to a light-to-dark shift, causing dramatic changes in gene expression and regulating ribosomal populations through HPF. By inducing high (p)ppGpp levels, we find that (p)ppGpp can control many fundamental cellular processes in *Synechococcus* (Figure 2-14).

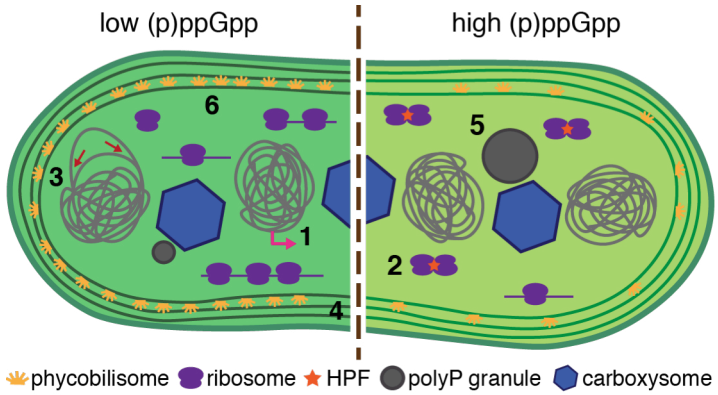

Figure 2-14. Model of (p)ppGpp regulation in *Synechococcus*. Our results indicate that many fundamental processes are regulated by (p)ppGpp in *Synechococcus*. These are schematicized in the figure above, and include (1) transcription, (2) translation, (3) DNA replication, (4) cell growth and division, (5) polyP granule formation, and (6) photosynthesis.

2.4.1 The stringent response as a coordinator of light/dark physiology in Synechococcus

It has been known for many years that cyanobacteria respond and adapt to both high light and low light conditions. While there is greater understanding of the photoprotective mechanisms that allow cells to adapt to high light (2), relatively little is known about how cells coordinate their response to darkness.

Our findings provide evidence that the stringent response helps *Synechococcus* adapt to darkness, and help explain previous observations about cyanobacterial physiology. In 1975, Singer and Doolittle reported that translation rates fall dramatically after a light/dark shift in *Synechococcus* (30). It is also known that treating *Synechococcus* with inhibitors of photosynthetic electron transport generally suppresses translation (40). We propose that loss of photosynthetic activity leads to increased (p)ppGpp levels, triggering increased HPF production. Higher levels of HPF dimerize ribosomes and likely work with additional cellular factors to decrease translation rates. High (p)ppGpp levels also suppress transcription of a subset of genes, slow or stop DNA replication, and prevent cell division in the dark (Figure 2-3).

Circadian rhythm is an important global regulator in *Synechococcus*, and is known to improve cellular fitness in oscillating light/dark cycles (41). It is interesting, therefore, that the capacity to stimulate ppGpp production seems to be independent of circadian rhythm. The experiments presented in Figure 2-1 were performed using replicate *Synechococcus* cultures harvested at different times during the circadian cycle, yet the relative ppGpp levels and kinetics of production are remarkably consistent across replicates. We have shown that the stringent response is important for responding to regular light/dark cycles (Figure 2-7B), but it is also activated during unexpected periods of darkness. It is likely that, in its native freshwater environment, *Synechococcus* could experience intermittent shading, a situation in which an adaptive response to darkness would be of significant benefit.

2.4.2 Conservation and adaptation of stringent response mechanisms in diverse bacteria

The stringent response was first identified in *E. coli* (42)*,* and more recent studies have uncovered targets and mechanisms of this pathway in *B. subtilis*, *C. crescentus,* and several bacterial pathogens (43-45). Although the stringent response works to restore metabolic homeostasis in both *E. coli* and *B. subtilis*, the specific targets of (p)ppGpp are distinct in these organisms. While (p)ppGpp binds directly to RNA polymerase and works with the transcription factor DksA in *E. coli* to control gene expression, (p)ppGpp regulates GTP biosynthesis in *B. subtilis* by directly inhibiting enzymes in this pathway, including guanylate kinase (GMK) (46). Altered GTP levels then affect gene expression in *B. subtilis* and other Firmicutes through the GTP-sensing transcription factor CodY (47). A recent phylogenetic analysis suggests that regulation of RNA polymerase by (p)ppGpp is conserved throughout the Proteobacteria, while regulation of GTP biosynthesis is conserved throughout the Firmicutes (48). This analysis does not predict a mechanism for the stringent response in cyanobacteria, but several observations suggest that neither of these strategies fully accounts for the global regulation enacted by (p)ppGpp in *Synechococcus*. *In vitro* assays with *Synechococcus* GMK have shown that it is insensitive to (p)ppGpp (49), and its genome lacks CodY and DksA homologs as well as the (p)ppGpp-interacting motif on RNA polymerase (50). Although it is likely that alteration of GTP pools as a result of (p)ppGpp synthesis could affect cell physiology and metabolic processes, we do not observe dramatic decreases in rRNA precursor levels when (p)ppGpp levels are high (Figure 2-12), even though GTP is the initiating nucleotide for rRNA transcription in *Synechococcus* (51).

As a photoautotroph, *Synechococcus* lives a very different metabolic lifestyle than the bacterial model systems in which the stringent response has been studied. Because photosynthesis forms the foundation of cyanobacterial growth, it is logical that (p)ppGpp would be synthesized in conditions that are unfavorable for photosynthesis, like darkness, and that this pathway can feed back to regulate levels of light-harvesting pigments. A study in the facultative phototroph *Rhodobacter capsulatus* suggested a link between the stringent response and regulation of photosynthetic gene expression/genome structure by the nucleoid protein HvrA (52), but this a-proteobacterium is only distantly related to cyanobacteria, and has greater metabolic

flexibility. It is likely that the strategies employed by cyanobacteria to respond to darkness differ from those employed by facultative phototrophs. We are beginning to appreciate the mechanisms behind the stringent response in *Synechococcus*, but much work remains to determine how (p)ppGpp levels can lead to altered physiology in phototrophic organisms.

2.4.3 HPF and translational regulation by (p)ppGpp

Regulation of translation is a classic mechanism of the stringent response. This can be accomplished by immediate action of (p)ppGpp on the translation apparatus, or by longer-term changes in gene expression of rRNAs, tRNAs, and ribosomal and ribosome-associated proteins. These are important adaptations during starvation since production of ribosomes can consume a significant fraction of the cell's energy supply (53). Immediately after encountering a stress, the cell contains its full complement of ribosomes and uses post-translational mechanisms to decrease the activity of these preexisting ribosomes. One way bacteria can do this is through direct inhibition of ribosomal GTPases by (p)ppGpp, as has been shown for the translation initiation factor IF2 (54) as well as for GTPases of *Staphylococcus aureus* (55). Alternatively, expression of factors such as HPF can modulate ribosome activity over longer timescales (56).

HPF is known to dimerize ribosomes in *Listeria monocytogenes, B. subtilis*, and *E. coli* in response to conditions that increase (p)ppGpp levels, such as stationary phase (57-59). We have shown that *hpf* expression is (p)ppGpp-regulated, and that *hpf* affects ribosomal status under conditions that decrease translation rates in *Synechococcus*, suggesting that it may contribute to this phenotype. Twenty years ago, HPF was identified as a protein made at high levels in the dark in *Synechococcus* sp. PCC 7002, and a mutation in this gene appears to alter patterns of protein synthesis after dark adaptation (60). This is an intriguing result, but little is known about the extent to which HPF affects translation rates *in vivo* in any organism or whether HPF might alter translational specificity. *Synechococcus* synthesizes a distinct set of 'dark-specific' polypeptides after a shift to darkness (8) – which is consistent with the transcriptional changes seen under these conditions – but the identities of these proteins and how production of specific proteins is controlled remain unknown.

2.4.4 Signals that trigger the stringent response are different in photosynthetic organisms

The range of stresses sensed by the stringent response encompasses carbon sources, nitrogen sources, and inorganic nutrients. Light represents an equally – if not more – important signal of nutritional status in *Synechococcus*. A cyanobacterial cell experiences dramatic intracellular changes in its redox state and pH, for example, depending on whether it is actively photosynthesizing (61). Redox state regulates centrally important metabolic enzymes in the cyanobacterium *Synechocystis* through thioredoxins, which mediate reduction of disulfides (62). Similar signals could trigger (p)ppGpp synthesis once photosynthesis stops. Inhibition of photosynthesis is known to

reduce translation in *Synechococcus* (40), an effect we also observe after inducing high (p)ppGpp levels. It would be interesting to determine whether inhibitors of photosynthesis mimic the effects of darkness and induce other physiological effects of the stringent response. Several observational studies have shown that ppGpp levels in *Synechococcus* rise in response to stresses such as elevated temperature (8) and nitrogen starvation (22, 63), but these studies did not investigate the mechanisms upstream of ppGpp synthesis or the physiological responses of the organism under these conditions.

Plants also contain (p)ppGpp metabolic enzymes (64). In *Arabidopsis thaliana* all of these proteins localize to the chloroplast (27, 65), and ppGpp levels rise in plants in response to darkness and other stresses, including wounding (66). Two recent studies have also shown that ppGpp levels affect photosynthetic capacity and chloroplast development in *Arabidopsis* (27, 67). Thus, it is likely that aspects of the stringent response pathway are conserved between cyanobacteria and chloroplasts.

Diverse bacterial taxa have different configurations of (p)ppGpp synthetases and hydrolases, but the fact that they are present in all but obligate pathogens suggests that they have been adapted to incredibly diverse lifestyles. Cyanobacteria represent an understudied group of organisms that could provide clues to the core principles and flexible components of this conserved bacterial stress response, while at the same time telling us about the unique stresses faced by phototrophs.

2.5 Acknowledgments

We thank A. Whiteley and the D. Portnoy laboratory for providing *E. coli* strains for and assistance with ppGpp detection experiments; K. Sogi and the S. Stanley laboratory for assistance with ^{14}C incorporation experiments and use of equipment; the UC Davis sequencing facility for constructing RNA-seq libraries, acquiring sequencing data, and initial data analysis; and V. Yu and the J. Cate laboratory for assistance with polysome experiments and use of equipment. We are grateful to R. Yokoo for critical reading of the manuscript, and C. Cassidy-Amstutz for help with statistical analysis. This work was supported by the DOE Office of Science Early Career Research Program (Grant number DE-SC0006394) through the Office of Basic Energy Sciences and an Alfred P. Sloan Research Fellowship to DFS. RDH and AF were supported by the National Science Foundation Graduate Research Fellowship Program.

2.6 References

1. Külheim C, Agren J, Jansson S (2002) Rapid regulation of light harvesting and plant fitness in the field. *Science* 297(5578):91–93.

2. Bailey S, Grossman A (2008) Photoprotection in cyanobacteria: regulation of light harvesting. *Photochem Photobiol* 84(6):1410–1420.

3. Ito H, et al. (2009) Cyanobacterial daily life with Kai-based circadian and diurnal genome-wide transcriptional control in Synechococcus elongatus. *Proc Natl Acad Sci USA* 106:14168–14173.

4. Vijayan V, Zuzow R, O'Shea EK (2009) Oscillations in supercoiling drive circadian gene expression in cyanobacteria. *Proc Natl Acad Sci USA* 106:22564–22568.

5. Doolittle WF (1979) The cyanobacterial genome, its expression, and the control of that expression. *Adv Microb Physiol* 20:1–102.

6. Binder BJ, Chisholm SW (1990) Relationship between DNA cycle and growth rate in Synechococcus sp. strain PCC 6301. *J Bacteriol* 172:2313–2319.

7. Mori T, Binder B, Johnson CH (1996) Circadian gating of cell division in cyanobacteria growing with average doubling times of less than 24 hours. *Proc Natl Acad Sci USA* 93:10183–10188.

8. Suranyi G, Korcz A, Palfi Z, Borbely G (1987) Effects of light deprivation on RNA synthesis, accumulation of guanosine 3'(2‘)-diphosphate 5’-diphosphate, and protein synthesis in heat-shocked Synechococcus sp. strain PCC 6301, a cyanobacterium. *J Bacteriol* 169:632–639.

9. Hosokawa N, et al. (2011) Circadian transcriptional regulation by the posttranslational oscillator without de novo clock gene expression in Synechococcus. *Proc Natl Acad Sci USA* 108:15396–15401.

10. Takano S, Tomita J, Sonoike K, Iwasaki H (2015) The initiation of nocturnal dormancy in Synechococcus as an active process. *BMC Biol* 13(1):36.

11. Allen MM (1968) Simple conditions for growth of unicellular blue-green algae on plates. *J Phycol* 4:1–4.

12. Engler C, Kandzia R, Marillonnet S (2008) A one pot, one step, precision cloning method with high throughput capability. *PLoS ONE* 3(11):e3647.

13. Bokinsky G, et al. (2013) HipA-Triggered Growth Arrest and -Lactam Tolerance in Escherichia coli Are Mediated by RelA-Dependent ppGpp Synthesis. *J Bacteriol* 195(14):3173–3182.

14. Sliusarenko O, Heinritz J, Emonet T, Jacobs-Wagner C (2011) High-throughput, subpixel precision analysis of bacterial morphogenesis and intracellular spatio-temporal dynamics. *Mol Microbiol* 80(3):612–627.

15. Yokoo R, Hood RD, Savage DF (2015) Live-cell imaging of cyanobacteria. *Photosynth Res* 126:33–46.

16. Aschar-Sobbi R, et al. (2008) High Sensitivity, Quantitative Measurements of Polyphosphate Using a New DAPI-Based Approach. *J Fluoresc* 18(5):859–866.

17. McClure R, et al. (2013) Computational analysis of bacterial RNA-Seq data. *Nucleic Acids Res* 41(14):e140.

18. Szekeres E, Sicora C, Dragoş N, Drugă B (2014) Selection of proper reference genes for the cyanobacterium SynechococcusPCC 7002 using real-time quantitative PCR. *FEMS Microbiol Lett* 359(1):102–109.

19. Traxler MF, et al. (2008) The global, ppGpp-mediated stringent response to amino acid starvation in Escherichia coli. *Mol Microbiol* 68(5):1128–1148.

20. Kuroda A, Murphy H, Cashel M, Kornberg A (1997) Guanosine Tetra- and Pentaphosphate Promote Accumulation of Inorganic Polyphosphate in Escherichia coli. *J Biol Chem* 272:21240–21243.

21. Seki Y, Nitta K, Kaneko Y (2014) Observation of polyphosphate bodies and DNA during the cell division cycle of Synechococcus elongatus PCC 7942. *Plant Biol (Stuttg)* 16(1):258–263.

22. Friga GM, Borbely G, Farkas GL (1981) Accumulation of guanosine tetraphosphate (ppGpp) under nitrogen starvation in Anacystis nidulans, a cyanobacterium. *Arch Microbiol* 129:341–343.

23. Nanamiya HH, et al. (2008) Identification and functional analysis of novel (p)ppGpp synthetase genes in Bacillus subtilis. *Mol Microbiol* 67(2):291–304.

24. Hogg T, Mechold U, Malke H, Cashel M, Hilgenfeld R (2004) Conformational Antagonism between Opposing Active Sites in a Bifunctional RelA/SpoT Homolog Modulates (p)ppGpp Metabolism during the Stringent Response. *Cell* 117:57–68.

25. Steinchen W, et al. (2015) Catalytic mechanism and allosteric regulation of an oligomeric (p)ppGpp synthetase by an alarmone. *Proc Natl Acad Sci USA* 112(43):13348–13353.

26. Collier JL, Herbert SK, Fork DC, Grossman AR (1994) Changes in the cyanobacterial photosynthetic apparatus during acclimation to macronutrient deprivation. *Photosynth Res* 42:173–183.

27. Maekawa M, et al. (2015) Impact of the plastidial stringent response in plant growth and stress responses. *Nat Plants*. doi:10.1038/nplants.2015.167.

28. Wang JD, Sanders GM, Grossman AD (2007) Nutritional control of elongation of DNA replication by (p)ppGpp. *Cell* 128(5):865–875.

29. Lesley JA, Shapiro L (2008) SpoT regulates DnaA stability and initiation of DNA replication in carbon-starved Caulobacter crescentus. *J Bacteriol* 190(20):6867–6880.

30. Singer RA, Doolittle WF (1975) Control of gene expression in blue-green algae. *Nature* 253:650–651.

31. Luque I, Forchhammer K (2008) Nitrogen assimilation and C/N balance sensing. *The Cyanobacteria: Molecular Biology, Genomics and Evolution*, eds Herrero A, Flores E (Caister Academic Press, Norfolk, UK), pp 335–382.

32. Garcia-Dominguez M, Reyes JC, Florencio FJ (1999) Glutamine synthetase inactivation by protein-protein interaction. *Proc Natl Acad Sci USA* 96(13):7161–7166.

33. Muro-Pastor MI, Reyes JC, Florencio FJ (2001) Cyanobacteria perceive nitrogen status by sensing intracellular 2-oxoglutarate levels. *J Biol Chem* 276(41):38320–38328.

34. Potrykus K, Cashel M (2008) (p)ppGpp: still magical? *Annu Rev Microbiol* 62:35–51.

35. Cangelosi GA, Brabant WH (1997) Depletion of pre-16S rRNA in starved Escherichia coli cells. *J Bacteriol* 179(14):4457–4463.

36. Ueta M, et al. (2008) Role of HPF (hibernation promoting factor) in translational activity in Escherichia coli. *J Biochem* 143(3):425–433.

37. Ueta M, et al. (2013) Conservation of two distinct types of 100S ribosome in bacteria. *Genes Cells* 18(7):554–574.

38. Polikanov YS, Blaha GM, Steitz TA (2012) How Hibernation Factors RMF, HPF, and YfiA Turn Off Protein Synthesis. *Science* 336(6083):915–918.

39. Qin D, Fredrick K (2013) Analysis of polysomes from bacteria. *Methods Enzymol* 530:159–172.

40. Schmitz O, Tsinoremas NF, Schaefer MR, Anandan S, Golden SS (1999) General effect of photosynthetic electron transport inhibitors on translation precludes their use for investigating regulation of D1 biosynthesis in Synechococcus sp. strain PCC 7942. *Photosynth Res* 62:261–271.

41. Woelfle MA, Ouyang Y, Phanvijhitsiri K, Johnson CH (2004) The Adaptive Value of Circadian Clocks: An Experimental Assessment in Cyanobacteria. *Curr Biol* 14(16):1481–1486.

42. Cashel M, Gallant J (1969) Two compounds implicated in the function of the RC gene of Escherichia coli. *Nature* 221:838–841.

43. Boutte CC, Crosson S (2011) The complex logic of stringent response regulation in Caulobacter crescentus: starvation signalling in an oligotrophic environment. *Mol Microbiol* 80(3):695–714.

44. Dalebroux ZD, Swanson MS (2012) ppGpp: magic beyond RNA polymerase. *Nat Rev Micro* 10(3):203–212.

45. Kriel A, et al. (2012) Direct regulation of GTP homeostasis by (p)ppGpp: a critical component of viability and stress resistance. *Mol Cell* 48(2):231–241.

46. Gaca AO, Colomer-Winter C, Lemos JA (2015) Many means to a common end: the intricacies of (p)ppGpp metabolism and its control of bacterial homeostasis. *J Bacteriol* 197(7):1146–1156.

47. Sonenshein AL (2005) CodY, a global regulator of stationary phase and virulence in Gram-positive bacteria. *Curr Opin Microbiol* 8(2):203–207.

48. Liu K, et al. (2015) Molecular Mechanism and Evolution of Guanylate Kinase Regulation by (p)ppGpp. *Mol Cell* 57:735–749.

49. Nomura Y, et al. (2014) Diversity in Guanosine 3“,5-”Bisdiphosphate (ppGpp) Sensitivity Among Guanylate Kinases of Bacteria and Plants. *J Biol Chem* 289(22):15631–15641.

50. Hauryliuk V, Atkinson GC, Murakami KS, Tenson T, Gerdes K (2015) Recent functional insights into the role of (p)ppGpp in bacterial physiology. *Nat Rev Micro* 13:298–309.

51. Kumano M, Tomioka N, Shinozaki K, Sugiura M (1986) Analysis of the promoter region in the rrnA operon from a blue-green alga, Anacystis nidulans 6301. *Mol Gen Genet* 202:173–178.

52. Masuda S, Bauer CE (2004) Null mutation of HvrA compensates for loss of an essential relA/spoT-like gene in Rhodobacter capsulatus. *J Bacteriol* 186(1):235–239.

53. Chubukov V, Gerosa L, Kochanowski K, Sauer U (2014) Coordination of microbial metabolism. *Nat Rev Micro* 12(5):327–340.

54. Milon P, et al. (2006) The nucleotide-binding site of bacterial translation initiation factor 2 (IF2) as a metabolic sensor. *Proc Natl Acad Sci USA* 103(38):13962–13967.

55. Corrigan RM, Bellows LE, Wood A, Gründling A (2016) ppGpp negatively impacts ribosome assembly affecting growth and antimicrobial tolerance in Gram-positive bacteria. *Proc Natl Acad Sci USA* 113(12):E1710–9.

56. Starosta AL, Lassak J, Jung K, Wilson DN (2014) The bacterial translation stress response. *FEMS Microbiol Rev* 38(6):1172–1201.

57. Wada A, Mikkola R, Kurland CG, Ishihama A (2000) Growth phase-coupled changes of the ribosome profile in natural isolates and laboratory strains of Escherichia coli. *J Bacteriol* 182(10):2893–2899.

58. Tagami K, et al. (2012) Expression of a small (p)ppGpp synthetase, YwaC, in the (p)ppGpp(0) mutant of Bacillus subtilis triggers YvyD-dependent dimerization of ribosome. *MicrobiologyOpen* 1(2):115–134.

59. Kline BC, McKay SL, Tang WW, Portnoy DA (2015) The Listeria monocytogenes Hibernation-Promoting Factor (HPF) is Required for the Formation of 100S Ribosomes, Optimal Fitness, and Pathogenesis. *J Bacteriol* 197(3):581–591.

60. Tan X, Varughese M, Widger WR (1994) A light-repressed transcript found in Synechococcus PCC 7002 is similar to a chloroplast-specific small subunit ribosomal protein and to a transcription modulator protein associated with sigma 54. *J Biol Chem* 269(33):20905–20912.

61. Tamoi M, Miyazaki T, Fukamizo T, Shigeoka S (2005) The Calvin cycle in cyanobacteria is regulated by CP12 via the NAD(H)/NADP(H) ratio under light/dark conditions. *Plant J* 42(4):504–513.

62. Lindahl M, Florencio FJ (2003) Thioredoxin-linked processes in cyanobacteria are as numerous as in chloroplasts, but targets are different. *Proc Natl Acad Sci USA* 100(26):16107–16112.

63. Borbely G, Kaki C, Gulyás A, Farkas GL (1980) Bacteriophage infection interferes with guanosine 3“-diphosphate-5-”diphosphate accumulation induced by energy and nitrogen starvation in the cyanobacterium Anacystis nidulans. *J Bacteriol* 144(3):859–864.

64. Atkinson GC, Tenson T, Hauryliuk V (2011) The RelA/SpoT Homolog (RSH) Superfamily: Distribution and Functional Evolution of ppGpp Synthetases and Hydrolases across the Tree of Life. *PLoS ONE* 6(8):e23479.

65. Masuda S, et al. (2008) The bacterial stringent response, conserved in chloroplasts, controls plant fertilization. *Plant Cell Physiol* 49(2):135–141.

66. Takahashi K, Kasai K, Ochi K (2004) Identification of the bacterial alarmone guanosine 5“-diphosphate 3-”diphosphate (ppGpp) in plants. *Proc Natl Acad Sci USA* 101(12):4320–4324.

67. Sugliani M, et al. (2016) An Ancient Bacterial Signaling Pathway Regulates Chloroplast Function to Influence Growth and Development in Arabidopsis. *The Plant Cell* 28(3):661–679.

Chapter 3

The stringent response helps *Synechococcus* adapt to a diverse range of stressors

3.1 Introduction

Growth of many bacteria is limited in their native environment due to a number of factors, such as competition or nutrient limitation. In aquatic environments, for example, nutrient availability can vary greatly and depends on both biotic and abiotic factors (1).

Cyanobacteria are abundant in aquatic environments – particularly in the ocean (2) – and play important roles as primary producers and in the carbon cycle. The metabolic requirements of a cyanobacterial cell are relatively simple: they need light for photosynthesis and inorganic nutrients containing carbon, nitrogen, sulfur, iron, phosphorus, calcium, and other trace elements.

Fluctuations in nutrient availability present challenges to any organism. For cyanobacteria – which are relatively self-sufficient, in the sense that they have many biosynthetic capabilities – these variations present differently than for more traditionally studied, heterotrophic bacteria like *Escherichia coli* and *Bacillus subtilis*. For one, light intensity and wavelength vary due to the time of day, weather conditions, and shading, and all of these changes affect photosynthetic metabolism. If there is too little light, the cell's ability to harvest and store energy is low, whereas if there is too much light, the cell can be subjected to high levels of reactive oxygen species (ROS) that trigger high light stress responses (3).

Starvation for inorganic nutrients can be equally trying, due to the interconnected nature of metabolism (Figure 1-2). If nitrogen sources are limited, for example, the carbon/nitrogen balance within the cell will be disrupted. This requires adjustments not only in nitrogen metabolism but also in central carbon metabolic pathways (4).

Bacteria respond to nutrient limitation in many ways, but in this work we have focused on when and how the stringent response helps the cyanobacterium *Synechococcus elongatus* (hereafter, *Synechococcus*) adapt to metabolic challenges. The stringent response is a conserved bacterial stress response mediated by the nucleotide second messengers ppGpp (guanosine 3'-diphosphate 5'-diphosphate) and pppGpp (guanosine 3'-diphosphate 5'-triphosphate), here collectively termed (p)ppGpp where appropriate. First, however, we will briefly review known responses to photosynthetic inhibition and nutrient starvation in *Synechococcus*.

3.1.1 Responses of Synechococcus *to photosynthetic inhibition*

Herbicides have been used for many years to perturb photosynthesis. One such herbicide, DCMU (3-(3,4-dichlorophenyl)-1,1-dimethylurea), inhibits electron transfer from photosystem II (PSII) to quinones in the thylakoid membrane (Figure 3-1). When

cultures of *Synechococcus* are treated with DCMU at levels that fully inhibit photosynthetic electron transfer (≥ 1 μM), many physiological responses ensue. Growth ceases (5), glycogen stores are broken down (6), translation generally decreases (7), DNA replication initiation stops (8), and activity of glutamine synthetase, a key enzyme of nitrogen metabolism, decreases (9). Altogether, the effects of DCMU generally mimic those of darkness, dramatically affecting nearly all aspects of *Synechococcus* physiology. However, many of the molecular mechanisms behind these responses remain unknown.

3.1.2 Responses of Synechococcus *to nutrient starvation*

Cyanobacteria bleach in response to starvation for nitrogen or sulfur, in a process called chlorosis (10). During chlorosis, cells degrade their photosynthetic pigments and protein complexes, thereby both increasing the availability of nitrogen- and sulfur-containing amino acids (11) and lowering the amount of light harvested. This allows cells to adjust to lower fluxes in downstream pathways that act as sinks of ATP and/or reducing power generated by photosynthesis. Within the first few days of nitrogen or sulfur deprivation, pigmentation decreases rapidly (12).

In the early 1990s, Collier and Grossman found that a small protein called NblA controls degradation of phycobilisomes, the major light-harvesting complexes in cyanobacteria (13). Expression of this gene is controlled by the response regulator NblR, as well as the nitrogen starvation-responsive transcription factor NtcA (14, 15). NblA is known to interact with both phycobiliproteins, which comprise the phycobilisome, and a chaperone of a cyanobacterial Clp protease, and is thought to target phycobiliproteins for degradation (16-18). NblA and its regulators have been well-studied in the context of nitrogen starvation, but additional questions remain. It is not well understood how general physiological responses to nutrient starvation are coordinated, nor how *Synechococcus* deals with starvation for nutrients other than nitrogen.

3.1.3 Objective

We showed previously that the stringent response becomes activated when *Synechococcus* encounters darkness, and that it is both necessary and sufficient to induce transcriptional, translational, and other physiological changes (Chapter 2). Following up on these observations, we set out to characterize other inputs into the pathway and to learn more about the mechanisms by which it regulates cellular physiology.

First, we determined whether the pathway is necessary for *Synechococcus* to survive exposure to several stressors. We followed up on these observations by measuring how the stringent response alters the photosynthetic machinery when the cell encounters metabolically unfavorable conditions. In this chapter, we also describe approaches that will allow us to learn more about how (p)ppGpp levels are controlled and how they affect downstream targets that lead to physiological responses of *Synechococcus*.

3.2 Materials and Methods

3.2.1 Bacterial strains and culture conditions

Synechococcus elongatus PCC 7942 was grown in BG-11 media (19) at 30°C with shaking (185 rpm) under white fluorescent lights at 60-100 µE. Cultures were grown either in a programmable photosynthetic incubator (Percival Scientific, Perry, IA) or in an environmental (30°C) room. Unless otherwise indicated, *Synechococcus* cultures were induced with 50 µM isopropyl β-D-1-thiogalactopyranoside (IPTG) when appropriate. Single antibiotics (chloramphenicol [Cm], kanamycin [Kan], spectinomycin [Sp]) were used at a final concentration of 10 µg/ml, and double antibiotics at 2 µg/ml each.

Cultures were treated with 1 µM DCMU (3-(3,4-dichlorophenyl)-1,1-dimethylurea; Sigma-Aldrich) where specified. Starvation media were prepared as follows: N-starvation media: replace 18 mM $NaNO_3$ with 18 mM NaCl; S-starvation media: replace 0.3 mM $MgSO_4$ with 0.3 mM $MgCl_2$; Fe-starvation media: omit 22 µM ammonium iron citrate from BG-11 and add 100 µM 2,2'-bipyridine (Sigma-Aldrich), an iron chelator; phosphate-starvation media: reduce phosphate levels in media from 175 µM HPO_4^{2-} 1000-fold, to 0.175 µM HPO_4^{2-}.

Escherichia coli was grown in LB media at 37°C with shaking (250 rpm), unless otherwise noted. When appropriate, chloramphenicol was used at 25 µg/ml, and kanamycin at 60 µg/ml for *E. coli*. Measurements of culture optical density (OD_{600} or OD_{750}, subscript indicating wavelength in nm) were performed using a Thermo Scientific Genesys 20 spectrophotometer (Waltham, MA).

3.2.2 Plasmid and strain construction

All plasmids were constructed using a Golden Gate cloning strategy (20) and were propagated in *E. coli* DH5α. Primers were designed to amplify genes such that a BsaI restriction enzyme site would be added onto both ends, and overhangs generated by digestion with BsaI would be complementary to those present in Golden Gate destination plasmids. Golden Gate reactions (incorporating cycles of restriction enzyme digestion and ligation) were incubated for 50 cycles of 45°C for 5 min and 16°C for 2 min, followed by incubations at 50°C for 10 min and 80°C for 10 min to inactivate the enzymes. Standard methods were used for PCR, gel purification of PCR products, *E. coli* transformation, and DNA sequencing to verify cloned constructs. Table 3-1 lists the plasmids and primers used in this chapter.

Table 3-1. Plasmids and primers used in Chapter 3.

plasmid name	reference
pNS1 (Sp^R)	Clerico, EM, Ditty, JL, and SS Golden (2007) Methods Mol Biol 362: 115-129
pNS1-BSU11600	this study
pNS2 (Kan^R)	Clerico, EM, Ditty, JL, and SS Golden (2007) Methods Mol Biol 362: 115-129
pNS2-BSU11600	Chapter 2
pNS2-BSU11600- Sp^R	this study
pNS2-BSU11600_D72G	Chapter 2
pNS2-BSU11600_D72G- Sp^R	this study
pNS2-Synpcc7942_1377	Chapter 2
pNS2-6xHis-Synpcc7942_1377	this study
pNS2-Synpcc7942_1377-FLAG	this study
pNS2-3xFLAG-Synpcc7942_1377	this study
pNS2-Synpcc7942_1377-3xFLAG	this study
pNS3 (Cm^R)	Clerico, EM, Ditty, JL, and SS Golden (2007) Methods Mol Biol 362: 115-129
pUC-ΔSynpcc7942_1377(rel)-Cm^R	Chapter 2
pUC-ΔSynpcc7942_2127(nblA)-Kan^R	this study
primer name	**primer sequence**
BSU11600-F-BsaI-GG	CACACCA GGTCTC A GTCC GATGACAAACAATGGGAGCG
BSU11600-R-stop-BsaI-GG	CACACCA GGTCTC A CGCT CTATTGTTGCTCGCTTCCTT
BSU11600-D72G-F-GG	CACACCA GGTCTC A GGTA TTGCTGGCCTTAGAATCATG
BSU11600-D72G-R-GG	CACACCA GGTCTC A TACC CTGCATGGTTTCAATTTCATGC
Synpcc7942_1377-F-BsaI-GG	CACACCA GGTCTC A GTCC ccgtcagccggtttgccg
Synpcc7942_1377-R-stop-BsaI-GG	CACACCA GGTCTC A CGCT tcacagctcatcatcgctgccg
Synpcc7942_1377-F-6xHis-BsaI-GG	CACACCA GGTCTC A GTCC caccatcaccatcaccat ccgtcagccggtttgccg
Synpcc7942_1377-R-FLAG-BsaI-GG	CACACCA GGTCTC A CGCT tca CTTATCGTCATCGTCTTTATAGTC cagctcatcatcgctgccg
Synpcc7942_1377-F-3xFLAG-BsaI-GG	CACCA GGTCTC A GTCC GACTACAAGGACCACGATGGAGATTACAAAGACCATGACATTGACTAC AAAGATGACGACGACAAG ccgtcagccggtttgccg
Synpcc7942_1377-R-3xFLAG-BsaI-GG	ACCA GGTCTC A CGCT tca CTTGTCGTCGTCATCTTTGTAGTCAATGTCATGGTCTTTGTAATCTCCAT CGTGGTCCTTGTAGTC cagctcatcatcgctgccg
rel-KO-up-F-BsaI-GG	CACACCA GGTCTC A CGCT ctggtcagcaagacttccagca
rel-KO-up-R-BsaI-GG	CACACCA GGTCTC A TACT cgaacgtgcgatcgctcc
rel-KO-down-F-BsaI-GG	CACACCA GGTCTC A TAGC tcactcagctatccaactgatg
rel-KO-down-R-BsaI-GG	CACACCA GGTCTC A GTCC ctggatctgaatccacacgatc
rel-KO-screen-F	catcgcctttcgcacagct
rel-KO-screen-R	cacagatcactgcagcactg
Cm^R-F-BsaI-GG	CACACCA GGTCTC A AGTA cactggagcacctcaa
Cm^R-R-BsaI-GG	CACACCA GGTCTC A GCTA ctgccaccgctgagc
nblA-KO-up-F-BsaI-GG	CACACCA GGTCTC A CGCT ctggcgatcgccgacgtag
nblA-KO-up-R-BsaI-GG	CACACCA GGTCTC A TACT gggagcctccggcactg
nblA-KO-down-F-BsaI-GG	CACACCA GGTCTC A TAGC accgtgtgcaagacttgcc
nblA-KO-down-R-BsaI-GG	CACACCA GGTCTC A GTCC gtcagccatcagccgctg
nblA-KO-screen-F	gtattgacggctcgtcaagc
nblA-KO-screen-R	gcctttgaagatgttctcgtgtg
Kan^R-F-BsaI-GG	CACACCA GGTCTC A AGTA agcttagatcgacctgcag
Kan^R-R-BsaI-GG	CACACCA GGTCTC A GCTA gcgctgaggtctgcctcg

Synechococcus was transformed by growing cultures to log phase (OD_{750} 0.2-0.6), harvesting cells by centrifugation (16000 g, 2 min, 25°C), washing cells once in 0.5X volume of 10 mM NaCl, and resuspending cells in 0.1X volume of BG-11 media. Approximately 200 ng of the plasmid to be transformed was added, and cultures were wrapped in foil and incubated overnight at 30°C. The next day, transformations were plated on BG-11 plates containing the appropriate selective antibiotic. All deletion strains were verified by colony PCR, using primers to detect both the native locus and the deletion construct, and were fully penetrant. Table 3-2 lists and describes the strains used in this chapter.

Table 3-2. Strains used in Chapter 3.

Strain name	Strain genotype	Resistance	Reference
Synechococcus elongatus PCC 7942 wild-type (WT)	WT	–	–
control (WT-Cm^R)	pNS3	Cm	Chapter 2
$ppGpp^+$	pNS2-BSU11600	Kan	Chapter 2
$ppGpp^+$ (Kan^R/Sp^R)	pNS2-BSU11600 + pNS1	Kan, Sp	this study
$ppGpp^+$ D72G	pNS2-BSU11600_D72G	Kan	Chapter 2
$ppGpp^+$ D72G (Kan^R/Sp^R)	pNS2-BSU11600_D72G + pNS1	Kan, Sp	this study
$ppGpp^{++}$	pNS2-BSU11600 + pNS1-BSU11600	Kan, Sp	this study
rel	pNS2-rel	Kan	this study
6xHis-rel	pNS2-6xHis-rel	Kan	this study
rel-FLAG	pNS2-rel-FLAG	Kan	this study
3xFLAG-rel	pNS2-3xFLAG-rel	Kan	this study
rel-3xFLAG	pNS2-rel-3xFLAG	Kan	this study
Δ*rel*	ΔSynpcc7942_1377-Cm^R	Cm	Chapter 2
Δ*rel* + vector	ΔSynpcc7942_1377-Cm^R +pNS2	Cm, Kan	Chapter 2
Δ*rel* + *rel*	ΔSynpcc7942_1377-Cm^R + pNS2-Synpcc7942_1377	Cm, Kan	Chapter 2
Δ*rel* + 3xFLAG-*rel*	ΔSynpcc7942_1377-Cm^R + pNS2-3xFLAG-Synpcc7942_1377	Cm, Kan	this study
Δ*rel* + *rel*-3xFLAG	ΔSynpcc7942_1377-Cm^R + pNS2-Synpcc7942_1377-3xFLAG	Cm, Kan	this study
Δ*nblA*	ΔSynpcc7942_2127-Kan^R	Kan	this study
Δ*nblA* $ppGpp^+$	ΔSynpcc7942_2127-Kan^R + pNS2- pNS2-BSU11600- Sp^R	Kan, Sp	this study
Δ*nblA* $ppGpp^+$ D72G	ΔSynpcc7942_2127-Kan^R + pNS2- pNS2-BSU11600_D72G- Sp^R	Kan, Sp	this study
Escherichia coli W3110 wild-type (CF1943)	WT	–	Michael Cashel (NIH)
E. coli W3110 *relA251::Kan* (CF1944)	*relA::Kan*	Kan	Michael Cashel (NIH)

3.2.3 Absorbance scans

Absorbance scans of *Synechococcus* cultures were performed using a Tecan Infinite M1000 Pro plate reader (Männedorf, Switzerland), measuring absorbance between 350-800 nm at 2 nm intervals. An identical absorbance scan was performed using sterile media, and these values were subtracted from culture readings.

3.2.4 SDS-PAGE

Pellets from *Synechococcus* cultures were resuspended in 1X SDS loading buffer, with the volume normalized according to culture density (~3 OD_{750} units of culture resuspended in ~100 µl buffer). One set of samples was left unboiled, while another was boiled at 95°C for 10 minutes. Samples were diluted 1:5 into 1X SDS loading buffer and run on a 10-20% gradient SDS-PAGE gel (Bio-Rad). Gels were imaged using a Bio-Rad Universal Hood III, both to measure fluorescence (phycobiliproteins naturally fluoresce in the YFP imaging channel, which uses an excitation filter with a range of 515-545 nm and an emission filter with a range of 582-632 nm) and after Coomassie staining, which was performed using Thermo Scientific GelCode blue stain reagent according to the manufacturer's protocol. Quantification of bands was performed using ImageJ.

3.2.5 ppGpp measurements

For *E. coli*, 250 ml cultures were grown to log phase (OD_{600} ~0.35), centrifuged to pellet cells, resuspended in 10 ml LB, and split into two cultures. Serine hydroxamate (Sigma) was added to cultures of the WT strain at a final concentration of 1 mg/ml, while the relA^{-} strain was left untreated. Cultures were incubated for 10 minutes with shaking at 37°C before harvesting the entire culture (~55 OD_{600} units). For *Synechococcus*, cultures were grown to log phase (OD_{750} ~0.6) and induced with 500 µM IPTG for 17 hours before harvesting 50 OD_{750} units per culture.

Cells were harvested by filtration, resuspended and lysed by vortexing in 500 µl 13 M formic acid, flash-frozen in liquid nitrogen, and stored at -80°C until further processing. Lysates were thawed at room temperature, subjected to three freeze/thaw cycles alternating between a dry ice/ethanol bath and room temperature, and were clarified by centrifugation (16000 g, 5 min, 4° C). The ppGpp standard was purchased from Trilink Biotechnologies. All samples – whether the ppGpp standard or cell extracts – were diluted to a final concentration of 1 M formic acid, and were filtered using 0.22-µm PES syringe filters before injection.

Samples were analyzed on a Bio-Rad FPLC (NGC chromatography system) using a GE Mono Q 5/50 GL anion exchange column, using a method modified from Traxler et al. (21). Buffer A consisted of 20 mM Tris pH 8.0, while buffer B consisted of 20 mM Tris, 1.5 M sodium formate pH 8.0. The analysis method consisted of: column equilibration, sample injection (injection volume for *E. coli* samples was 300 µl, while for *Synechococcus* samples it was ~3.5 ml), gradient elution (0-55% buffer B for 15 column

volumes), and column washing. Absorbance was monitored at 254 nm, and peaks were integrated using Bio-Rad ChromLab software.

3.2.6 Immunoprecipitation

Synechococcus cultures (250 ml) were grown to an OD_{750} of ~0.1, induced with IPTG for 24 hours (to an OD_{750} of 0.2-0.5), concentrated by centrifugation (4000 g, 20 min, 25°C), resuspended in 10 ml BG-11, and split into 2 x 5 ml tubes. One tube was incubated in the light, and the other in the dark, each for 30 minutes at room temperature. Formaldehyde was added to a final concentration of 1%, and crosslinking was allowed to proceed for 2 minutes before quenching by addition of Tris (pH 8.0) to a final concentration of 0.5 M. Cross-linked cultures were centrifuged (4000 g, 10 min, 25°C), pellets were washed once in 10 ml BG-11, and were stored at -80°C until further processing.

Immunoprecipitation was performed using a method modified from Gerace and Moazed (22). Cell pellets were thawed on ice, resuspended in 800 µl IP lysis buffer (50 mM Na-HEPES pH 7.5, 150 mM NaCl, 1 mM EDTA, 0.5% Triton X-100, 10% glycerol, 0.5 mM DTT, 1 mM PMSF), and lysed by bead beating (3 x 1 min cycles, with 1 minute on ice in between each beating). Tubes were centrifuged quickly (1000 g, 30 sec, 4°C) to sediment beads, the supernatant was transferred to a new tube, and the lysate was clarified by centrifugation (16000 g, 10 min, 4°C). Meanwhile, protein G magnetic beads (Bio-Rad; 33 µl used per reaction) were washed 4 times in IP lysis buffer on a magnetic tube rack. Clarified cell lysate (400 µl) and α-3xFLAG antibody (1.5 µl; Cell Signaling Technologies) were added to washed beads and were incubated at 4°C with rotation for 2 hours. Using a magnetic tube rack, beads were washed 2 times with IP wash buffer 1 (50 mM Na-HEPES pH 7.5, 150 mM NaCl, 1 mM EDTA, 0.5% Triton X-100, 5% glycerol, 0.5 mM DTT, 1 mM PMSF) and 1 time with IP wash buffer 2 (50 mM Na-HEPES pH 7.5, 150 mM NaCl, 1 mM EDTA, 5% glycerol, 1 mM PMSF). Protein was eluted from beads using IP elution buffer (25 mM Na-HEPES pH 7.5, 100 mM NaCl, 1 mM PMSF) containing 200 µg/ml 3xFLAG peptide (Sigma-Aldrich), and was collected after incubation at 4°C with vortexing for 30 min followed by incubation at room temperature for 10 min. Eluates were analyzed by SDS-PAGE, as described in Section 3.2.4, except that silver staining was performed using a Thermo Scientific Pierce silver stain kit according to the manufacturer's protocol.

3.2.7 Suppressor experiments and EMS mutagenesis

To select for spontaneous suppressor mutants of the $ppGpp^{++}$ strain, cultures were grown to log phase, concentrated by centrifugation (4000 g, 15 min, 25°C), plated on BG-11 + 500 µM IPTG, and grown in constant light. Colonies began to appear within ~2 weeks after plating.

To select for spontaneous suppressor mutants of the Δ*rel* strain, cultures were grown to log phase, treated with 1 µM DCMU for 4 days, concentrated by centrifugation (4000 g,

15 min, 25°C), plated, and grown in constant light. Colonies began to appear after 2-3 weeks.

EMS mutagenesis was performed according to (23). Cultures were grown to an OD_{750} of ~1, 5 OD_{750} units were centrifuged (4000 g, 15 min, 25°C), and pellets were resuspended in 0.5 ml BG-11 + 0.5 ml 30 mM potassium phosphate, pH 7.0. EMS (Sigma-Aldrich) was added to a final concentration of 400 mM, tubes were incubated in a heat block at 37°C for 30 min, and 10 ml of 5% sodium thiosulfate was added. Cultures were centrifuged (4000 g, 15 min, 25°C), and pellets were washed twice before resuspension in 5 ml BG-11 with the appropriate antibiotic. EMS-mutagenized cultures (and controls to which no EMS was added) were allowed to recover under low light (~25 μE) for 2 days before backdilution and DCMU treatment.

3.3 Results

3.3.1 The stringent response helps Synechococcus *survive photosynthetic inhibition*

Levels of ppGpp rise in *Synechococcus* in response to a light to dark shift (Figure 2-1). However, the input(s) that signal this shift to darkness remain unknown. To test whether cessation of photosynthesis is sufficient to trigger this response, we used the herbicide DCMU to inhibit linear photosynthetic electron flow (Figure 3-1A).

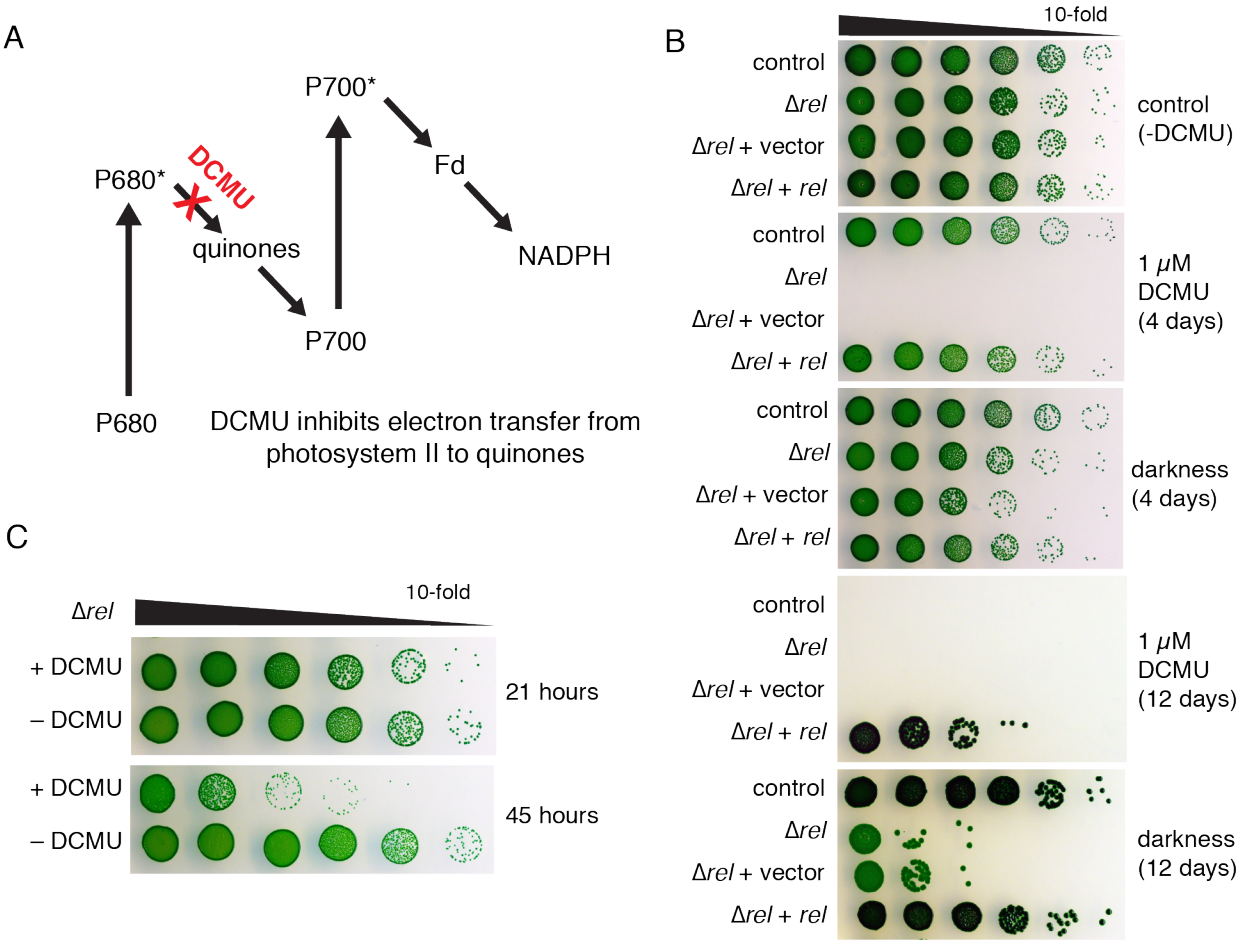

Figure 3-1. Strains unable to synthesize (p)ppGpp are sensitive to photosynthetic inhibition by DCMU. (A) Mechanism of photosynthetic inhibition by DCMU. This molecule interferes with electron transfer from photosystem II to quinones in the thylakoid membrane, thereby inhibiting linear photosynthetic electron flow. (B and C) Tenfold serial dilutions of cultures were plated after the indicated treatment/time and grown in constant light. (B) Survival of the Δ*rel* mutant is more impaired in response to DCMU treatment than incubation in darkness. Images shown are representative of at least two independent experiments. (C) The Δ*rel* mutant starts to lose viability after two days of treatment with 1 μM DCMU.

We tested a panel of *Synechococcus* strains for their ability to survive treatment with 1 μM DCMU, a concentration which inhibits growth of wild-type (WT) cultures. While WT cells retained full viability compared to untreated controls, the Δ*rel* mutant, which cannot make (p)ppGpp, completely lost viability under these conditions (Figure 3-1B). When an IPTG-inducible copy of the *rel* gene was expressed for 27 hours before DCMU treatment, Δ*rel* regained viability equal to that of the WT.

We conclude that the stringent response is activated upon inhibition of photosynthesis by DCMU. We also note that the Δ*rel* mutant loses viability much more quickly in response to DCMU than in response to darkness (Figure 3-1B). While it usually takes at least 4-5 days for the Δ*rel* mutant to lose viability in constant darkness, its viability starts dropping precipitously within 2 days of DCMU treatment (Figure 3-1C). (In other experiments not shown here, viability sometimes drops off even earlier, within ~24 hours of DCMU treatment.)

We hypothesize that this additional toxicity may be due to the presence of light while cells are encountering metabolic disruptions. Since DCMU-treated cultures are incubated under standard light levels (80-100 μE), there may be additional factors contributing to decreased survival of the Δ*rel* mutant, such as increased ROS (23). Without activating the many downstream effects of the stringent response, the Δ*rel* mutant may not be able to mount adaptive responses to this oxidative stress. Preliminary experiments have supported this idea: both WT and Δ*rel* strains retain viability longer when incubated under lower light levels (25 μE) compared to under standard light levels (75 μE) after DCMU treatment (data not shown).

3.3.2 The stringent response helps Synechococcus *survive nutrient starvation*

In other bacteria, (p)ppGpp is made in response to many types of starvation, including deprivation of amino acids, phosphate, and carbon-, iron-, and nitrogen-containing compounds (24). *Synechococcus* is known to respond to nitrogen, sulfur, iron, and phosphate starvation, so we tested whether the stringent response helps cells respond to these insults.

We predicted that mutants unable to induce the stringent response would not survive these challenges as well as WT cells. This was indeed the case, with the effect being strongest in response to nitrogen starvation. After 4 days without a nitrogen source (nitrate), the viability of the Δ*rel* mutant was ~1000-fold lower than that of the WT (Figure 3-2). After 12 days, the only strain that could recover from nitrogen deprivation was the complemented Δ*rel* strain (Δ*rel* + *rel*), which had been pre-induced with IPTG for 27 hours before starvation. We hypothesize that the protective nature of *rel* overexpression is due to stronger activation of the stringent response upon the transition to starvation. This could manifest as higher (p)ppGpp levels produced, which might affect its molecular targets more strongly and lead to more dramatic physiological responses.

The stringent response also helps cells adapt to sulfur or iron starvation. In both cases, the viability of the Δ*rel* mutant was ~10-fold lower than that of the WT after 4 days, and at least 100-fold lower after 12 days (Figure 3-2). We conclude that this stress response pathway helps cells survive starvation for nitrogen, sulfur, and iron, particularly when starvation is more prolonged. We predict that the pathway is more important during the transition to starvation (nutrient downshift), but we cannot rule out that it may play a role during nutrient upshift, since this assay measures both survival and resumption of growth after stress.

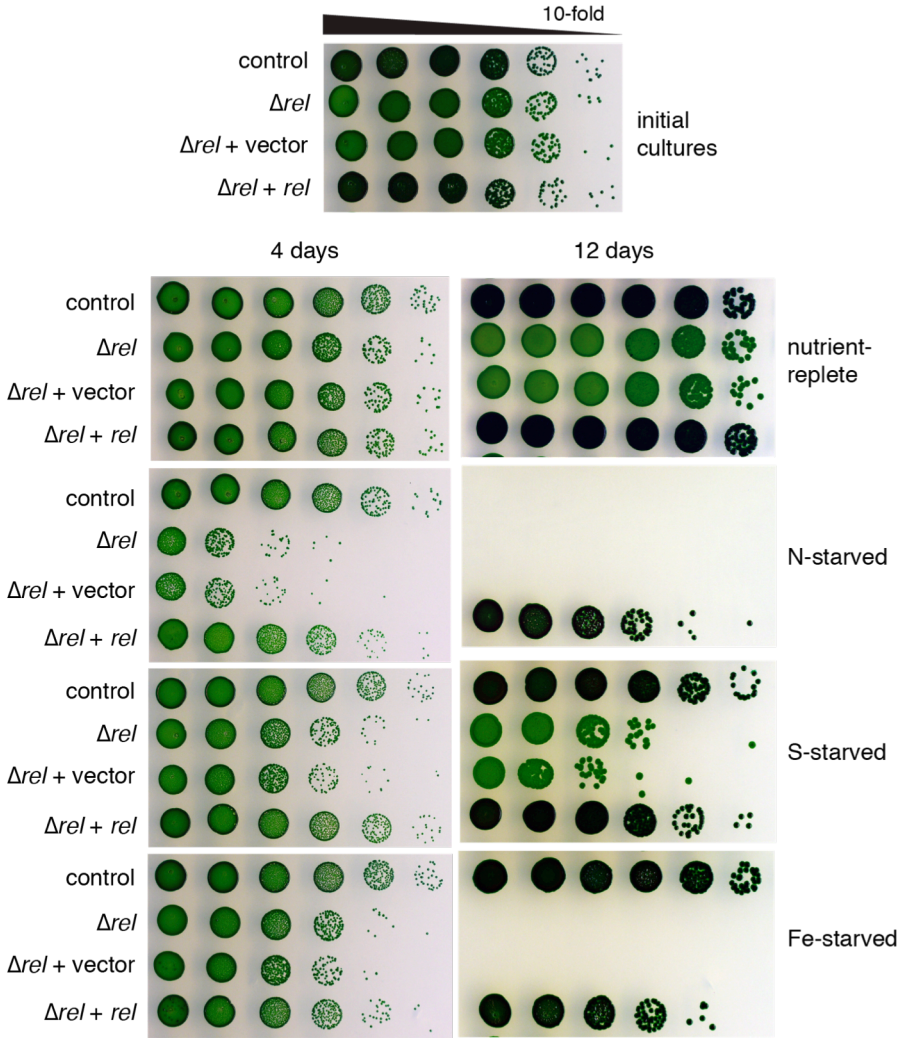

Figure 3-2. Strains unable to make (p)ppGpp cannot survive nutrient starvation as well as wild-type cells. Cultures were grown to log phase and resuspended in media lacking the indicated nutrient (except for nutrient-replete controls, which were resuspended in nutrient-replete media), and incubated in the light. At the indicated time, tenfold serial dilutions were spotted onto nutrient-replete plates and grown in constant light. The Δ*rel* + vector and Δ*rel* + rel strains were induced with IPTG for 27 hours before starvation. Images are representative of at least two independent experiments.

3.3.3 Production of (p)ppGpp is necessary and sufficient to trigger chlorosis, including phycobilisome degradation mediated by nblA

We tested whether the stringent response controls chlorosis, and found that it can be both necessary and sufficient for this process. Wild-type *Synechococcus* normally breaks down its phycobilisomes in response to nitrogen or sulfur starvation, but a mutant lacking the *nblA* gene (Δ*nblA*) does not. Using WT and Δ*nblA* strains as controls, we performed absorbance scans of *Synechococcus* cultures incubated in nutrient-replete media, or media lacking nitrogen or sulfur. (Absorbance scans are typically used as a proxy for the light-harvesting capacity of the cell, and to indicate how the photosynthetic machinery adapts to different growth conditions.)

Absorbance profiles of WT and Δ*rel* strains reveal opposite phenotypes in nitrogen starvation and nutrient-replete conditions. After 4 days of growth in nutrient-replete media, levels of phycobilins (phycobilisome pigments) and chlorophyll are lower in Δ*rel* than in WT (Figure 3-3). This may be related to the fact that growth of Δ*rel* is slightly impaired compared to WT as cultures enter stationary phase (Figure 2-7A).

After nitrogen deprivation, however, phycobilin absorbance is higher in Δ*rel*, indicating that this strain does not degrade its phycobilisomes to the same extent as the WT. While levels of phycobilins and chlorophyll decrease rapidly within the first two days of nitrogen starvation in WT cells, this occurs to a lesser extent in the Δ*rel* strain (Figure 3-3). In comparison, the Δ*nblA* mutant retains high levels of phycobilins over the course of the experiment, while its chlorophyll levels are similar to those of the WT and Δ*rel* strains.

When cultures are starved of sulfur, the WT and Δ*rel* strains behave similarly, showing rapid decreases in phycobilin and chlorophyll pigmentation, while Δ*nblA* again retains high levels of phycobilins (Figure 3-4). In all, these results suggest that the stringent response regulates pigment degradation in response to nitrogen starvation (and possibly stationary phase), but not sulfur starvation. Preliminary results suggest that the stringent response may regulate degradation of photosynthetic complexes during phosphate starvation as well (data not shown).

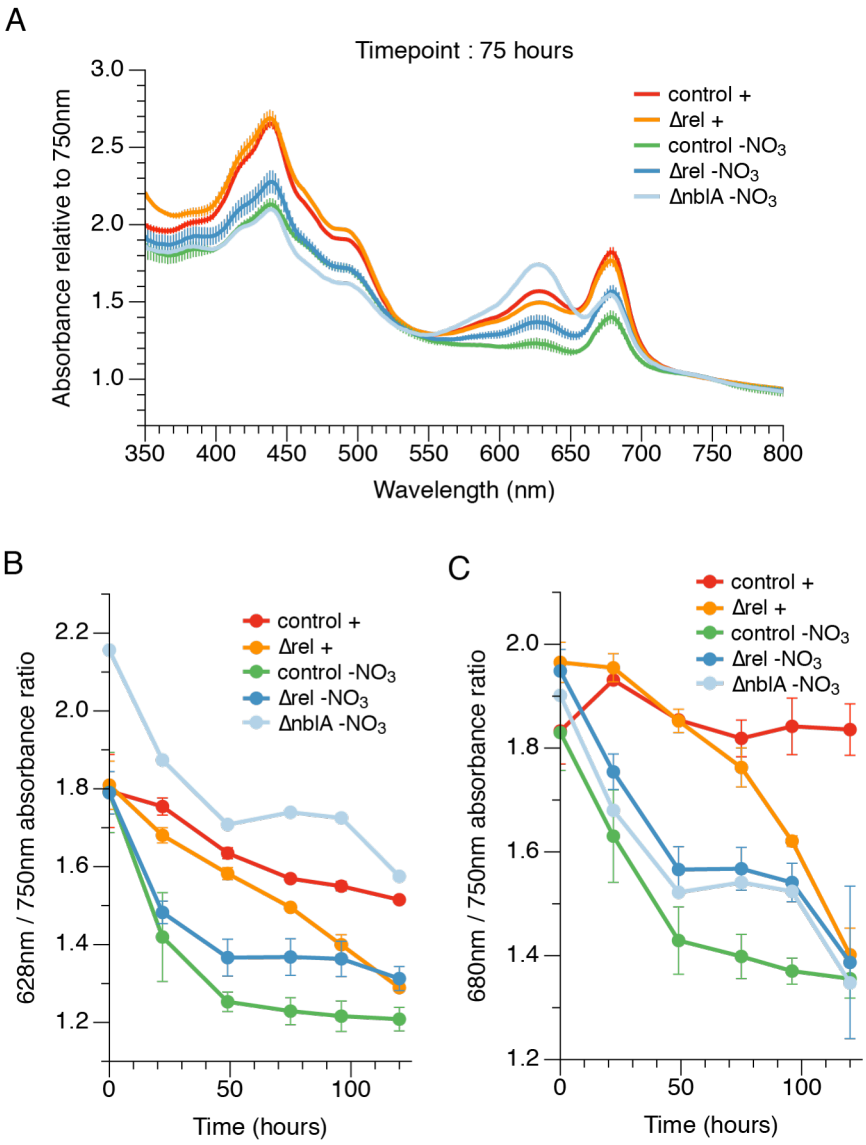

Figure 3-3. The stringent response is involved in degradation of photosynthetic pigments during nitrogen starvation. Cultures were grown to log phase, resuspended in the indicated medium (+, nutrient-replete; -NO_3, N-starvation), and incubated in the light. Absorbance scans were performed at the indicated times and are normalized by absorbance at 750 nm to account for differences in culture density. Data are plotted as mean ± SD, and all conditions are n=3, except for Δ*nblA*, which is n=1. (A) Absorbance scans reveal dramatic changes in pigment absorbance after 75 hours of nitrogen starvation. (B) Absorbance of phycobilisome pigments (phycobilins, which peak at 628 nm) remains higher in the Δ*rel* mutant than in the WT control following nitrogen starvation. Phycobilin absorbance of the Δ*nblA* control remains much higher than any other strain tested. (C) Absorbance of chlorophyll (which peaks at 680 nm) decreases following nitrogen starvation, but remains somewhat higher in Δ*rel* and Δ*nblA* than in the WT control.

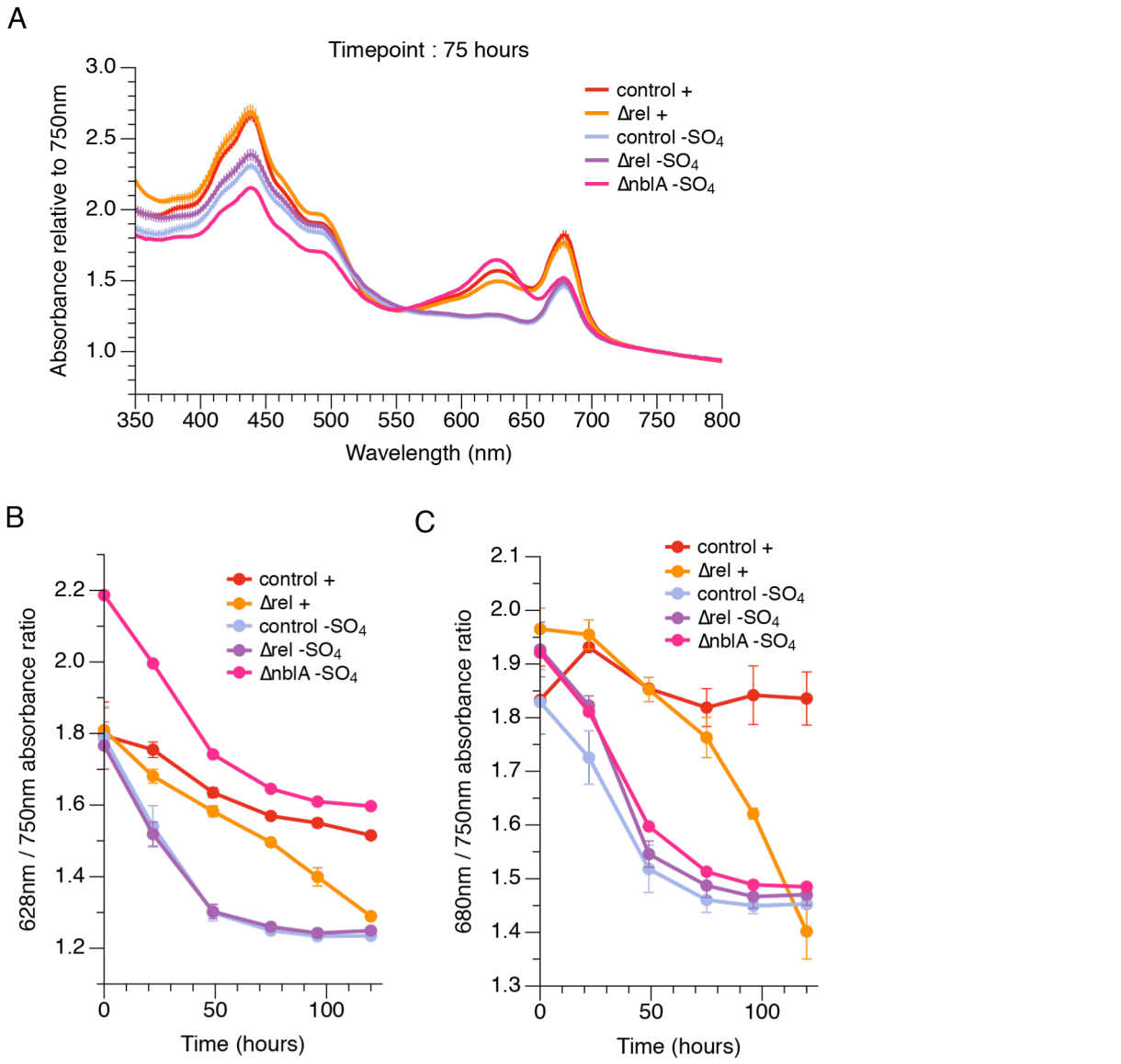

Figure 3-4. The stringent response is not involved in pigment degradation during sulfur starvation. Cultures were grown to log phase, resuspended in the indicated medium (+, nutrient-replete; -SO_4, S-starvation), and incubated in the light. Absorbance scans were performed at the indicated times and are normalized by absorbance at 750 nm to account for differences in culture density. Data are plotted as mean ± SD, and all conditions are n=3, except for Δ*nblA*, which is n=1. (A) Absorbance scans reveal that both the WT control and the Δ*rel* mutant have mostly degraded their phycobilisomes after 75 hours of sulfur starvation. (B) Absorbance of phycobilisome pigments (phycobilins, which peak at 628 nm) falls dramatically in both WT and Δ*rel* following sulfur starvation, while remaining high in the Δ*nblA* control. (C) Absorbance of chlorophyll (which peaks at 680 nm) decreases in all strains following sulfur starvation.

Having seen that the starvation responses of the Δ*rel* mutant are impaired – thus showing that the stringent response is necessary for regulating photosynthetic pigments and proteins in response to starvation – we looked at whether (p)ppGpp is sufficient to do so. We had previously profiled gene expression by RNA-seq (as described in Chapter 2), and noticed that the *nblA* gene was upregulated in the ppGpp$^+$ strain (Figure 3-5A). This was intriguing, and led us to test whether the phycobilisome degradation we had previously observed in this strain (Figures 2-3 and 2-5) is mediated by *nblA*.

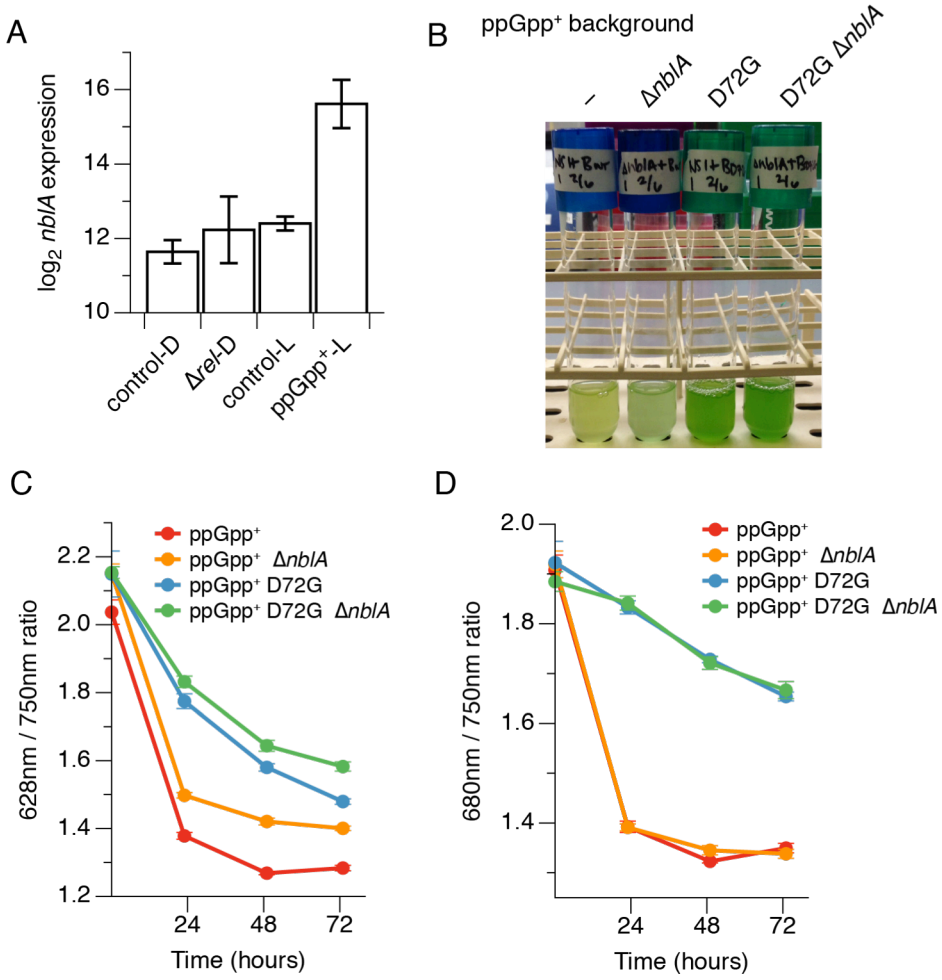

Figure 3-5. Phycobilisome degradation in ppGpp$^+$ works through *nblA*. (A) Expression of *nblA* is increased in the ppGpp$^+$ strain. Data are expression values from the RNA-seq experiment described in Chapter 2. Data are plotted as mean ± SD (n≥3). (B) Relative to ppGpp$^+$, the ppGpp$^+$ Δ*nblA* strain is visibly greener. Photo of cultures used for absorbance scans in (C) and (D), at 73 hours after IPTG induction. (C) The ppGpp$^+$ Δ*nblA* strain does not degrade its phycobilisomes as much as ppGpp$^+$. Absorbance of phycobilins (which peaks at 628 nm) is higher in the ppGpp$^+$ Δ*nblA* strain. (D) Deleting *nblA* does not affect chlorophyll absorbance (which peaks at 680 nm). For (C) and (D), data are plotted as mean ± SD (n≥3), and are normalized by absorbance at 750 nm to account for differences in culture density.

If (p)ppGpp upregulates *nblA*, which is responsible for phycobilisome breakdown, we expected that knocking out *nblA* in the ppGpp$^+$ background should result in higher phycobilisome levels. Indeed, ppGpp$^+$ Δ*nblA* was visibly greener than ppGpp$^+$ within a couple days of IPTG induction (Figure 3-5B). Absorbance scans showed that *nblA* mediates phycobilisome degradation in the ppGpp$^+$ strain, but has no effect on chlorophyll levels (Figures 3-5C, 3-5D, and 3-6). This pattern holds true even in the ppGpp$^+$ D72G strain, which does not make elevated levels of (p)ppGpp, indicating that *nblA* may play a role in regulating phycobilisome levels even under our standard culture conditions.

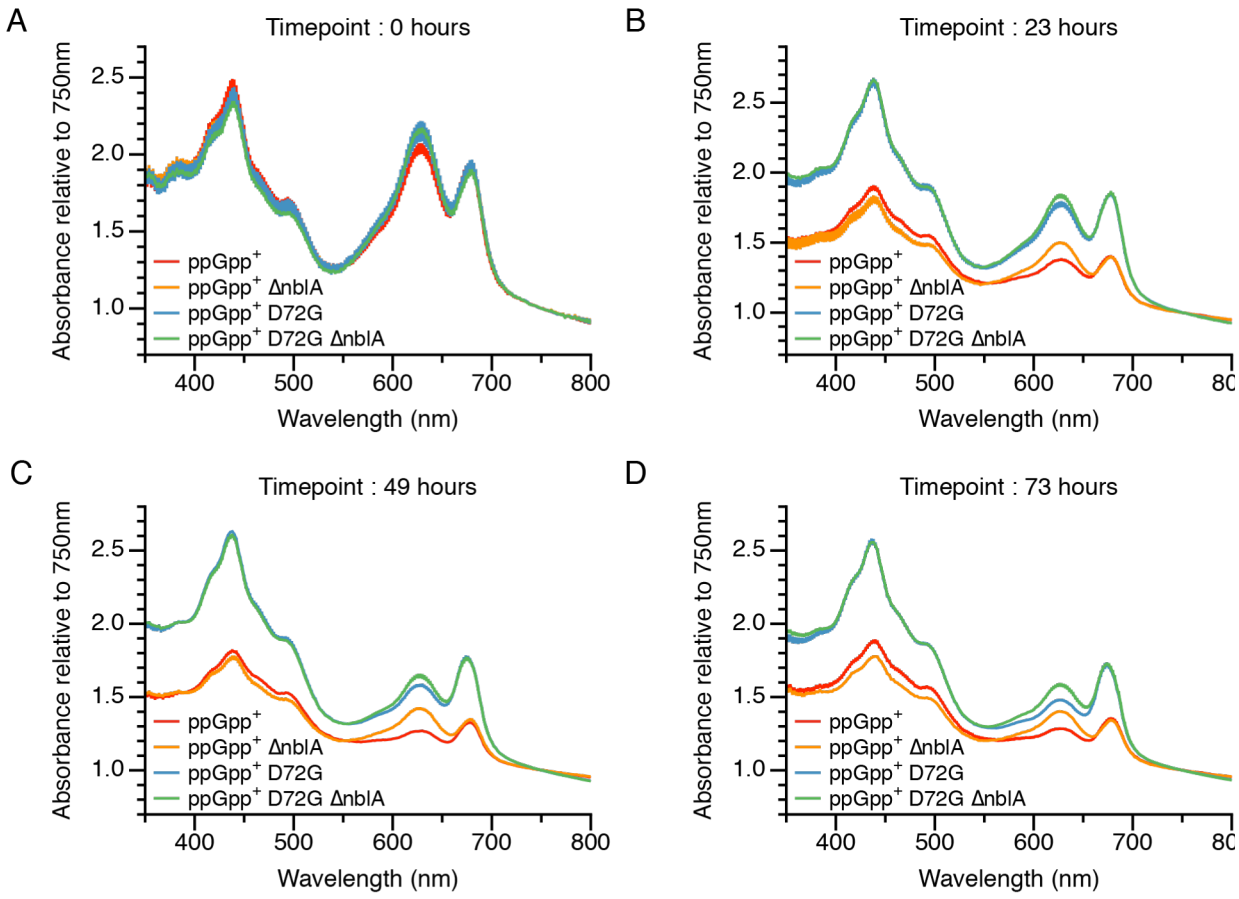

Figure 3-6. Complete absorbance scans confirm the specific role of *nblA* in phycobilisome degradation in the ppGpp$^+$ strain. Cultures were grown to log phase, induced with IPTG at time = 0 hours, and absorbance scans were performed at the indicated times. Data are plotted as mean ± SD (n≥3), and are normalized by absorbance at 750 nm to account for differences in culture density. Data shown were measured 0 (A), 23 (B), 49 (C), or 73 (D) hours after induction of the (p)ppGpp synthetase in the ppGpp$^+$ strain.

While we see a specific effect of *nblA* in regulating phycobilisome degradation, levels of phycobilins and chlorophyll both generally decrease in the ppGpp$^+$ strain, in an *nblA*-independent manner. This suggests that other mechanisms are at work – these could include post-translational mechanisms other than *nblA* that cause degradation of phycobilisomes and photosystems, and/or downregulation of genes encoding pigment-synthesizing enzymes or subunits of the light-harvesting complexes themselves. We know that phycobiliprotein genes are highly downregulated in the ppGpp$^+$ strain, as noted in Chapter 2 (Figure 2-8), which at least partially explains these phenotypes.

Based on the absorbance scans presented above, we surmise that (p)ppGpp is both necessary and sufficient to trigger degradation of light-harvesting complexes in *Synechococcus*. To verify that these changes are indeed occurring at the protein level, we analyzed cell lysates from the panel of ppGpp$^+$ strains tested above by SDS-PAGE. Quantification of phycobiliproteins relative to the carbon fixation enzyme Rubisco, whose levels remain relatively unchanged across these conditions, mirrors the trends seen in the absorbance scans (Figure 3-7). We find that phycobiliprotein levels are indeed lower in ppGpp$^+$ than in ppGpp$^+$ Δ*nblA*.

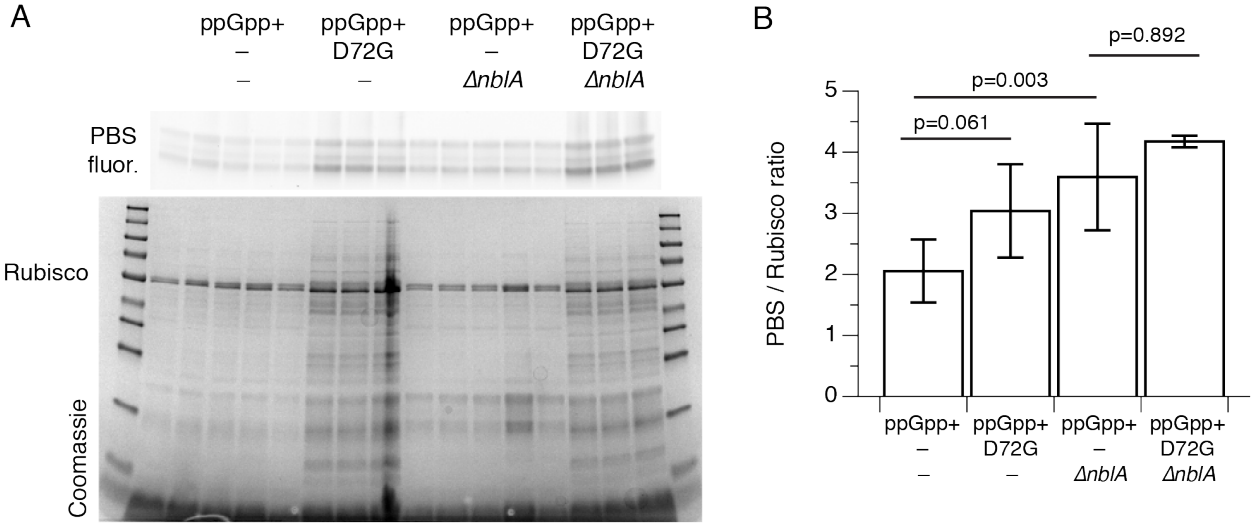

Figure 3-7. Phycobilisome protein levels decrease in an *nblA*-dependent fashion in the ppGpp$^+$ strain. SDS-PAGE analysis of phycobilisome (PBS) proteins and Rubisco from *Synechococcus* lysates. (A) Cultures from the same experiment as in Figures 3-5 and 3-6 were harvested after 73 hours of IPTG induction. Cell lysates were prepared by normalizing for absorbance at 750 nm. Lysates were unboiled (top, PBS fluor.) or boiled (bottom, Coomassie) and run on SDS-PAGE gels. The natural fluorescence of PBS proteins was imaged using a YFP filter set (top; see Materials and Methods), while total protein (including Rubisco) was imaged by Coomassie staining. (B) Quantification of protein bands from gels shown in (A). Data are plotted as mean ± SD (n≥3), and p-values shown result from a two-tailed t-test.

3.3.4 Measuring (p)ppGpp levels in response to metabolic stressors

We showed above (in Sections 3.3.1 and 3.3.2) that *rel* helps *Synechococcus* survive DCMU treatment and nitrogen starvation; thus, we predict that (p)ppGpp levels rise under these circumstances. Though we have previously measured ppGpp, both by HPLC and ^{32}P-labeling (Figures 2-1 and 2-2), we decided to work out a different ppGpp measurement method based on the work of Traxler et al (21). This method is more quantitative than ^{32}P-labeling, and we needed to use different instrumentation than we had used for our previous HPLC measurements. Thus, we conducted preliminary experiments toward the goal of measuring ppGpp by anion exchange FPLC. Analysis of serial dilutions of a ppGpp standard shows a linear range of detection between 3-100 µM ppGpp and a limit of detection of ~2 µM (Figure 3-8A).

We analyzed control *E. coli* extracts to identify ppGpp elution conditions (Figure 3-8B), and have also detected ppGpp from extracts of *Synechococcus* ppGpp$^+$ cultures (Figure 3-8C). We plan to extract nucleotides from WT *Synechococcus* cultures at multiple time intervals after DCMU treatment and starvation for nitrogen, sulfur, and iron, and quantify ppGpp levels. There is precedent in the literature for ppGpp levels rising in response to both DCMU treatment (5) and nitrogen starvation in *Synechococcus* (25, 26).

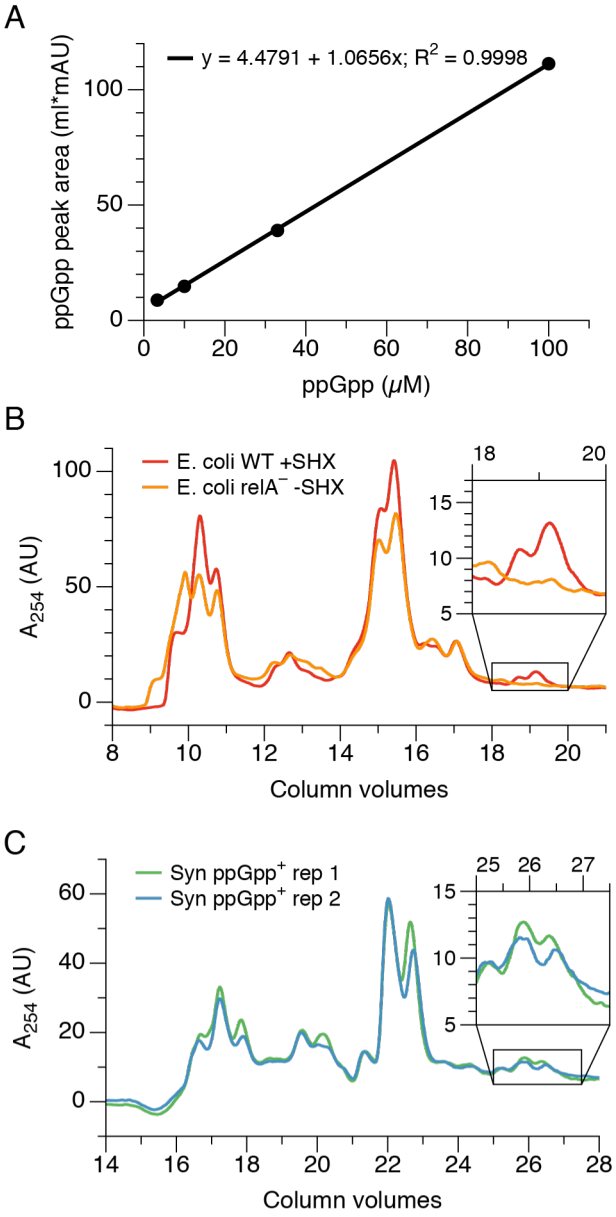

Figure 3-8. Development and validation of a ppGpp measurement method using anion exchange chromatography. (A) Standard curve showing a linear range of ppGpp detection between 3-100 μM. Based on this method, which uses a Mono Q anion exchange column on an FPLC system, the limit of detection is estimated at 2 μM ppGpp. (B and C) ppGpp can be measured in formic acid extracts of *E. coli* and *Synechococcus*. (B and C, inset) Zoomed-in views of ppGpp peaks. (B) Analysis of control *E. coli* extracts. The WT strain was treated with serine hydroxamate (SHX), which is a known trigger of ppGpp production and serves as a positive control. The relA$^-$ strain was used as a negative control. (C) Analysis of extracts from two *Synechococcus* ppGpp$^+$ cultures. Numerical differences on the x-axis (column volumes) in (B) and (C) are due to differences in the injection volumes for *E. coli* and *Synechococcus* samples.

3.3.5 Towards the identification of Rel interaction partners

Little is known about regulation of (p)ppGpp synthesis and hydrolysis at the level of Rel activity. However, the mechanism of the distantly related (p)ppGpp synthetase RelA from *E. coli* has been well-studied. RelA is activated upon binding to ribosomes containing uncharged tRNAs at the A site, but this enzyme is found only in Proteobacteria (27-30). Other notable findings in (p)ppGpp biochemistry include a demonstrated interaction between *E. coli*'s bifunctional (p)ppGpp synthetase/hydrolase SpoT and acyl carrier protein (31), as well as the partial crystal structure of *Streptococcus equisimilus* Rel (32). This structure provides information about the N-terminal half of the protein, which includes its (p)ppGpp hydrolase and synthetase domains, but lacks its C-terminal regulatory domains. A crystal structure of a small (p)ppGpp synthetase from *B. subtilis* – the protein overproduced by our *Synechococcus* $ppGpp^+$ strain – has also been determined (33). The Rel protein of cyanobacteria is similar to that of the Gram-positive Firmicutes (like *S. equisimilus*), and is predicted to be a bifunctional (p)ppGpp synthetase and hydrolase (27). We hypothesize that identifying interaction partners of *Synechococcus* Rel will inform our knowledge of how (p)ppGpp synthesis and/or hydrolysis are controlled at a biochemical level.

Toward this goal, we constructed epitope-tagged *rel* alleles and tested their functionality. First, we tested whether overexpression of these alleles affects growth of *Synechococcus*. When expressed in a WT background, none of the C-terminally-tagged constructs tested exhibit toxic effects (Figure 3-9A). However, N-terminal 6xHis or 3xFLAG tags decreased growth and induced chlorosis at concentrations of 50 μM IPTG or higher (Figure 3-9A). The (p)ppGpp hydrolase domain is located at the N-terminus of the Rel protein, and it is possible that adding an N-terminal tag disrupts the balance between hydrolase and synthetase activity. This would be consistent with the reciprocal regulation model for these domains, as was proposed by Hogg et al. (32).

We next tested the ability of these tagged *rel* alleles to complement the Δ*rel* mutant phenotype. Each construct was expressed for 21 hours before shifting cells to the dark for one week. Under these conditions, Rel proteins with 3xFLAG tags on either the N or C terminus complement the mutation, though the N-terminally-tagged protein does so to a lesser extent (Figure 3-9B). Based on the ability of each of these *rel* alleles to at least partially complement the Δ*rel* mutation, we conclude that a 3xFLAG tag on either the N- or C-terminus of Rel results in a functional protein that can be used for further investigation.

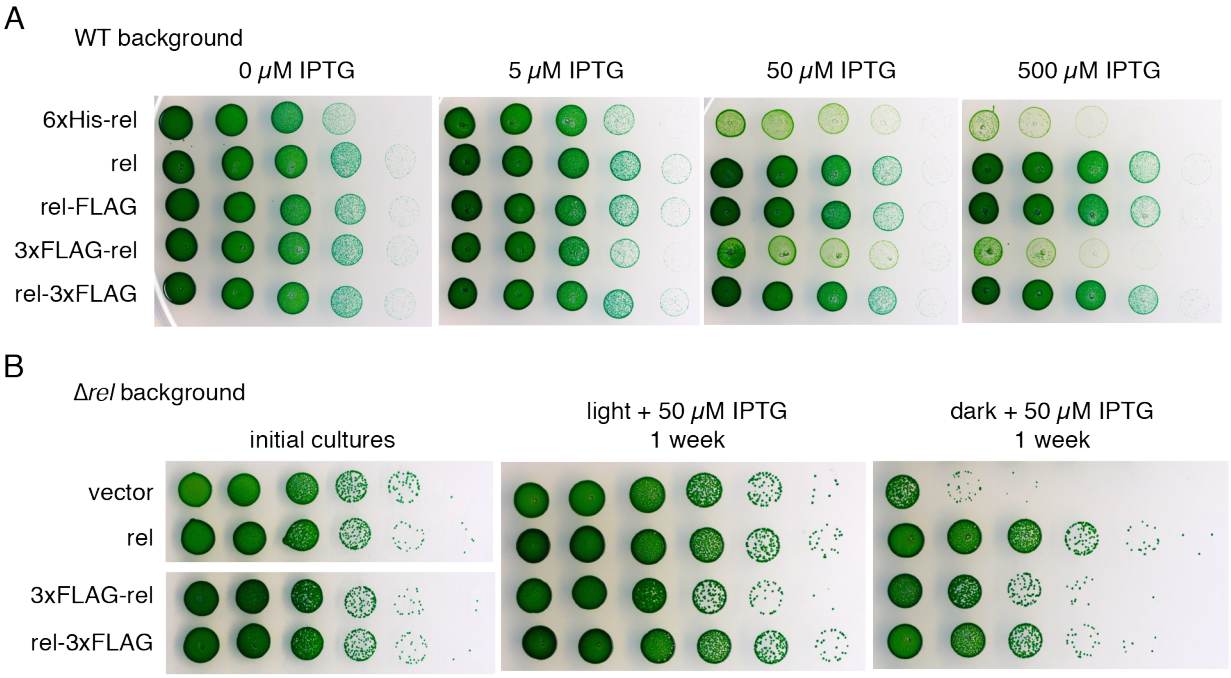

Figure 3-9. 3xFLAG-tagged *rel* alleles are functional, but exhibit varying degrees of toxicity when expressed in *Synechococcus*. (A) N-terminally tagged *rel* alleles exhibit toxic effects when overexpressed in WT *Synechococcus*. Cultures of the indicated strains were serially diluted tenfold, spotted onto plates containing the indicated concentrations of IPTG, and grown in constant light. (B) 3xFLAG-tagged *rel* alleles complement the Δ*rel* mutation, improving survival of dark incubation. Both N- and C-terminal tags result in functional proteins, though the C-terminally-tagged protein better rescues the mutant. Cultures of the indicated strains were incubated under the specified conditions, serially diluted tenfold, spotted onto plates lacking IPTG, and grown in constant light.

Working towards identifying protein interaction partners of *Synechococcus* Rel, we performed immunoprecipitation experiments with the 3xFLAG-tagged alleles characterized above. Analysis of pulldown eluates by silver staining shows bands corresponding to 3xFLAG-Rel and Rel-3xFLAG (Figure 3-10). Untagged Rel is not detected by this method, demonstrating its specificity for the 3xFLAG-tagged variants. However, no additional bands, which could clearly indicate Rel binding partners, are visible from conditions in which Rel was enriched. The next step is to perform a similar pulldown experiment and identify proteins present in the sample by mass spectrometry. This more sensitive method may identify proteins not visible by silver staining.

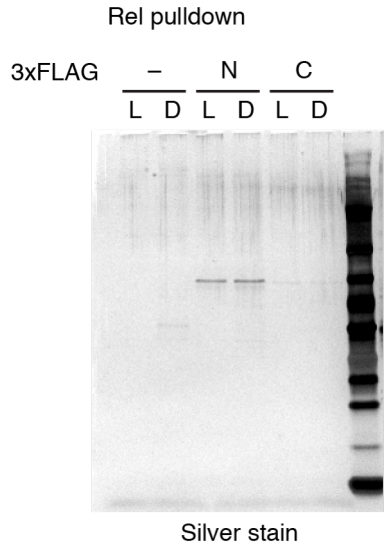

Figure 3-10. Immunoprecipitation of 3xFLAG-tagged Rel proteins from *Synechococcus* lysates. Cultures of the indicated strains (–, *rel*; N, *3xFLAG-rel*; C, *rel-3xFLAG*) were incubated in the light (L) or dark (D) for 30 minutes, crosslinked with 1% formaldehyde, and lysed. Immunoprecipitations were performed using an α-3xFLAG antibody and protein G magnetic beads. After eluting proteins with a 3xFLAG peptide, proteins were analyzed by silver staining. The 3xFLAG-Rel protein is most enriched, though some Rel-3xFLAG can also be detected. Untagged Rel is not enriched, demonstrating the specificity of the method.

3.3.6 Investigating targets of (p)ppGpp through mutagenesis and identification of suppressor mutations

Suppressor mutagenesis has provided great insight into the targets and mechanisms of (p)ppGpp in several bacteria. In *E. coli*, for example, a strain that cannot make (p)ppGpp cannot grow on minimal media lacking amino acids. Suppressor mutants that can grow under these conditions have been mapped to RNA polymerase, demonstrating the importance of the (p)ppGpp-RNA polymerase interaction for *E. coli*'s stringent response (34). Suppressor mutagenesis has also been applied recently in *Synechococcus*, and allowed Diamond and colleagues to unravel why mutation of the transcription factor *rpaA* causes lethality during light/dark cycles (23).

In order to identify suppressor mutations, a stringent selection system with low background is necessary. Our study of the cyanobacterial stringent response lends itself to two different approaches to suppressor mutagenesis. The first uses a (p)ppGpp overproduction system based on the ppGpp$^+$ strain, which stops growing upon induction of the (p)ppGpp synthetase with IPTG (Figure 2-3). Initial tests looking for suppressors of the ppGpp$^+$ strain that could grow on plates containing IPTG demonstrated a high frequency of spontaneous mutations (~1 x 10^{-4}), many of which were located within the promoter region or coding sequence of the (p)ppGpp synthetase.

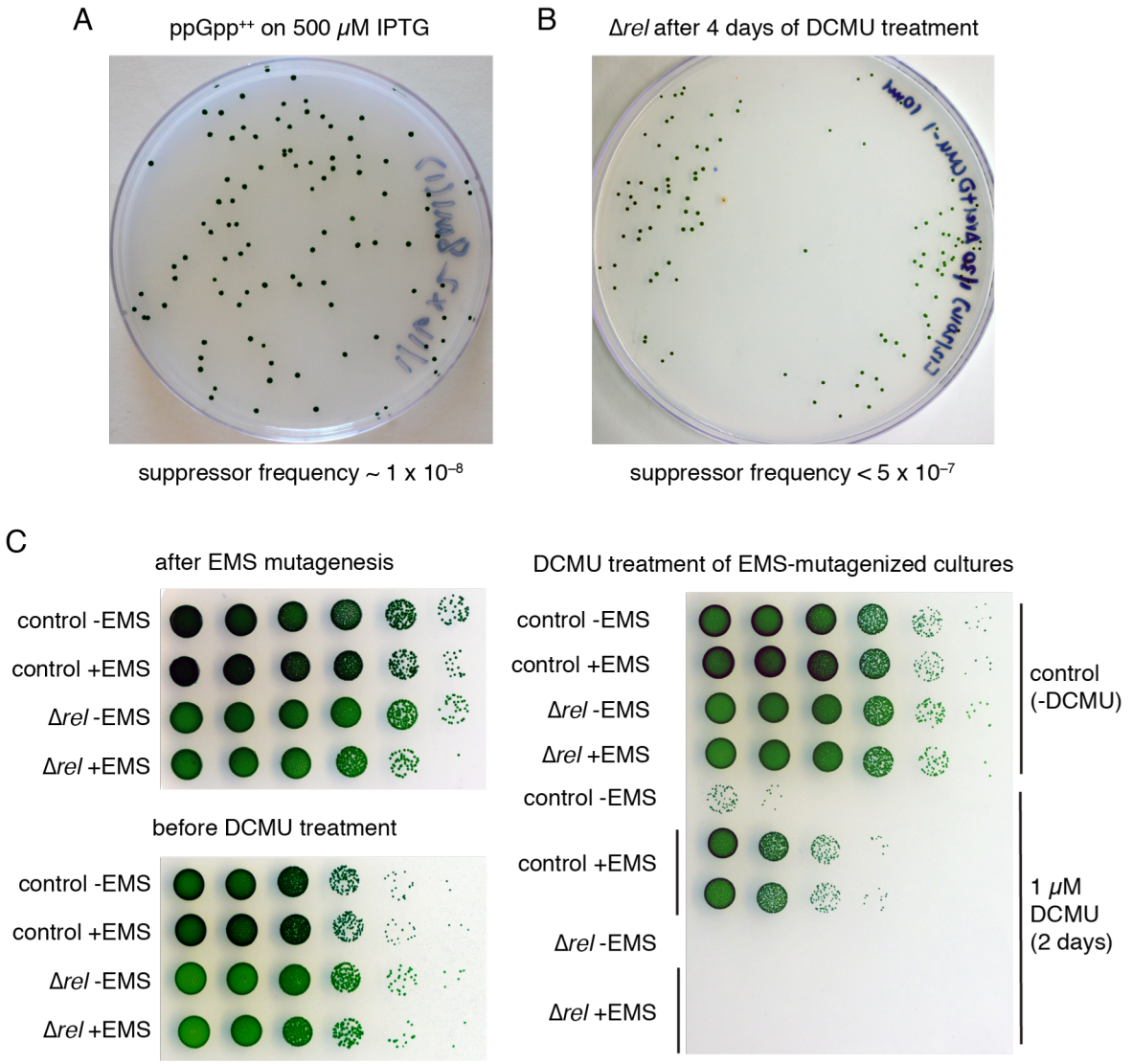

Figure 3-11. Suppressor mutagenesis of ppGpp^{++} and Δ*rel* strains. (A) The ppGpp^{++} strain was grown to log phase, concentrated, and plated on 500 μM IPTG. Spontaneous suppressor mutants appear at a frequency of approximately 1 x 10^{-8}. (B) The Δ*rel* mutant was treated with DCMU for four days, concentrated, and plated on media lacking DCMU. Spontaneous suppressor mutants appear at a frequency of less than 5 x 10^{-7}. (C) EMS mutagenesis of control and Δ*rel* results in viable cultures, and survival of control (WT-Cm^{R}) cultures after DCMU treatment indicates that EMS mutagenesis will boost suppressor frequencies. Cultures were treated with EMS, allowed to recover, backdiluted, and either treated with DCMU or left untreated. Cultures were serially diluted tenfold, spotted onto plates, and grown in constant light after the indicated treatment.

In an effort to decrease the background of these undesired spontaneous mutations, we introduced an additional, identical copy of this gene at a different neutral site on the *Synechococcus* chromosome. We call this strain ppGpp^{++}. When ppGpp^{++} is induced with IPTG, its mutational background is significantly lower (~1 x 10^{-8}; Figure 3-11A), making the system feasible for use in suppressor experiments. Preliminary Sanger sequencing results of ppGpp^{++} suppressors indicate that while some of them contain obvious mutations in the promoter and/or coding sequence of the synthetase, others – many of which grow more slowly and display altered pigmentation phenotypes – do not have obvious mutations in these regions and may be promising candidates for further investigation.

Another useful background for suppressor experiments comes from the sensitivity of the Δ*rel* mutant to treatment with DCMU, as described in Section 3.3.1. When Δ*rel* cultures are plated after 4 days of DCMU treatment, colonies representing spontaneous suppressor mutants sometimes appear within 2-3 weeks (Figure 3-11B; frequency estimated as < 5 x 10^{-7}). Previous studies have identified genetic mutations that prevent binding of DCMU to photosystem II proteins and thereby confer resistance to this herbicide in WT *Synechococcus* (35). Any Δ*rel* + DCMU suppressor mutants should first be screened to test whether PSII mutations are responsible for their resistance phenotype, and only colonies with wild-type PSII sequences will be analyzed further.

Going forward, a promising approach is to mutagenize *Synechococcus* cultures, of both WT and Δ*rel* strains, with ethyl methanesulfonate (EMS). This treatment should increase the frequency and diversity of mutations found within a given culture, and will allow us to identify a broader range of mutations that permit the Δ*rel* mutant to grow during DCMU treatment. Preliminary experiments have shown that EMS-treated WT cultures survive DCMU treatment better than untreated WT cultures (Figure 3-11C), a promising indication that mutation frequency has increased. Unfortunately, selection conditions for the Δ*rel* mutant were overly stringent in this particular experiment and no colonies formed in either EMS-treated or untreated cultures after DCMU treatment (Figure 3-11C). Preliminary results have shown that EMS also increases the frequency of Δ*rel* suppressors after DCMU treatment (data not shown).

We are interested in identifying suppressors of the Δ*rel* phenotype that have mutations in genes involved in the cyanobacterial stringent response. Because the Δ*rel* mutant does not produce (p)ppGpp in response to stress (Figure 2-1), mutations in (p)ppGpp target genes could allow cells to circumvent this pathway, such that (p)ppGpp is no longer necessary for activation or repression of these genes/proteins. This could allow the Δ*rel* mutant to better survive stressful conditions, though its growth will likely be slower than that of the WT under the same conditions. We do not know how many targets of the stringent response exist in *Synechococcus*, but it is likely that it has multiple targets rather than acting through one master regulator. Therefore, mutating only one gene may not be sufficient to fully restore growth of the Δ*rel* mutant. However, even strains with slow-growing phenotypes could provide valuable insights into the biology behind the stringent response of *Synechococcus.*

3.4 Discussion

This work has broadened our understanding of the stringent response in *Synechococcus*. We have shown that the pathway helps cells respond to several stresses other than darkness – namely, photosynthetic inhibition by DCMU treatment, and starvation for nitrogen, sulfur, and iron. We have also found that the stringent response can be involved in chlorosis, a characteristic stress response of cyanobacteria. Our recent work has laid the foundation for gaining a more detailed, mechanistic understanding of how (p)ppGpp and the stringent response control *Synechococcus* physiology in response to diverse environmental stressors. This will allow us to learn more about both inputs into the pathway and the molecular underpinnings of its physiological outputs.

3.4.1 The stringent response may be involved in both general and nutrient-specific stress responses in Synechococcus

Across diverse bacteria, the stringent response senses and responds to many types of starvation signals (though in many cases, how those specific signals are sensed remains unknown). Once starvation triggers (p)ppGpp production, the pathway enacts changes throughout the cell by reallocating resources to where they are most needed and thereby facilitating adaptation. Some of these changes are general mechanisms that help cells adapt no matter which type of starvation they encounter – in many cases it is beneficial to stop growth and division because the resources to produce healthy progeny cells are not available. On the other hand, some of these changes are (and must be) nutrient-specific, and therefore involve more specific metabolic responses. When *E. coli* is starved for amino acids, several mechanisms operate to increase amino acid availability in this organism: short-term strategies include degradation of existing proteins, while long-term strategies involve increasing expression of necessary amino acid biosynthetic genes (36, 37).

Our studies of the stringent response in *Synechococcus* have shown that different types of stress can lead to different physiological responses. For example, only some of the stressors that induce the stringent response trigger chlorosis. While decreases in pigmentation become very obvious following nitrogen starvation – and are partially dependent upon the stringent response – inhibition of photosynthesis does not trigger chlorosis (as also noted in (38)). *Synechococcus* cultures that have been incubated in continuous darkness for several weeks do not bleach; when treated with DCMU, they only start to lose pigmentation once cells become inviable. Chlorotic nitrogen-starved cells, on the other hand, retain a higher degree of viability (39).

In the case of DCMU treatment, changes in pigmentation may be in response to toxic side effects of the drug (as discussed above in Section 3.3.1). One cause of DCMU toxicity in the Δ*rel* mutant could be accumulation of ROS. If one branch of photosynthesis (PSII) is blocked and cultures are incubated in the light, levels of ROS could increase, making the Δ*rel* mutant especially sensitive if it lacks detoxification mechanisms. It would be interesting to test whether the Δ*rel* mutant does in fact have

higher ROS levels than the WT after DCMU treatment. If so, further experiments could be performed to determine whether its survival increases when incubated in lower light, which would be expected to decrease oxidative stress. Diamond and colleagues found that growth of an ROS-sensitive mutant of *Synechococcus* improved when light levels were decreased (23).

Another indication that the stringent response can have distinct mechanistic effects under different circumstances comes from results of the RNA-seq experiment described in Chapter 2 (discussed in Section 2.3.4). Although transcriptional responses to darkness and (p)ppGpp production in the light overlap in some regards, many genes are differentially expressed in the dark compared to in the ppGpp$^+$ strain (Figures 2-8 and 2-9). One notable example is that of *nblA*, which is highly expressed only in the ppGpp$^+$ strain (Figure 3-5A). There are likely many other genes that fit this pattern, as 455 genes were differentially expressed in the ppGpp$^+$ strain but not in response to darkness (Figure 2-9).

3.4.2 Connecting previously known cyanobacterial stress responses with the stringent response

The stringent response plays a role in adapting to different metabolic challenges, but it is not the only stress response that occurs under these conditions. This is clear from the cyanobacterial literature (40), as well as from (p)ppGpp-independent responses evident in our data. During nitrogen starvation, for example, levels of phycobilins decrease in Δ*rel* even though this strain cannot make (p)ppGpp, indicating that mechanisms other than the stringent response are involved in phycobilisome degradation (Figure 3-3). Since the Δ*rel* mutant encodes *nblA*, it could be that this gene is upregulated by other pathways. Future work could measure *nblA* expression under these conditions – based on our observations, we would expect expression of this gene to be higher in WT than in Δ*rel* following nitrogen starvation.

Though chlorosis is a specific stress response in the sense that it occurs only during certain types of nutrient deprivation (10), it has also been observed as a phenotype of several knockout strains in *Synechococcus* other than the Δ*rel* mutant. A strain in which the circadian-regulated transcription factor *rpaA* is inactivated, for example, shows decreases in phycobilin absorbance after entering darkness, a condition in which it rapidly loses viability (23). The chlorotic phenotype is visually striking and can be easily measured by performing absorbance scans, which probably leads to its frequent observation. While this can make it seem like chlorosis is a nonspecific response, it also highlights the fundamental nature of photosynthetic metabolism and its regulation when other branches of metabolism, or regulatory systems in the cell, are disrupted.

Stress responses work by coordinating cellular processes and promoting metabolic homeostasis. Studies in *Synechococcus* have shown that glycogen is an important component of the nitrogen starvation response, and its levels are known to vary not only in response to nitrogen starvation, but also in response to darkness and DCMU treatment (6, 41). We have not tested whether glycogen levels might be affected in the

Δ*rel* mutant (or vice versa), but considering the metabolic importance of glycogen to cyanobacteria, there may very well be interactions between central carbon metabolism and the stringent response.

3.4.3 Outlook

We have shown that the stringent response is important for helping cells survive environmental stressors, yet it represents only one network within a much larger framework of cellular metabolism, fundamental cellular processes, and regulatory pathways. Thus, future experiments addressing the context of the stringent response in the cell, and its interactions with other processes, will be interesting, informative, and important.

3.5 Acknowledgments

We are grateful to C. Cassidy-Amstutz and L. Oltrogge for assistance with ppGpp detection experiments, S. Diamond for assistance with EMS mutagenesis, and other members of the Savage lab for feedback. This work was supported by the DOE Office of Science Early Career Research Program (Grant number DE-SC0006394) through the Office of Basic Energy Sciences and an Alfred P. Sloan Research Fellowship to DFS. RDH was supported by the National Science Foundation Graduate Research Fellowship Program.

3.6 References

1. Mackey KRM, et al. (2015) Divergent responses of Atlantic coastal and oceanic Synechococcus to iron limitation. *Proc Natl Acad Sci USA* 112(32):9944–9949.

2. Flombaum P, et al. (2013) Present and future global distributions of the marine Cyanobacteria Prochlorococcus and Synechococcus. *Proc Natl Acad Sci USA* 110(24):9824–9829.

3. Latifi A, Ruiz M, Zhang C-C (2009) Oxidative stress in cyanobacteria. *FEMS Microbiol Rev* 33(2):258–278.

4. Muro-Pastor MI, Reyes JC, Florencio FJ (2001) Cyanobacteria perceive nitrogen status by sensing intracellular 2-oxoglutarate levels. *J Biol Chem* 276(41):38320–38328.

5. Smith RJ (1977) The regulation of stable RNA synthesis in the blue-green alga Anacystis nidulans, the effect of DCMU inhibition. *FEMS Microbiol Lett* 1:129–132.

6. Lehmann M, Wober G (1976) Accumulation, mobilization and turn-over of glycogen in the blue-green bacterium Anacystis nidulans. *Arch Microbiol* 111:93–97.

7. Schmitz O, Tsinoremas NF, Schaefer MR, Anandan S, Golden SS (1999) General effect of photosynthetic electron transport inhibitors on translation precludes their use for investigating regulation of D1 biosynthesis in Synechococcus sp. strain PCC 7942. *Photosynth Res* 62:261–271.

8. Ohbayashi R, et al. (2013) DNA replication depends on photosynthetic electron transport in cyanobacteria. *FEMS Microbiol Lett* 344:138–144.

9. Marques S, Merida A, Candau P, Florencio FJ (1992) Light-mediated regulation of glutamine synthetase activity in the unicellular cyanobacterium Synechococcus sp. PCC 6301. *Planta* 187:247–253.

10. Collier JL, Grossman AR (1992) Chlorosis induced by nutrient deprivation in Synechococcus sp. strain PCC 7942: not all bleaching is the same. *J Bacteriol* 174(14):4718–4726.

11. Kiyota H, Hirai MY, Ikeuchi M (2014) NblA1/A2-Dependent Homeostasis of Amino Acid Pools during Nitrogen Starvation in Synechocystis sp. PCC 6803. *Metabolites* 4(3):517–531.

12. Collier JL, Herbert SK, Fork DC, Grossman AR (1994) Changes in the cyanobacterial photosynthetic apparatus during acclimation to macronutrient deprivation. *Photosynth Res* 42:173–183.

13. Collier JL, Grossman AR (1994) A small polypeptide triggers complete degradation of light-harvesting phycobiliproteins in nutrient-deprived cyanobacteria. *EMBO J* 13(5):1039–1047.

14. Luque I, Zabulon G, Contreras A, Houmard J (2001) Convergence of two global transcriptional regulators on nitrogen induction of the stress-acclimation gene nblA in the cyanobacterium Synechococcus sp. PCC 7942. *Mol Microbiol* 41(4):937–947.

15. Luque I, Forchhammer K (2008) Nitrogen assimilation and C/N balance sensing. *The Cyanobacteria: Molecular Biology, Genomics and Evolution*, eds Herrero A, Flores E (Caister Academic Press, Norfolk, UK), pp 335–382.

16. Karradt A, Sobanski J, Mattow J, Lockau W, Baier K (2008) NblA, a Key Protein of Phycobilisome Degradation, Interacts with ClpC, a HSP100 Chaperone Partner of a Cyanobacterial Clp Protease. *J Biol Chem* 283(47):32394–32403.

17. Sendersky E, et al. (2014) The proteolysis adaptor, NblA, initiates protein pigment degradation by interacting with the cyanobacterial light-harvesting complexes. *Plant J* 79(1):118–126.

18. Sendersky E, et al. (2015) The proteolysis adaptor, NblA, is essential for degradation of the core pigment of the cyanobacterial light-harvesting complex. *Plant J* 83(5):845–852.

19. Allen MM (1968) Simple conditions for growth of unicellular blue-green algae on plates. *J Phycol* 4:1–4.

20. Engler C, Kandzia R, Marillonnet S (2008) A one pot, one step, precision cloning method with high throughput capability. *PLoS ONE* 3(11):e3647.

21. Traxler MF, et al. (2011) Discretely calibrated regulatory loops controlled by ppGpp partition gene induction across the “feast to famine” gradient in Escherichia coli. *Mol Microbiol* 79(4):830–845.

22. Gerace E, Moazed D (2015) Affinity Pull-Down of Proteins Using Anti-FLAG M2 Agarose Beads. *Methods Enzymol* 559:99–110.

23. Diamond S, et al. (2017) Redox crisis underlies conditional light-dark lethality in cyanobacterial mutants that lack the circadian regulator, RpaA. *Proc Natl Acad Sci USA* 114:E580–E589.

24. Boutte CC, Crosson S (2013) Bacterial lifestyle shapes stringent response activation. *Trends Microbiol* 21(4):174–180.

25. Borbely G, Kaki C, Gulyás A, Farkas GL (1980) Bacteriophage infection interferes with guanosine 3“-diphosphate-5-”diphosphate accumulation induced by energy and nitrogen starvation in the cyanobacterium Anacystis nidulans. *J Bacteriol* 144(3):859–864.

26. Friga GM, Borbely G, Farkas GL (1981) Accumulation of guanosine tetraphosphate (ppGpp) under nitrogen starvation in Anacystis nidulans, a cyanobacterium. *Arch Microbiol* 129:341–343.

27. Atkinson GC, Tenson T, Hauryliuk V (2011) The RelA/SpoT Homolog (RSH) Superfamily: Distribution and Functional Evolution of ppGpp Synthetases and Hydrolases across the Tree of Life. *PLoS ONE* 6(8):e23479.

28. Arenz S, et al. (2016) The stringent factor RelA adopts an open conformation on the ribosome to stimulate ppGpp synthesis. *Nucleic Acids Res* 44(13):6471–6481.

29. Brown A, Fernández IS, Gordiyenko Y, Ramakrishnan V (2016) Ribosome-dependent activation of stringent control. *Nature* 534(7606):277–280.

30. Loveland AB, et al. (2016) Ribosome-RelA structures reveal the mechanism of stringent response activation. *eLife* 5:e17029.

31. Battesti A, Bouveret E (2006) Acyl carrier protein/SpoT interaction, the switch linking SpoT-dependent stress response to fatty acid metabolism. *Mol Microbiol* 62(4):1048–1063.

32. Hogg T, Mechold U, Malke H, Cashel M, Hilgenfeld R (2004) Conformational Antagonism between Opposing Active Sites in a Bifunctional RelA/SpoT Homolog Modulates (p)ppGpp Metabolism during the Stringent Response. *Cell* 117:57–68.

33. Steinchen W, et al. (2015) Catalytic mechanism and allosteric regulation of an oligomeric (p)ppGpp synthetase by an alarmone. *Proc Natl Acad Sci USA* 112(43):13348–13353.

34. Murphy H, Cashel M (2003) Isolation of RNA polymerase suppressors of a (p)ppGpp deficiency. *Methods Enzymol* 371:596–601.

35. Golden SS, Haselkorn R (1985) Mutation to herbicide resistance maps within the psbA gene of Anacystis nidulans R2. *Science* 229(4718):1104–1107.

36. Kuroda A, et al. (1999) Inorganic polyphosphate kinase is required to stimulate protein degradation and for adaptation to amino acid starvation in Escherichia coli. *Proc Natl Acad Sci USA* 96(25):14264–14269.

37. Traxler MF, et al. (2008) The global, ppGpp-mediated stringent response to amino acid starvation in Escherichia coli. *Mol Microbiol* 68(5):1128–1148.

38. Grossman AR, van Waasbergen LG, Kehoe DM (2003) Environmental regulation of phycobilisome biosynthesis. *Light-Harvesting Antennas*, eds Green B, Parson W (Kluwer Academic Publishers), pp 471–493.

39. Sauer J, Schreiber U, Schmid R, Volker U, Forchhammer K (2001) Nitrogen Starvation-Induced Chlorosis in Synechococcus PCC 7942. Low-Level Photosynthesis As a Mechanism of Long-Term Survival. *Plant Physiology* 126:233–243.

40. Schwarz R, Forchhammer K (2005) Acclimation of unicellular cyanobacteria to macronutrient deficiency: emergence of a complex network of cellular responses. *Microbiology* 151:2503–2514.

41. Hickman JW, et al. (2013) Glycogen synthesis is a required component of the nitrogen stress response in Synechococcus elongatus PCC 7942. *Algal Research* 2(2):98–106.

Chapter 4

Exploring the roles of polyphosphate in *Synechococcus*

4.1 Introduction

Cyanobacteria have evolved specialized intracellular structures to compartmentalize and regulate their metabolic pathways (Figures 1-1 and 1-2). Several decades of study investigating cyanobacterial ultrastructure have shown that carboxysomes, the location of the carbon-fixing enzyme Rubisco, often associate with granules of polyphosphate (1, 2). Polyphosphate (polyP) is a linear polymer of inorganic phosphate (P_i) molecules linked by the same high-energy phosphoanhydride bonds found in nucleoside triphosphates like ATP.

The association observed between carboxysomes and polyP granules suggests that there could be a functional relationship between these two structures – indeed, in some cases, polyphosphate has even been observed within carboxysomes (3). This intriguing finding raises questions about the roles of polyP in cyanobacteria, and form the basis of the investigations presented in this chapter. The remainder of this introduction will provide some background on how polyP levels are controlled in bacteria, and will highlight findings in the polyP literature that have demonstrated roles for this compound in diverse organisms.

4.1.1 Control of polyphosphate levels in bacteria and links to the stringent response

Three enzymes are of particular importance in controlling polyP synthesis and degradation in bacteria, and are widely conserved (Table 4-1) (4). PolyP kinase (PPK) is the principal enzyme that synthesizes polyP, generally from ATP, and can also catalyze the reverse reaction in which polyP is used to produce ATP. Another enzyme, polyP phosphotransferase (PPT), can also synthesize polyP, though it primarily uses polyP to phosphorylate either AMP or ADP. The major enzyme involved in polyP degradation in bacteria is exopolyphosphatase (PPX), which hydrolyzes the terminal phosphate from a polyP chain, releasing P_i.

Table 4-1. Important enzymes in polyP metabolism.

Gene name	Protein encoded	Activity
ppk	polyP kinase	polyP synthesis
ppt	phosphotransferase	transfer of phosphate from polyP to AMP/ADP
ppx	exopolyphosphatase	hydrolysis of terminal phosphate from polyP

Interestingly, activity of at least one of these enzymes can be regulated by the stringent response. In *Escherichia coli*, (p)ppGpp directly inhibits PPX activity. Thus, when (p)ppGpp levels are high, PPX cannot hydrolyze polyP but PPK continues to synthesize it. This leads to dramatic increases in polyP accumulation when cells are starved (5).

Inspired by these findings, we tested whether the two are linked in *Synechococcus*, and showed that high levels of (p)ppGpp lead to accumulation of polyP in this cyanobacterium (Figure 2-3).

4.1.2 Roles of polyphosphate in diverse organisms

PolyP has been detected in very diverse organisms, ranging from bacteria to animals, including humans, though it generally accumulates to higher levels in single-celled organisms (6). Reducing polyP levels by inactivating *ppk* in several bacteria – including *E. coli, Salmonella typhimurium, Shigella flexneri,* and *Pseudomonas aeruginosa* – decreases survival in response to a variety of stresses, but the molecular mechanisms by which polyP mediates these responses remain largely unknown (4). In a number of cases, (p)ppGpp and polyP seem to exert similar effects on cell physiology and stress tolerance.

One of the most specific functions proposed for polyP is in ribosomal protein degradation in *E. coli*. Upon amino acid starvation, levels of (p)ppGpp rise, inhibit PPX activity, and lead to increases in polyP (5). This polyP can bind to free ribosomal proteins and target them for degradation by the Lon protease, thereby freeing up amino acids and helping to restore homeostasis (7).

4.1.3 Objective

PolyP has been studied in several heterotrophic bacteria, especially *E. coli*, but few studies have investigated the roles of polyP in photosynthetic or autotrophic microbes. These organisms use significantly different metabolic strategies than heterotrophs to derive their energy, and therefore could take advantage of the versatility of polyP in different ways. To address these questions, we have begun an investigating into the roles of polyphosphate in *Synechococcus.* We have measured cellular polyP content under different conditions, and have also started to characterize the phenotypes of knockout mutants of the three key polyP enzymes described above.

4.2 Materials and Methods

4.2.1 Bacterial strains and culture conditions

Synechococcus elongatus PCC 7942 was grown in BG-11 media (8) at 30°C with shaking (185 rpm) under white fluorescent lights at 60-100 µE. Cultures were grown either in a programmable photosynthetic incubator (Percival Scientific, Perry, IA) or in an environmental (30°C) room. All processing of samples under dark conditions was performed in a dark room with a minimal amount of light provided by a green LED. Starvation media were prepared as follows: N-starvation media: replace 18 mM $NaNO_3$ with 18 mM NaCl; S-starvation media: replace 0.3 mM $MgSO_4$ with 0.3 mM $MgCl_2$.

Unless otherwise indicated, *Synechococcus* cultures were induced with 50 µM isopropyl β-D-1-thiogalactopyranoside (IPTG) when appropriate. Single antibiotics (chloramphenicol, kanamycin) were used at 10 µg/ml, and double antibiotics at 2 µg/ml each. *Escherichia coli* was grown in LB media at 37°C with shaking (250 rpm), unless otherwise noted. When appropriate, chloramphenicol was used at 25 µg/ml, and kanamycin at 60 µg/ml for *E. coli*. Measurements of culture optical density (OD_{600} or OD_{750}, subscript indicating wavelength in nm) were performed using a Thermo Scientific Genesys 20 spectrophotometer (Waltham, MA).

4.2.2 Plasmid and strain construction

Plasmids were constructed using either traditional restriction enzyme cloning or a Golden Gate cloning strategy (9) and were propagated in *E. coli* DH5α. For Golden Gate cloning, primers were designed to amplify genes such that a BsaI restriction enzyme site would be added onto both ends, and overhangs generated by digestion with BsaI would be complementary to those present in Golden Gate destination plasmids. Golden Gate reactions (incorporating cycles of restriction enzyme digestion and ligation) were incubated for 50 cycles of 45°C for 5 min and 16°C for 2 min, followed by incubations at 50°C for 10 min and 80°C for 10 min to inactivate the enzymes. Standard methods were used for PCR, gel purification of PCR products, restriction enzyme cloning, *E. coli* transformation, and DNA sequencing to verify cloned constructs. Table 4-2 lists the plasmids and primers used in this chapter.

Table 4-2. Plasmids and primers used in Chapter 4.

plasmid name	reference
pNS2 (Kan^R)	Clerico, EM, Ditty, JL, and SS Golden (2007) Methods Mol Biol 362: 115-129
pNS2-Synpcc7942_1377(rel)	Chapter 2
pNS2-Synpcc7942_1566(ppk)	this study
pNS3 (Cm^R)	Clerico, EM, Ditty, JL, and SS Golden (2007) Methods Mol Biol 362: 115-129
pUC-ΔSynpcc7942_1377(rel)-Cm^R	Chapter 2
pUC-ΔSynpcc7942_1566(ppk)-Cm^R	constructed by D. Savage (unpublished)
pUC-ΔSynpcc7942_1965(ppx)-Cm^R	this study
pUC-ΔSynpcc7942_0493(ppt)-Cm^R	this study
primer name	**primer sequence**
Synpcc7942_1377-F-BsaI-GG	CACACCA GGTCTC A GTCC ccgtcagccggtttgccg
Synpcc7942_1377-R-stop-BsaI-GG	CACACCA GGTCTC A CGCT tcacagctcatcatcgctgccg
Synpcc7942_1566-F-SpeI	ATTAGC ACTAGT catcccttgctaggatcag
Synpcc7942_1566-R-NS-XbaI-stop-HindIII-NotI	ATTAGC GCGGCCGCAAGCTTTTATCTAGA gcgggtggtagccgcg
rel-KO-up-F-BsaI-GG	CACACCA GGTCTC A CGCT ctggtcagcaagacttccagca
rel-KO-up-R-BsaI-GG	CACACCA GGTCTC A TACT cgaacgtgcgatcgctcc
rel-KO-down-F-BsaI-GG	CACACCA GGTCTC A TAGC tcactcagctatccaactgatg
rel-KO-down-R-BsaI-GG	CACACCA GGTCTC A GTCC ctggatctgaatccacacgatc
rel-KO-screen-F	catcgcctttcgcacagct
rel-KO-screen-R	cacagatcactgcagcactg
Cm^R-F-BsaI-GG	CACACCA GGTCTC A AGTA cactggagcacctcaa
Cm^R-R-BsaI-GG	CACACCA GGTCTC A GCTA ctgccaccgctgagc
ppxKO-Up-F -EcoRI	GATAGC GAATTC gtcacagcaaccaagctcc
ppxKO-Up-R -SpeI	GATAGC ACTAGT gggcgcagggttccaag
ppxKO-Dn-F-HindIII	GATAGC AAGCTT tttctctcacctgacttct
ppxKO-Dn-R-NotI	GATAGC GCGGCCGC gaaaggaaaagcgagcagc
pptKO-Up-F-ApaI	GATAGC GGGCCC ctgttcaggtcgcaaaaag
pptKO-Up-R-SpeI	GATAGC ACTAGT tcttctcaacttgccacagc
pptKO-Dn-F-HindIII	GATAGC AAGCTT aagttctggaaactgtgacg
pptKO-Dn-R-NotI	GATAGC GCGGCCGC caaataaccagacacgatcg
CmR-KO-screen-R	ccaggttttcaccgtaacacg
ppk-KO-screen-F	tcgcgacgaagaagagtatcg
ppk-KO-screen-R	gcgaaatactgatcgaggtatc
ppx-KO-screen-F	gatgcggctttattatcccac
ppx-KO-screen-R	ctaaaccgacttcatggatgac
ppt-KO-screen-F	cagaaactgggtctaggtcatc
ppt-KO-screen-R	ctgacatgcatccagagtttg

Synechococcus was transformed by growing cultures to log phase (OD_{750} 0.2-0.6), harvesting cells by centrifugation (16000 g, 2 min, 25°C), washing cells once in 0.5X volume of 10 mM NaCl, and resuspending cells in 0.1X volume of BG-11 media. Approximately 200 ng of the plasmid to be transformed was added, and cultures were wrapped in foil and incubated overnight at 30°C. The next day, transformations were plated on BG-11 plates containing the appropriate selective antibiotic. All deletion strains were verified by colony PCR, using primers to detect both the native locus and the deletion construct, and were fully penetrant. Table 4-3 lists and describes the strains used in this chapter.

Table 4-3. Strains used in Chapter 4.

Strain name	Strain genotype	Resistance	Reference
Synechococcus elongatus PCC 7942 wild-type (WT)	WT	–	–
control (WT-Cm^R)	pNS3	Cm	Chapter 2
Δ*rel*	ΔSynpcc7942_1377-Cm^R	Cm	Chapter 2
Δ*rel* + *rel*	ΔSynpcc7942_1377-Cm^R + pNS2-Synpcc7942_1377	Cm, Kan	Chapter 2
Δ*ppk*	ΔSynpcc7942_1566-Cm^R	Cm	this study
Δ*ppk* + *ppk*	ΔSynpcc7942_1566-Cm^R + pNS2-Synpcc7942_1566	Cm, Kan	this study
Δ*ppx*	ΔSynpcc7942_1965-Cm^R	Cm	this study
Δ*ppt*	ΔSynpcc7942_0493-Cm-Kan^R	Cm	this study

4.2.3 Microscopy and image analysis

For the experiment shown in Figure 4-1, *Synechococcus* cultures were incubated under the indicated conditions, cell pellets were resuspended in BG-11 + 2% glutaraldehyde and incubated at 30°C for 15 minutes. Fixed cells were washed two times in BG-11 before continuing with DAPI staining. For all other DAPI staining experiments, live cells were used for staining.

Cells were stained with 4',6-diamidino-2-phenylindole (DAPI; Sigma-Aldrich) at 1 mg/ml for 15 minutes in the dark at room temperature. Stained cells were washed two times in phosphate-buffered saline (PBS) and resuspended in BG-11 medium. Cells were immobilized by spotting cultures onto agarose pads (2% agarose in BG-11 medium). Imaging was performed on a Zeiss AXIO Observer.Z1 inverted microscope (Oberkochen, Germany) equipped with a 100X phase-contrast oil objective (NA 1.4) and an Excelitas Technologies X-Cite 120Q fluorescent light source (Fremont, CA). Images were acquired using a Hamamatsu Photonics ORCA-Flash4.0 sCMOS camera (Hamamatsu City, Japan) and Zeiss ZEN 2012 software.

Cyanobacteria naturally fluoresce in the red portion of the visible spectrum due to both chlorophyll-containing photosystems and the light-harvesting pigments present in phycobilisomes, both of which are found in the thylakoid membranes (10). Pigment fluorescence was assayed using a standard red fluorescent protein (RFP) filter set (excitation 572 nm; emission 629 nm). Polyphosphate (polyP) was imaged using a standard cyan fluorescent protein (CFP) filter set (excitation 436 nm; emission 480 nm). Upon binding to negatively-charged polyP, the positively-charged DAPI molecule exhibits a spectral Stokes shift that permits DAPI-polyP fluorescence to be distinguished from DAPI-DNA fluorescence using these wavelengths (11). At the same time, a standard DAPI filter set was used to assay DAPI-DNA fluorescence (excitation 365 nm; emission 445 nm). Microscopy images were analyzed using MicrobeTracker and SpotFinder, bacterial image analysis programs written in Matlab (12). Segmentation of cells was manually verified and corrected when necessary.

4.3 Results and Discussion

4.3.1 Levels of polyphosphate rise in the dark

PolyP granules can be visualized *in vivo* using DAPI staining and fluorescence microscopy. While typically used to stain DNA, DAPI also binds to polyP and exhibits a spectral red shift, allowing specific visualization of the polyP-DAPI complex (11). To test whether polyP abundance varies depending on metabolic activity, we compared polyP levels in cells growing under constant light to cells that had been incubated in the dark for 24 hours (Figure 4-1A). Both the number and the size of polyP granules increase in the dark in wild-type cells (Figures 4-1B and 4-1C).

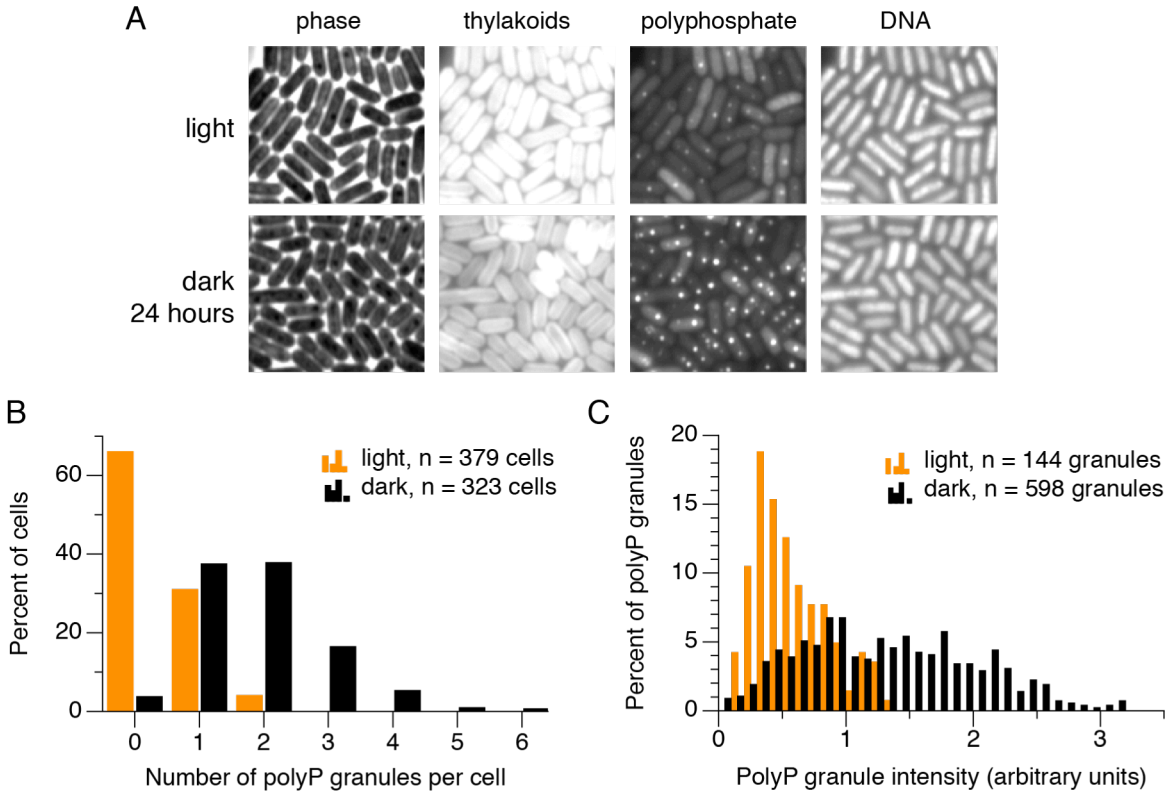

Figure 4-1. Polyphosphate levels increase in the dark. Both the number of granules per cell and the size of the granules increases after a 24-hour dark incubation. (A) Wild-type cultures were incubated in the light or dark before fixation with 2% glutaraldehyde. Fixed cells were stained with DAPI and imaged by fluorescence microscopy. (B,C) Images were analyzed using MicrobeTracker and SpotFinder.

The finding that polyP levels increase in the dark was initially surprising – we had hypothesized that polyP could serve as an energy storage reservoir when cells are not photosynthesizing. Since these experiments were performed, another group has also shown that polyP levels rise in the dark in *Synechococcus* (13), lending support to our finding.

We know that polyP increases in *Synechococcus* when (p)ppGpp levels are high (Figure 2-3), and that (p)ppGpp increases in the dark, but we have not directly connected these observations. We still do not know whether cells accumulate polyP in the dark because it is preferentially used in the light (for a pathway like carbon fixation, for example), or because it accumulates in response to metabolic changes and stress responses during darkness. To test whether (p)ppGpp is responsible for increasing polyP levels in the dark, future experiments could determine polyP levels when the Δ*rel* mutant – which cannot synthesize (p)ppGpp – is subjected to darkness. If our hypothesis is correct, polyP levels should be lower in this strain than in the wild-type.

4.3.2 A Δ**ppk** *mutant lacks polyphosphate granules and displays altered cellular morphology*

To determine whether *ppk* drives polyP formation in *Synechococcus*, we constructed and analyzed a knockout mutant of this gene. DAPI staining and fluorescence microscopy show that polyP granules are not detectable in the Δ*ppk* strain, indicating that this enzyme is indeed required for polyP synthesis (Figures 4-2A and 4-2B).

A notable phenotype of this strain is its altered cellular morphology. Cells of the Δ*ppk* mutant are noticeably smaller than those of the wild-type (Figure 4-2C). This suggests that cell division might be affected in the Δ*ppk* mutant, which could have a variety of causes. PolyP has been implicated in nucleoid structure in *P. aeruginosa* (14) and localization of basic proteins in *E. coli* (15), and could contribute to cellular organization.

A role in intracellular organization could also explain the interaction observed *in vivo* between polyP granules and carboxysomes. Preliminary experiments in the Savage lab have shown that carboxysomes co-localize with the nucleoid in *Synechococcus*, and this holds true even when nucleoid structure is disrupted by the DNA gyrase inhibitor ciprofloxacin (D. Savage, unpublished). If polyP is somehow involved in regulating nucleoid structure, it could also be involved in positioning carboxysomes within the cell. This could be tested by analyzing localization of carboxysomes labeled with green fluorescent protein in polyP mutant strains (Δ*ppk*/Δ*ppx*/Δ*ppt*) by fluorescence microscopy. Further experiments could also characterize the morphology of the Δ*ppk* mutant in greater detail, and determine whether it does in fact have cell division defects or abnormalities.

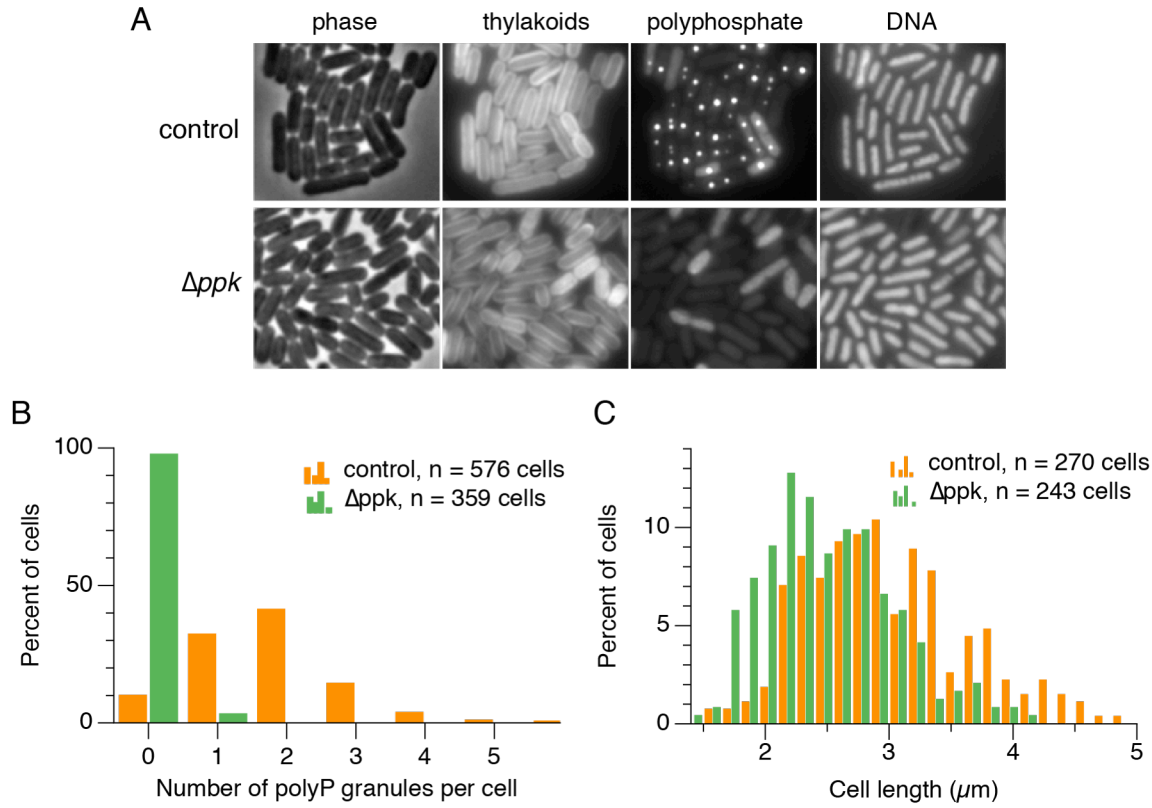

Figure 4-2. A Δ*ppk* mutant lacks polyphosphate granules and displays altered cellular morphology. (A) Cultures of the indicated strains were stained with DAPI and imaged by fluorescence microscopy. (B,C) Images were analyzed using MicrobeTracker and SpotFinder. Results are representative of three independent experiments.

4.3.3 Mutants lacking ppx *or* ppt *do not have obvious phenotypes*

We also knocked out the genes encoding *ppx* and *ppt*, both of which are involved in controlling polyP levels (Table 4-1). Analysis of polyP content in these strains indicates that polyP levels may be slightly higher than the wild-type control. Further experimentation will be necessary, however, to determine whether these mutations have any measurable effects on growth or physiology of *Synechococcus*. We have also constructed a triple mutant, Δ*ppk* Δ*ppx* Δ*ppt*, in which all polyP metabolic genes have been knocked out. The phenotypes of this mutant could also be tested to see if they differ from those of the individual mutants. Preliminary results show that this mutant lacks polyP, so its phenotypes may be similar to those of the Δ*ppk* mutant (data not shown).

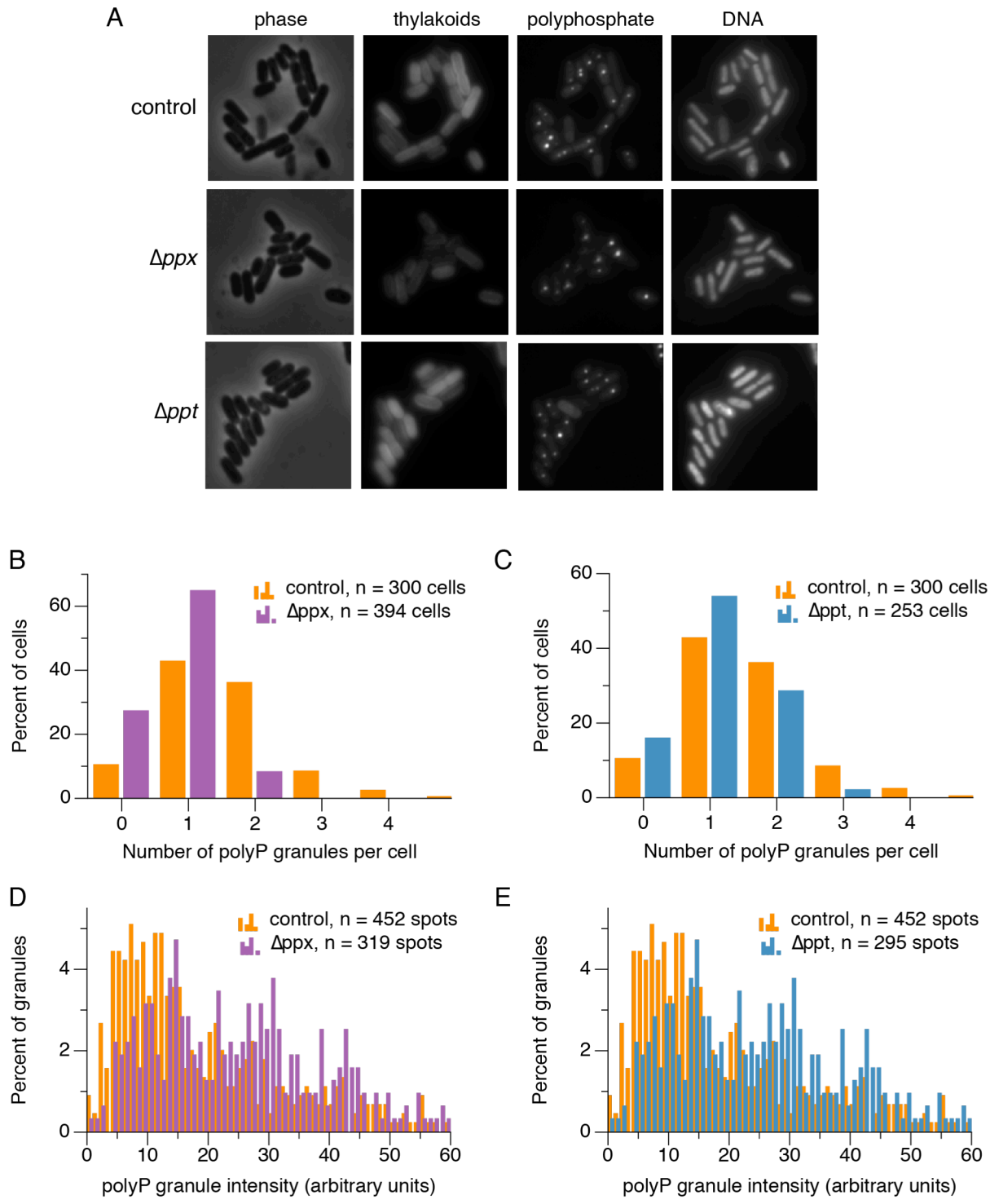

Figure 4-3. Mutants lacking *ppx* or *ppt* do not have obvious phenotypes. (A) Cultures of the indicated strains were stained with DAPI and imaged by fluorescence microscopy. (B-E) Images were analyzed using MicrobeTracker and SpotFinder.

4.3.4 The Δppk *mutant shows impaired survival in response to stress*

It has been found previously that Δ*ppk* mutants of various bacterial species do not survive stress as well as the wild-type strain (4). We tested whether survival of the Δ*ppk* mutant is impaired after darkness or starvation for nitrogen or sulfur (Figure 4-4). The Δ*ppk* strain survived exposure to darkness or nitrogen starvation as well as the wild-type, but its growth was impaired after sulfur starvation. This effect could be complemented by expressing an IPTG-inducible copy of the *ppk* gene elsewhere on the chromosome.

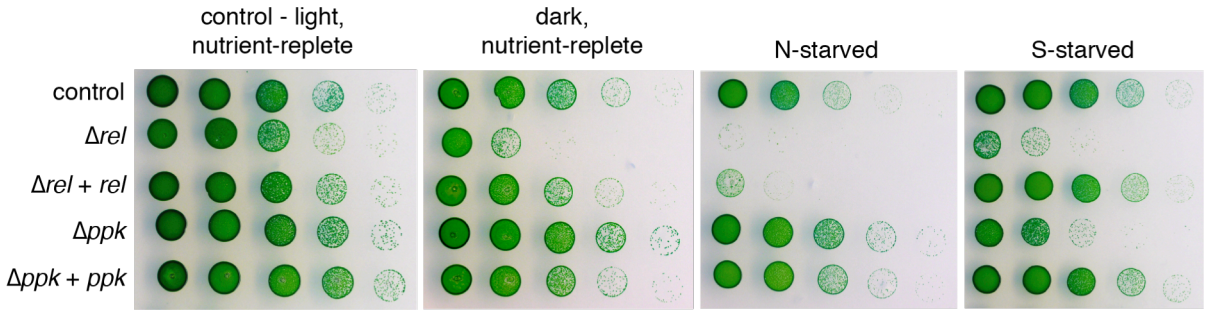

Figure 4-4. The Δ*ppk* mutant may not survive sulfur starvation as well as the wild-type. Cultures were resuspended in media lacking the indicated nutrient (except for nutrient-replete controls, which were resuspended in nutrient-replete media), and incubated under the indicated condition. After 6 days, tenfold serial dilutions were spotted onto nutrient-replete plates and grown in constant light. The Δ*rel* + *rel* and Δ*ppk* + *ppk* strains were induced with IPTG for 21 hours before starvation.

Though these results are preliminary and bear repeating, it would also be interesting to test other stressors, including iron and phosphate starvation and treatment with the photosynthetic inhibitor DCMU. These experiments could also include the triple mutant (Δ*ppk* Δ*ppx* Δ*ppt*), to see if abolishing all polyP metabolism affects survival to a greater extent. Finally, a reciprocal experiment would be to determine how polyP levels change under starvation conditions. During nitrogen deprivation, for example, polyP granules are made in *P. aeruginosa* (16), and we might predict to see the same effect in *Synechococcus* due to the metabolic imbalances that result from starvation.

4.3.5 Conclusions

One of the primary functions of polyP is undoubtedly as a phosphate storage compound (17). Field studies have shown that polyP can be detected in free-living and symbiotic cyanobacteria in the ocean, and have proposed that it serves important storage functions in these environments (18, 19). PolyP reserves can be mobilized in *Synechococcus* for RNA synthesis and other cellular functions (20). However, other roles – both proven and proposed – have also expanded far further than that (4). There are still many unknowns in the field of polyP biology, but it is likely that there are interesting answers to be found in *Synechococcus*.

4.4 References

1. Jensen TE (1968) Electron microscopy of polyphosphate bodies in a blue-green alga, Nostoc pruniforme. *Archiv fur Mikrobiologie* 62:144–152.

2. Nierzwicki-Bauer SA, Dalkwill DL, Stevens SE (1983) Three-dimensional ultrastructure of a unicellular cyanobacterium. *J Cell Biol* 97:713–722.

3. Iancu CV, et al. (2010) Organization, Structure, and Assembly of α-Carboxysomes Determined by Electron Cryotomography of Intact Cells. *Journal of Molecular Biology* 396(1):105–117.

4. Rao NN, Gómez-García MR, Kornberg A (2009) Inorganic Polyphosphate: Essential for Growth and Survival. *Annu Rev Biochem* 78(1):605–647.

5. Kuroda A, Murphy H, Cashel M, Kornberg A (1997) Guanosine Tetra- and Pentaphosphate Promote Accumulation of Inorganic Polyphosphate in Escherichia coli. *J Biol Chem* 272:21240–21243.

6. Kulaev IS, Vagabov V, Kulakovskaya T (2004) *The Biochemistry of Inorganic Polyphosphates* (John Wiley & Sons, Ltd). 2nd Ed.

7. Kuroda A, et al. (2001) Role of Inorganic Polyphosphate in Promoting Ribosomal Protein Degradation by the Lon Protease in E. coli. *Science* 293(5530):705–708.

8. Allen MM (1968) Simple conditions for growth of unicellular blue-green algae on plates. *J Phycol* 4:1–4.

9. Engler C, Kandzia R, Marillonnet S (2008) A one pot, one step, precision cloning method with high throughput capability. *PLoS ONE* 3(11):e3647.

10. Yokoo R, Hood RD, Savage DF (2015) Live-cell imaging of cyanobacteria. *Photosynth Res* 126:33–46.

11. Aschar-Sobbi R, et al. (2008) High Sensitivity, Quantitative Measurements of Polyphosphate Using a New DAPI-Based Approach. *J Fluoresc* 18(5):859–866.

12. Sliusarenko O, Heinritz J, Emonet T, Jacobs-Wagner C (2011) High-throughput, subpixel precision analysis of bacterial morphogenesis and intracellular spatio-temporal dynamics. *Mol Microbiol* 80(3):612–627.

13. Seki Y, Nitta K, Kaneko Y (2014) Observation of polyphosphate bodies and DNA during the cell division cycle of Synechococcus elongatus PCC 7942. *Plant Biol (Stuttg)* 16(1):258–263.

14. Fraley CD, et al. (2007) A polyphosphate kinase 1 (ppk1) mutant of Pseudomonas aeruginosa exhibits multiple ultrastructural and functional defects. *Proc Natl Acad Sci USA* 104:3526–3531.

15. Zhao J, et al. (2008) Group II Intron Protein Localization and Insertion Sites Are Affected by Polyphosphate. *Plos Biol* 6(6):e150.

16. Racki LR, et al. (2017) Polyphosphate granule biogenesis is temporally and functionally tied to cell cycle exit during starvation in Pseudomonas aeruginosa. *Proc Natl Acad Sci USA* 114(12):E2440–E2449.

17. Allen MM (1984) Cyanobacterial cell inclusions. *Annu Rev Microbiol* 38:1–25.

18. Martin P, Dyhrman ST, Lomas MW, Poulton NJ, Van Mooy BAS (2014) Accumulation and enhanced cycling of polyphosphate by Sargasso Sea plankton in response to low phosphorus. *Proc Natl Acad Sci USA* 111(22):8089–8094.

19. Zhang F, et al. (2015) Phosphorus sequestration in the form of polyphosphate by microbial symbionts in marine sponges. *Proc Natl Acad Sci USA* 112(14):4381–4386.

20. Grillo JF, Gibson J (1979) Regulation of Phosphate Accumulation in the Unicellular Cyanobacterium Synechococcus. *J Bacteriol* 140(2):508–517.

Chapter 5

Conclusions

5.1 Summary

This work has shown that the stringent response is a major regulator of metabolism and physiology in the cyanobacterium *Synechococcus elongatus*. Amazingly, usage of the second messenger (p)ppGpp to convey cellular nutritional status has been conserved in bacteria that live in an incredibly wide range of environments on the planet: from oceans to land; cold to hot; wet to dry; nutrient-rich to nutrient-poor; free-living bacteria to pathogens. By continuing to learn more about the importance and functions of this response in diverse bacteria, we can learn more not only about the organisms themselves, but also about the environments in which they live and the challenges they encounter.

Chapter 1 begins by providing background on the ecological importance of cyanobacteria and their cell biology, metabolism, and physiology. Many aspects of these organisms' biology must be taken into account when considering stress responses, since understanding these responses requires a holistic view of the cell and how it coordinates many simultaneous pathways and processes.

In Chapter 2, we show that darkness is analogous to starvation in *Synechococcus*. When *Synechococcus* enters the dark, increased levels of (p)ppGpp trigger widespread changes in gene expression and alter ribosomal populations, possibly affecting translation rate or altering specificity. We also show that (p)ppGpp can affect many aspects of *Synechococcus* physiology, though not all of these changes occur during the (p)ppGpp-mediated response to darkness.

Chapter 3 takes a broader look at the role of the stringent response in *Synechococcus*. We show that it helps this cyanobacterium survive exposure to other stresses it might encounter in its environment, including nitrogen deprivation. The ability to make (p)ppGpp also helps cells adapt to treatment with DCMU, an inhibitor of photosynthesis. Under certain conditions, the stringent response seems to regulate photosynthetic flux by altering the quantity and/or composition of light-harvesting protein complexes. In this chapter, we also outline approaches we are currently taking to learn more about both upstream inputs and downstream effects of the stringent response in *Synechococcus*, which we will also discuss below.

Finally, in Chapter 4, we determine that levels of the stringent response-linked molecule polyphosphate increase in response to darkness, that its synthesis is controlled by the enzyme PPK, and that it – like the stringent response – may help *Synechococcus* respond to stress. Our results indicate that it may also play some role in regulating cellular organization and/or division.

5.2 Discussion and future directions

Our work has begun to characterize how (p)ppGpp affects *Synechococcus* physiology in response to stress. Little was known about the mechanistic effects of this pathway before this work, and we have made good progress, but there are still many unknowns. Our findings have also provided a lens through which previous studies of cyanobacterial physiology can be viewed (as reviewed in (1)).

5.2.1 Inputs of the stringent response

Given that *Synechococcus* Rel is most likely a bifunctional enzyme that can both synthesize and hydrolyze (p)ppGpp, how are these opposing activities regulated? The first question might be, then, under which conditions is (p)ppGpp made? We – and others – have shown that darkness triggers ppGpp production (Figure 2-1; (2, 3)). We have evidence showing that (p)ppGpp synthesis is important for responding to photosynthetic inhibition (DCMU treatment) and nitrogen starvation, among other types of nutrient starvation. Indeed, previous studies have shown that DCMU and nitrogen deprivation do trigger (p)ppGpp synthesis (3-5). We are currently working to repeat these experiments, using the updated method described in Section 3.3.4. Our current method cannot measure pppGpp, however, and thus we still do not know how much of this compound is being produced or how important it is in *Synechococcus*.

In a larger sense, what actually modulates Rel activity? This most likely occurs through allosteric mechanisms, either by binding of another protein or by a small molecule. RelA, a (p)ppGpp synthetase from *E. coli,* can be allosterically activated through a feedback mechanism mediated by ppGpp itself (6). The activity of RelA is affected by its binding to the ribosome, and this also holds true with a bifunctional Rel from *Mycobacterium tuberculosis* (7-10). It is currently unknown whether *Synechococcus* Rel interacts with the ribosome and responds to low amino acid levels or stalled translation.

What could be the signals that convey that photosynthesis has stopped, or that nitrogen is unavailable, in *Synechococcus*? When photosynthesis stops, cellular redox state and pH change. One candidate for the 'dark signal' might be a redox-sensing protein that could interact with Rel and thereby affect its activity, or perhaps Rel itself is redox-sensitive. Some nitrogen responsive-proteins, like NtcA and P_{II}, detect changes in levels of the metabolite α-ketoglutarate, which increases during nitrogen starvation (11). A more general stress response like the stringent response, however, might not sense such a specific metabolite. Perhaps nutrient-specific regulators could interact with Rel, or affect its activity indirectly, to control (p)ppGpp synthesis as well? We do not know where Rel is localized in the cyanobacterial cell, and whether its localization might change depending on nutritional status, but these experiments may provide some clues about its regulation.

5.2.2 Downstream effects of the stringent response / targets of (p)ppGpp in **Synechococcus**

Transcription

We have found that many genes are (p)ppGpp-regulated in *Synechococcus* (Chapter 2). This is consistent with what has been observed in many other bacteria, though the mechanisms driving these changes are likely not conserved in *Synechococcus*. *Synechococcus* lacks homologs to the transcription factors DksA, which works with (p)ppGpp to reprogram gene expression in Proteobacteria, as well as CodY, a major regulator of gene expression in Firmicutes during the stringent response (12). We do not know whether (p)ppGpp binds directly to any transcription factors, or how it otherwise signals to RNA polymerase and its regulators in *Synechococcus*. It would be interesting to test whether cyanobacterial sigma factors are necessary to observe stringent response-dependent transcriptional changes. Transcriptional regulators might be one possible hit from the ppGpp suppressor experiments described in Section 3.3.6. Clearly, we do not know how transcription is reprogrammed in response to (p)ppGpp, but we also know nothing about the functions of many genes induced in response to high (p)ppGpp levels (Tables 2-3 and 2-4).

Translation

Different proteins are translated in the dark than in the light (13, 14), but their identities remain unknown. Similarly, it seems reasonable to hypothesize that only a small, specific subset of proteins would be translated under nutrient starvation. Ribosome profiling experiments could show which proteins are actively being translated under such conditions (15). Based on our results showing that HPF causes ribosomes to dimerize in the dark (Figure 2-11), we tested whether the Δ*hpf* mutant had either altered translation rates (by measuring the degree of ^{14}C-Leu incorporation into proteins) or altered translational specificity (by ^{35}S-Met labeling of newly synthesized proteins) in the dark, but did not observe any differences between the wild-type and Δ*hpf*. It has recently been shown that HPF from *Pseudomonas aeruginosa* helps preserve ribosomal integrity during nutrient starvation (16) – an intriguing finding that could be tested in *Synechococcus* as well. Another possible role for (p)ppGpp in regulating translation might be through interacting with GTP-binding translation proteins, as has been shown in several other bacteria. For example, Corrigan et al. (17) showed that (p)ppGpp binds directly to GTPases involved in ribosome assembly in *Staphylococcus aureus*.

Metabolism

We have identified several downstream targets of the stringent response that regulate key metabolic pathways, including photosynthetic light-harvesting complexes and glutamine synthetase, the primary enzyme of nitrogen assimilation (Chapters 2 and 3). This points to a general role of the stringent response in balancing different branches of metabolism during stress conditions. Changing (p)ppGpp levels almost certainly affects nucleotide pools, and regulation of GTP levels is a major effect of (p)ppGpp in *Bacillus subtilis* (18). As discussed in Chapter 1, cyanobacteria accumulate glycogen when they are photosynthetically active, and use it both for energy and as an electron sink. It

would be interesting to test whether levels of glycogen and other metabolites differ depending on whether cells have the ability to synthesize (p)ppGpp or not.

Polyphosphate
Levels of polyphosphate (polyP) are regulated by the stringent response in *Synechococcus*, as we have shown in Chapter 2. Although we describe preliminary experiments into polyP functions in Chapter 4, we still know very little about what it does in *Synechococcus*. Methods for studying polyP are somewhat limited – for example, intact polyP granules cannot be isolated directly from cells. In the past few years, however, two particularly interesting findings/hypotheses have been reported about polyP. Gray et al. (19) reported that polyP can serve a chaperone-like function, protecting proteins (and *E. coli*) from oxidative stress. As a negatively-charged chain of phosphates, polyP can also mimic nucleic acid backbones, in some cases competing with DNA or RNA to bind particular proteins (20). Recently, Racki et al. (21) concluded that polyP plays a role in nucleoid organization in *P. aeruginosa*. This led the authors to propose that polyP could serve as a phosphate storage polymer, a source of phosphate for regulatory proteins like kinases (as has been shown for the kinase MprB of *M. tuberculosis*; (22)), and/or that polyP granules could create phase-separated microenvironments in which particular enzymatic activities are localized. These latter two are intriguing possibilities, and though they require further experimentation, might inform future directions into the roles of polyP in *Synechococcus*.

DNA replication, cell division, etc.
When (p)ppGpp levels are high, DNA replication slows or stops and cell division seems to be affected in *Synechococcus* (Figure 2-3). These phenotypes are consistent with what has been seen in other bacteria (23-26), but further studies will be necessary to elucidate the mechanisms behind these effects. Determining which *Synechococcus* proteins directly bind (p)ppGpp could be achieved using an approach like that of Corrigan et al. (17), and might provide insight into how these processes are regulated.

5.2.3 Interplay between the stringent response and other regulatory systems

A number of other regulatory systems operate in cyanobacteria, and respond to some of the same triggers as the stringent response. Circadian rhythm is probably the best-studied of these (as described in Chapter 1), but signaling also occurs via a variety of two-component systems and transcription factors. Since none of these systems act in isolation, it would be interesting to investigate cross-talk between these pathways. For example, one could envision testing whether circadian rhythm is altered in the Δ*rel* mutant, or whether growth of a Δ*rel* mutant that also lacks circadian rhythm is even more impaired in light/dark cycles. It has recently been found that *Synechococcus* makes cyclic-di-AMP upon a shift from light to dark (27), and responses to cyclic-di-AMP and (p)ppGpp are known to overlap in some Gram-positive bacteria (28, 29). Whether these two nucleotides or their responses are linked in *Synechococcus* is currently unknown.

5.2.4 Broadening our view of bacterial physiology from the E. coli *model*

E. coli has long been, and continues to be, *the* model bacterium. We have learned a great deal from studying this organism in depth, but assuming that other bacteria will fit the mold of *E. coli* biology not only leads to incorrect assumptions, it also does not encourage us to appreciate the diversity of bacterial lifestyles and environments. In the last couple decades, mechanistic studies of the stringent response have finally expanded beyond the *E. coli* paradigm, and have provided insight into the elegant strategies by which different bacteria sense and respond to the world around them. I'm sure this trend will continue in the years to come, and that many more fascinating findings will come out of these studies.

5.2.5 Beyond cyanobacteria – the stringent response in other photosynthetic organisms

As the progenitors of chloroplasts, what we learn from studies of cyanobacteria can also, in some cases, inform our understanding of algal and plant physiology. Plants and algae encode multiple families of (p)ppGpp synthetases/hydrolases (30, 31) and make ppGpp in response to darkness, wounding, and other stresses (32). Studies have also shown that (p)ppGpp can decrease the activity of chloroplast RNA polymerase, thereby generally suppressing transcription. These nucleotides can also affect photosynthesis and chloroplast physiology (32-34), as we observe for *Synechococcus.*

The amazing ability of photosynthetic organisms to harvest light energy from the sun and convert it to chemical energy sustains life on Earth. Learning more about how these organisms regulate their metabolism is of fundamental importance, both from a microbiological perspective and from an ecological standpoint.

5.3 References

1. Doolittle WF (1979) The cyanobacterial genome, its expression, and the control of that expression. *Adv Microb Physiol* 20:1–102.

2. Mann N, Carr NG, Midgley J (1975) RNA synthesis and the accumulation of guanine nucleotides during growth down shift in the blue-green alga Anacystis nidulans. *Biochim Biophys Acta* 402:41–50.

3. Borbely G, Kaki C, Gulyás A, Farkas GL (1980) Bacteriophage infection interferes with guanosine 3“-diphosphate-5-”diphosphate accumulation induced by energy and nitrogen starvation in the cyanobacterium Anacystis nidulans. *J Bacteriol* 144(3):859–864.

4. Smith RJ (1977) The regulation of stable RNA synthesis in the blue-green alga Anacystis nidulans, the effect of DCMU inhibition. *FEMS Microbiol Lett* 1:129–132.

5. Friga GM, Borbely G, Farkas GL (1981) Accumulation of guanosine tetraphosphate (ppGpp) under nitrogen starvation in Anacystis nidulans, a cyanobacterium. *Arch Microbiol* 129:341–343.

6. Shyp V, et al. (2012) Positive allosteric feedback regulation of the stringent response enzyme RelA by its product. *EMBO Rep* 13(9):835–839.

7. Avarbock D, Avarbock A, Rubin H (2000) Differential regulation of opposing RelMtb activities by the aminoacylation state of a tRNA.ribosome.mRNA.RelMtb complex. *Biochemistry* 39(38):11640–11648.

8. Arenz S, et al. (2016) The stringent factor RelA adopts an open conformation on the ribosome to stimulate ppGpp synthesis. *Nucleic Acids Res* 44(13):6471–6481.

9. Brown A, Fernández IS, Gordiyenko Y, Ramakrishnan V (2016) Ribosome-dependent activation of stringent control. *Nature* 534(7606):277–280.

10. Loveland AB, et al. (2016) Ribosome-RelA structures reveal the mechanism of stringent response activation. *eLife* 5:e17029.

11. Muro-Pastor MI, Reyes JC, Florencio FJ (2001) Cyanobacteria perceive nitrogen status by sensing intracellular 2-oxoglutarate levels. *J Biol Chem* 276(41):38320–38328.

12. Gaca AO, Colomer-Winter C, Lemos JA (2015) Many means to a common end: the intricacies of (p)ppGpp metabolism and its control of bacterial homeostasis. *J Bacteriol* 197(7):1146–1156.

13. Singer RA, Doolittle WF (1975) Control of gene expression in blue-green algae. *Nature* 253:650–651.

14. Suranyi G, Korcz A, Palfi Z, Borbely G (1987) Effects of light deprivation on RNA synthesis, accumulation of guanosine 3'(2‘)-diphosphate 5’-diphosphate, and protein synthesis in heat-shocked Synechococcus sp. strain PCC 6301, a cyanobacterium. *J Bacteriol* 169:632–639.

15. Ingolia NT (2014) Ribosome profiling: new views of translation, from single codons to genome scale. *Nat Rev Genet* 15(3):205–213.

16. Akiyama T, et al. (2017) Resuscitation of Pseudomonas aeruginosa from dormancy requires hibernation promoting factor (PA4463) for ribosome preservation. *Proc Natl Acad Sci USA* 114(12):3204–3209.

17. Corrigan RM, Bellows LE, Wood A, Gründling A (2016) ppGpp negatively impacts ribosome assembly affecting growth and antimicrobial tolerance in Gram-positive bacteria. *Proc Natl Acad Sci USA* 113(12):E1710–9.

18. Kriel A, et al. (2012) Direct regulation of GTP homeostasis by (p)ppGpp: a critical component of viability and stress resistance. *Mol Cell* 48(2):231–241.

19. Gray MJ, et al. (2014) Polyphosphate Is a Primordial Chaperone. *Mol Cell*:1–11.

20. Nomura K, Kato J, Takiguchi N, Ohtake H, Kuroda A (2004) Effects of Inorganic Polyphosphate on the Proteolytic and DNA-binding Activities of Lon in Escherichia coli. *J Biol Chem* 279(33):34406–34410.

21. Racki LR, et al. (2017) Polyphosphate granule biogenesis is temporally and functionally tied to cell cycle exit during starvation in Pseudomonas aeruginosa. *Proc Natl Acad Sci USA* 114(12):E2440–E2449.

22. Sureka KK, et al. (2007) Polyphosphate kinase is involved in stress-induced mprAB-sigE-rel signalling in mycobacteria. *Mol Microbiol* 65(2):261–276.

23. Wang JD, Sanders GM, Grossman AD (2007) Nutritional control of elongation of DNA replication by (p)ppGpp. *Cell* 128(5):865–875.

24. Srivatsan A, Wang JD (2008) Control of bacterial transcription, translation and replication by (p)ppGpp. *Curr Opin Microbiol* 11(2):100–105.

25. Ferullo DJ, Lovett ST (2008) The stringent response and cell cycle arrest in Escherichia coli. *PLoS Genet* 4(12):e1000300.

26. Maciąg M, Kochanowska M, Łyżeń R, Węgrzyn G, Szalewska-Pałasz A (2010) ppGpp inhibits the activity of Escherichia coli DnaG primase. *Plasmid* 63(1):61–67.

27. Rubin BE, Golden SS, personal communication.

28. Whiteley AT, Pollock AJ, Portnoy DA (2015) The PAMP c-di-AMP Is Essential for Listeria Growth in Macrophages and Rich but Not Minimal Media due to a Toxic Increase in (p)ppGpp. *Cell Host Microbe* 17(6):788–798.

29. Corrigan RM, Bowman L, Willis AR, Kaever V, Gründling A (2015) Crosstalk between two Nucleotide-Signaling Pathways in Staphylococcus aureus. *J Biol Chem* 290:5826–5839.

30. Atkinson GC, Tenson T, Hauryliuk V (2011) The RelA/SpoT Homolog (RSH) Superfamily: Distribution and Functional Evolution of ppGpp Synthetases and Hydrolases across the Tree of Life. *PLoS ONE* 6(8):e23479.

31. Ito D, Ihara Y, Nishihara H, Masuda S (2017) Phylogenetic analysis of proteins involved in the stringent response in plant cells. *J Plant Res*. doi:10.1007/s10265-017-0922-8.

32. Takahashi K, Kasai K, Ochi K (2004) Identification of the bacterial alarmone guanosine 5“-diphosphate 3-”diphosphate (ppGpp) in plants. *Proc Natl Acad Sci USA* 101(12):4320–4324.

33. Maekawa M, et al. (2015) Impact of the plastidial stringent response in plant growth and stress responses. *Nat Plants*. doi:10.1038/nplants.2015.167.

34. Sugliani M, et al. (2016) An Ancient Bacterial Signaling Pathway Regulates Chloroplast Function to Influence Growth and Development in Arabidopsis. *The Plant Cell* 28(3):661–679.